Spring 2017

Investigation of local velocities and phase holdups, and flow regimes and maldistribution identification in a trickle bed reactor

Mohd Fitri Bin Abdul Rahman

Department: Chemical and Biochemical Engineering

INVESTIGATION OF LOCAL VELOCITIES AND PHASE HOLDUPS, AND FLOW REGIMES AND MALDISTRIBUTION IDENTIFICATION IN A TRICKLE BED REACTOR

by

MOHD FITRI ABDUL RAHMAN

A DISSERTATION

Presented to the Graduate Faculty of the

MISSOURI UNIVERSITY OF SCIENCE AND TECHNOLOGY

In Partial Fulfillment of the Requirements for the Degree

DOCTOR OF PHILOSOPHY

in

CHEMICAL ENGINEERING

2017

Approved

Muthanna Al Dahhan, Advisor
Parthasakha Neogi
Joseph D. Smith
Douglas K. Ludlow
Shoaib Usman

PUBLICATION DISSERTATION OPTION

This dissertation consists of the following three articles which have been submitted for publication as follows:

PAPER I: pages 15-45 have been submitted to Chemical Engineering & Processing: Process Intensification Journal.

PAPER II: pages 46-84 have been submitted to the Flow Measurement and Instrumentation.

PAPER III: pages 85-110 have been submitted to International Journal of Multiphase Flow.

ABSTRACT

Trickle bed reactors are packed beds of catalyst on which gas and liquid reactants flow concurrently downward. In this work, the experimental work was carried out in 0.14 m diameter Plexiglas column using air-water system flowing over a packed bed of 3 mm glass bead particles. The local liquid and gas velocities, phase saturation and their time series have been investigated for the first time by developing, validating, and implementing a new two-tip optical fiber probe technique. It was found the radially and axially the liquid and gas velocities and their saturation vary and they also vary with times. In various locations, due to non-uniform distribution of the flowing phases, there are windows of time where the gas phase does not pass through that location where the optical fiber probe was put at. The non-invasive gamma-ray densitometry (GRD) technique has been implemented for the first time in trickle bed reactor as in online monitoring technique to identify flow regime, gross maldistribution and liquid distribution. The GRD technique was able to identify trickle and pulse flow regime and their transition. The findings have been consistent with what have been reported in the literature. The measurement of these techniques was conducted at various axial and radial positions with the superficial liquid velocity varies in the range 0.004 – 0.016 m/s and the superficial gas velocity varies in the range of 0.03-0.27 m/s covering trickling and pulsing flow regime. The results obtained confirm that these techniques can be used with fidelity for measurements and the studies mentioned above and can be employed in various sizes of reactor operated at industrial conditions including harsh conditions of corrosion materials, high pressure, and high temperatures.

ACKNOWLEDGMENTS

First of all, praise belongs to God (ALLAH) for his kindness and for providing many blessings in my life.

I express gratitude from the depth of my heart to my advisor, Professor Muthanna H. Al-Dahhan, for his supervision, advice, knowledge and support which have made this work possible. I would also like to acknowledge the members of my committee, namely, Prof. Parthasakha Neogi, Prof. Joseph Smith, Prof. Douglas Ludlow (Department of Chemical and Biochemical Engineering), and Prof. Shoaib Usman (Department of Nuclear Engineering) for taking interest in my work and examining my dissertation.

I would like to acknowledge the Malaysian Ministry Of Science and Technology (MOSTI) for sponsoring my study at the Chemical and Biochemical Engineering Department at Missouri University of Science and Technology. Special thanks to Dean Lenz from the Chemical and Biochemical Engineering Department who helped us design and install the experimental setup.

I express a deep sense of appreciation to my mother, brothers and sisters for their unconditional support. Words are far from adequate to thank them, and what I can do is to keep this deep feeling in my heart forever. During the most challenging and painful years of my life, my wife Noor Huda, daughters (Kauthar & Khaulah) and sons (Ahmad Nabil, Ahmad Nasif & Ahmad Naeem) shared both the happiness and sadness along with me, as we faced the ups and downs of our lives together. Without their encouragement and confidence, I would have failed many times due to hesitance and doubt.

TABLE OF CONTENTS

Page

PUBLICATION DISSERTATION OPTION ……iii

ABSTRACT……... iv

ACKNOWLEDGEMENTS…… v

LIST OF ILLUSTRATIONS……. x

LIST OF TABLES……... xiv

NOMENCLATURE…..…….xv

SECTION

1. INTRODUCTION 1

1.1. SCOPE 1

1.2. MOTIVATION 6

1.3. RESEARCH OBJECTIVES 9

1.4. DISSERTATION ORGANIZATION 10

REFERENCES.. ……11

PAPER

I. FLOW REGIME IDENTIFICATION USING ON-LINE GAMMA-RAY DENSITOMETRY FOR TRICKLE BED REACTORS (TBRs)..... 15

ABSTRACT…….15

1. INTRODUCTION 16

2. EXPERIMENTAL WORK..... 23

2.1. TRICKLE BED REACTOR EXPERIMENTAL SETUP. 23

2.2. GAMMA RAY DENSITOMETRY (GRD) TECHNIQUE. 25

2.3. GRD SIGNALS AND THEIR ANALYSIS FOR FLOW REGIME IDENTIFICATION. 27

3. RESULTS AND DISCUSSION 28

3.1 RESULTS OF STATISTICAL ANALYSIS 28

3.2 RESULT OF SPECTRAL ANLAYSIS 34

3.3 RESULT OF AUTOCORRELATION 35

3.4 RESULT OF KOLMOGOROV ENTROPY (KE) 38

4. REMARKS 41

ACKNOWLEDGEMENT 42

REFERENCES 43

II. NOVEL MEASUREMENT TECHNIQUE BASED ON OPTICAL PROBE TO MEASURE LOCAL FLOW DYNAMICS IN PACKED BED REACTORS 46

ABSTRACT 46

1. INTRODUCTION 47

2. TWO TIP OPTICAL PROBE 50

2.1. MEASUREMENT PRINCIPLE FOR OPTICAL PROBES. 51

2.2. THE OPTICAL FIBER PROBE TIP BEHAVIOR INSIDE THE GAS-LIQUID SYSTEMS. 53

2.3. DESIGN AND FABRICATION OF TWO-TIP OPTICAL PROBE. 56

3. PARAMETERS MEASURED FROM TWO-TIP OPTICAL PROBE 58

4. PROCEDURE TO DETERMINE LOCAL HYDRODYNAMIC PARAMETERS FROM TWO-TIP OPTICAL PROBE 62

4.1. RAW SIGNAL. 62

4.2. FILTERED SIGNAL. 63

4.3. SMOOTHING OF FILTERED SIGNAL.. 63

4.4. DETERMINATION OF LOCAL GAS AND LIQUID SATURATION. 64

4.5. DETERMINATION OF LOCAL GAS AND LIQUID VELOCITIES. 66

5. VALIDATION OF TWO-TIP OPTICAL PROBE TECHNIQUE 70

5.1. VALIDATION WITH X-RAY DIGITAL INDUSTRIAL RADIOGRAPHY TECHNIUQE (DIR) MOHD SALLEH ET AL. (2014), MOHD SALLEH (2014). 70

5.2. VALIDATION WITH KNOWN LIQUID VELOCITY. 72

6. EXPERIMENTAL SETUP 74

7. RESULT OF LOCAL LIQUID AND GAS VELOCITY 75

8. RESULT OF LOCAL LIQUID AND GAS SATURATIONS 78

9. REMARKS 80

ACKNOWLEDGEMENT 81

REFERENCES 82

III. OVERALL DISTRIBUTION IDENTIFICATION AND EFFECT ON INLET DISTRIBUTOR ON THE PHASE HOLDUP IN A TRICKLE BED REACTOR USING GAMMA-RAY DENISTOMETRY (GRD)……..…85

ABSTRACT…….…….85

1. INTRODUCTION 86

2. EXPERIMENAL SETUP 91

3. METHOD OF ANALYSIS 94

3.1. EXPERIMENTAL DETERMINATION OF PHASE HOLDUPS……...95

4. RESULT AND DISCUSSION 97

4.1. PHASE HOLDUP WITH SINGLE INLET NEAR TO COLUMN WALL. 97

4.2. PHASE HOLDUP WITH SINGLE INLET IN THE CENTER …….. 99

4.3. PHASE HOLDUP WITH PROPER SHOWER INLET..... 103

5. REMARKS 107

ACKNOWLEDGMENT……..107

REFERENCES……109

SECTION

2. OVERALL CONCLUSION AND RECOMMENDATION 111

2.1. OVERALL CONCLUSION 111

2.2. FLOW REGIME IDENTIFICATION USING ON-LINE GAMMA RAY DENSITOMETER FOR TRICKLE BED REACTORS..... 111

2.3. NOVEL MEASUREMENT TECHNIQUE BASED ON OPTICAL PROBE TO MEASURE LOCAL FLOW DYNAMICS IN PACKED BED REACTORS..... 112

2.4. OVERALL DISTRIBUTION IDENTIFICATION AND EFFECT OF INLET DISTRIBUTOR ON THE PHASE HOLDUP IN A TRICKLE BED REACTOR USING GAMMA-RAY DENSITOMETRY (GRD). 113

2.5. RECOMMENDATIONS FOR FUTURE WORK 114

APPENDICES

A. PROCEDURE MAKING TWO-TIP OPTICAL FIBER PROBE...……115

B. MATLAB PROGRAM FOR TWO-TIP OPTICAL PROBE…….……..121

C. PROGRAM OF KOLMOGOROV ENTROPY CALCULATION……..127

VITA……....130

LIST OF ILLUSTRATIONS

Page

Figure 1.1. Schematic Diagram of a TBR..... 1

Figure 1.2. A Sample of Flow Regime Map (Taken from Sie & Krishna, 1998)..... 5

PAPER I

Figure 1. Typical Results of Pressure Fluctuation Time Series without any Data Analysis (Taken from Horowitz et al., 1997) 20

Figure 2. Trickle Bed Reactor Experimental Setup (A: Pressure drop probe, B: Shower Head C: Distributor, D: Mesh Support E: Inlet) 24

Figure 3. Scan Positions in Trickle Bed Reactor 25

Figure 4. Time Series Signals of the Photon Count Baseline of the Condition of the TBR Packed with the Particles without Flowing of Gas and Liquid..... 28

Figure 5. Time Series Signals of the Photon Counts at Ul = 0.01 m/s and Ug = 0.06 m/s at Z/D = 5 and r/R = 0. 29

Figure 6. Average Count (Mean) of GRD for TBR with Different Superficial Liquid Flow Rate at Z/D = 2 at Ug = 0.09 m/s at the middle scans of the TBR 32

Figure 7. Standard Deviation of GRD Counts for TBR with Different Superficial Liquid Flow Rate at Z/D = 2 at Ug = 0.09 m/s at the middle scans of the TBR. 32

Figure 8. Standard Deviation versus Different Superficial Liquid and Gas Velocities at Z/D = 5 and r/R = 0..... 33

Figure 9. Flow Regime Identification Using Pressure Drop Measurement with different Ug at Z/D = 5 and r/R =0. 33

Figure 10. a) PSD for U_l = 0.008 m/s (trickle regime) , (b) U_l = 0.010 m/s (trickle regime), (c) PSD for U_l = 0.010 m/s (pulse regime) and (d) PSD for U_l = 0.014 m/s (pulse regime) all plot with constant Ug = 0.09 m/s with axial at Z/D = 5 and r/R=0. 36

Figure 11. Results of Autocorrelation for Z/D =5 and r/R=0 with different Ul with constant Ug = 0.09 m/s 38

Figure 12. Superficial Liquid Velocity versus Kolmogorov Entropy at Different Ug, Z/D = 5 and r/R = 0. 40

PAPER II

Figure 1. Snell's Law 52

Figure 2. (a) Angle of Incidence is Less Than Critical Angle; Light bends toward interface without total internal reflection (b) Angle of Incidence Greater than Critical Angle; Total Internal Reflection Occurs. 52

Figure 3. Light Propagation inside the Optical Fiber Probe. 53

Figure 4. (a) Optical fiber probe tip made into conical shape (b) Refraction phenomena gas touches the probe tip (c) Reflection phenomena when liquid touches the probe tip. (Xue et al. (2003)) 54

Figure 5. Schematic of Optical Fiber Box (Kagumba & Al-Dahhan (2015)) 55

Figure 6. The step response of a bubble striking a single probe tip. 56

Figure 7. Orientation of Two-Tip Optical Probe 57

Figure 8. (a) Two-tip optical probe (b) Placement of two-tip optical probe at local locations inside packed bed 57

Figure 9. Raw Signal Obtained from Two-Tip Optical Probe 58

Figure 10. Schematic of Probe Response of Two-Tips Of Optical Probe 60

Figure 11. (a) Raw Time Series Data of The Frame Between 17.5 Sec And 20 Sec (B) Raw Time Series Data of The Frame Between 20 Sec And 22.5 Sec 62

Figure 12. (a) Filtered Time Series Data of the Frame Between 17.5 Sec And 20 Sec (b) Filtered Time Series Data of the Frame Between 20 Sec And 22.5 Sec 63

Figure 13. The histogram plot of raw signal;(a)For the upper probe (b) For the lower probe 65

Figure 14. Smoothed Signal of Filtered Data of Two-Tip Optical Probe; (a) For Time Frame 17.5 Sec To 20 (b) For Time Frame 20 Sec To 22.5 66

Figure 15. Detected bubbles and validation test: (1) accepted, (2) rejected, (3) rejected, and (4) rejected (Magaud et al. (2001),Aloui & Souhar (1996) 66

Figure 16. Selection Criteria for Local Gas Velocity Calculation in Two-Tip Optical Probe; Bubbles Similar to Green Circled are Accepted and Bubbles Similar to Black Circled are Rejected..... 68

Figure 17. Selection Criteria for Local Liquid Velocity Calculation in Two-Tip Optical Probe; Bubbles Similar to Green Circled are Accepted and Bubbles Similar to Black Circled are Rejected..... 69

Figure 18. The Two-inch TBR Setup with (a) Fiber Optic Probe and (b) Radiographic Image Port Located at each Z/D Mohd Salleh (2014)..... 71

Figure 19. Localized Position of Optical Probe and whole section scanned by DIR (Mohd Salleh (2014))..... 71

Figure 20. Syringe Pump with Two-Tip Optical Probe..... 73

Figure 21. Schematic Diagrams of Optical Probe Measurement Points with Axial and Radial Scan Locations..... 75

Figure 22. Number of Occurrences Liquid Velocities at Different Axial Locations and Varying Flow Conditions..... 76

Figure 23. Range of Liquid Velocities at Different Axial Locations and Varying Flow Conditions..... 77

Figure 24. Number of Occurrences Gas Velocities at Different Axial Locations and Varying Flow Conditions..... 79

Figure 25. Range of Gas Velocities at Different Axial Locations and Varying Flow Conditions..... 79

Figure 26. Liquid Saturation Values at Different Axial Location and Varying Liquid Flow Condition..... 80

Figure 27. Gas Saturation Values at Different Axial Location and Varying Liquid Flow Condition..... 80

PAPER III

Figure 1. Experimental setup..... 92

Figure 2. Single Inlet Near The Wall..... 93

Figure 3. Single Inlet/Distributor At The Center Of The Column..... 93

Figure 4. Proper Shower Inlet/Distributor..... 94

Figure 5. Liquid Distribution for Single Inlet Near the Wall Column..... 98

Figure 6. Liquid Holdup for Single Inlet Near The Wall in TBR Of 0.14m Internal Diameter (ID)..... 99

Figure 7. The Liquid Holdup for Different Gas Flow Rate With Constant Ul = 0.012 m/s Single Inlet Near the Wall at Axial Position Z/D = 5. 100

Figure 8. Liquid Distribution for Single Inlet Near The Center..... 100

Figure 9. Liquid Holdup for Single Inlet in The Center In TBR 0.14m (ID)..... 101

Figure 10. Gas Holdup for Single Inlet at The Center In TBR Of 0.14m Internal Diameter (ID)..... 101

Figure 11. Solid Holdup for Single Inlet in The Center In TBR Of 0.14m Internal Diameter (ID)..... 102

Figure 12. The Liquid Holdup for Different Gas Flow Rate with Constant Ul = 0.012 m/s Single Inlet In The Center At Axial Position Z/D = 5. 103

Figure 13. Liquid Holdup from GRD for TBR 0.14 m Internal Diameter (ID) at the Different Axial Position of Z/D 2, 5 and 7..... 104

Figure 14. Gas Holdup from GRD For TBR 0.14m Internal Diameter (ID) at Different Axial Position of Z/D 2, 5 And 7. 105

Figure 15. Solid Holdup from GRD For TBR 0.14m Internal Diameter (ID) at Different Axial Position Of Z/D 2, 5 And 7. 105

Figure 16. Liquid Holdup for TBR from Gamma Ray Computed Tomography (Taken from Kuzeljevic, 2010)..... 106

Figure 17. The Liquid Holdup for 0.14m TBR From GRD With Different Ug 106

LIST OF TABLES

Page

Table 1.1. Comparison between Laboratory, Pilot Plant Scale and Industrial Scale Reactor Parameters 2

Table 1.2. Advantages and Disadvantages of TBRs..... 3

PAPER I

Table 1. Summary some Studies on the Flow Regime with the Techniques Used……...18

PAPER II

Table 1. Comparison between Mean, Standard Deviation (σ), Variance (σ2), Degree of Freedom (df), t-Value, and p-Value (α level 0.05) Generated by Statistical Analysis Software (SAS) between the Measured ULL(OP) by Optical Probe (OP) And ULL(DIR) by X-Ray Digital Industrial Radiography (DIR) in a Two-inch TBR (Blue Dashed Circle). (Mohd Salleh (2014))……..72

Table 2. Comparison of Actual and Measured Liquid Velocity……73

PAPER III

Table 1. A selected summary of investigations of local maldistribution in TBRs. 90

NOMENCLATURE

Symbol	Description
U_g	Superficial Gas Velocity
U_l	Superficial Liquid Velocity
σ	Standard Deviation
U_{GG}	Measured Gas Velocity
U_{LL}	Measured Liquid Velocity
μ	Attenuation coefficient
μm	Micrometer
β_L	Liquid Retention
ρ	Density
t	Time
τ	Time lag
ψ	Wavelet
T	Transmission ratio
I_o	Incident radiation
I	Detected radiation
l	Length
$\varepsilon_{(G,L,S)}$	Holdups of gas or liquid or solid
$V_{G,L,S}$	Volume of gas or liquid or solid
$t_{(G,L,S)}$	Time average of gas or liquid or solid
R	Autocorrelation
C	Autocorrelation function
k	relative permeability
Re	Reynolds numbers
Ga	Galileo numbers
Fl	Flow number
Fr	Froude number

Abbreviations:

TTOFP	Two tip Optical Fiber Probe
CFD	Computer Fluid Dynamics
PTV	Particle Tracking Velocimetry
MRI	Magnetic Resonance Imaging
PIV	Particle Imaging Velocimetry
TBR	Trickle Bed Reactor
DAQ	Data Acquisition
DIR	Digital Imaging Radiography
ASPEN	Process simulation software for chemical engineering industry
LDV	Laser Doppler Velocimetry
LDA	Laser Doppler Anemometer
MATLAB	A type of scientific software for calculation and programming
WTMM	Wavelet transform modulus maxima
CWT	Continous wavelet transform
DWT	Discrete wavelet transform
G-L-S	Gas, Liquid or Solid Systems
PDD	Probability Density Distribution

1. INTRODUCTION

1.1 SCOPE

One of the major reactors in refineries and chemical plants is a trickle bed reactor (TBR). Billions of dollars have been spent to both build and maintain the quality performance of these reactors. A better understanding of the trickle beds reactor helps the industrial processes for better and efficient performance and energy saving operation.

TBRs are packed beds in which gas and liquid flow concurrently downward. The gas and liquid come into contact with fixed solid particles that act as catalysts. These catalyst particles are always porous and are typically spherical, cylindrical, lumps of irregularly shaped which are extrudes and granules between 1.0 mm and 3.2 mm in size (Al-Dahhan et al., 1997; Pushnov, 2006). Figure 1.1 is an illustration of a typical TBR.

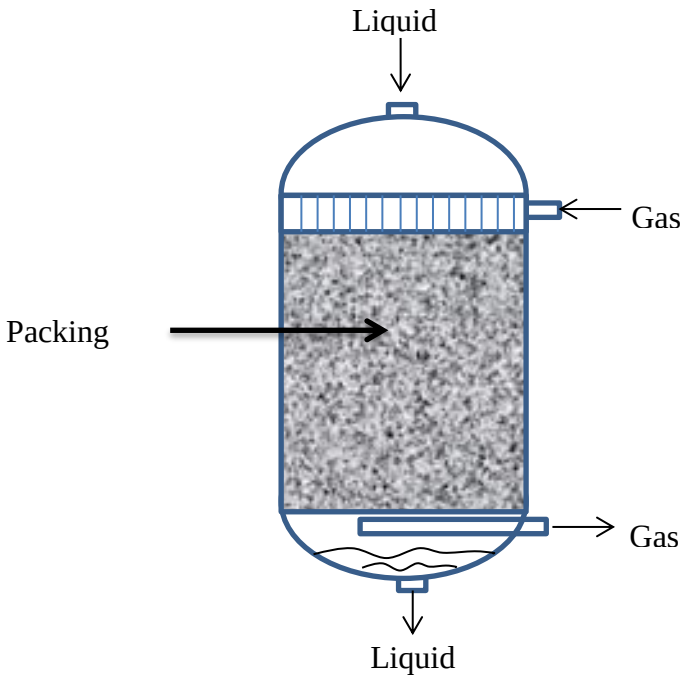

Figure 1.1. Schematic Diagram of a TBR

The comparison between typical laboratory, pilot plant, and industrial scale reactor parameters are shown in Table 1.1 (Adapted from Gunjal & Ranade, 2007).

Table 1.1. Comparison between Laboratory, Pilot Plant Scale and Industrial Scale Reactor Parameters

Reactor variables	**Laboratory**	**Pilot reactor**	**Industrial reactor**
Length, m	0.3-1.5	0.5 - 2.0	10 – 25
Diameter, m	0.12-0.5	0.5 – 2	1 - 4
Liquid superficial velocity, m/s	2.52e-04-1.01e-03	0.0008 – 0.0025	0.008 – 0.025
Gas superficial velocity, m/s	5.04e-04-6.05e-03	0.0148	0.148 – 22
Dispersion	Significant	Significant	Poor
Wetting	0.1-0.7	0.1 – 0.6	0.6 – 1
Maldistribution	Significant	Significant	Significant
Wall effect	Considerable	Considerable	Negligible

Trickle beds have been applied in petroleum refining, petrochemical, and chemical industries. The application process includes hydrogenation, desulphurization, oxidation, and hydrocracking. In addition, TBRs are used in the process of production of commodity and in the specialty chemicals (Al-Dahhan et al., 1997; Nigam et al., 2005; Huerta et al., 2014; Shen et al., 2014). TBRs are also used as organic filters in water treatment (Lopes et al., 2010; Lei et al., 2013; Kaplan et al., 2014) and biochemical processing (Dudukovic et al., 2002; Burkhardt & Busch, 2013).

Nevertheless, when gas and liquid phases are flowing concurrently downward through a packed bed of solid particles, the situation is more complex compared to that associated with a single-phase flow. Both the advantages and disadvantages of using TBRs are listed in Table 1.2. Although there are some disadvantages, TBRs are still one

of the main reactors in the refinery. The comparisons between three phase reactor types are discussed by many researchers (Matsunaga et al., 2009; Wenmakers et al., 2010; Haase et al., 2013)

Table 1.2. Advantages and Disadvantages of TBRs

Advantages	Disadvantages
The catalyst, or packing, is static.	Operations are limited to a non-viscous fluid.
The liquid flow closes to the plug flow.	The laboratory-to-industrial scaling up process is difficult.
They require low operating costs and investments.	They have a low reaction rate due to a large catalyst size.
The operations of TBRs are more flexible in terms of process.	They are not only sensitive to thermal effects, but also inefficient at heat removal.
They are operable at higher temperatures and pressures.	They are usually facing the problem of incomplete of catalyst wetting and channeling.
Low liquid-solid volume ratio: fewer occurrences of homogeneous side reactions.	Long term catalyst stability and high crushing strength are required.
Longer reactor sizes.	The risk of increasing pressure drop or obstructing catalyst pores when side reactions lead to fouling products.

The studies reported in the literature for TBRs investigation are broad. Many review and technical papers discussed various parameters such as pressure drop, holdup, bed properties, heat and mass transfer, dispersion of mass and heat, kinetics, conversion, macroscale/microscale phenomena and inlet distributor designs (Sundaresan, 2013; Mederos et al., 2009). Recently, a number of studies have been conducted on pressure drop (Giri & Majumder, 2014), bed properties (Janecki et al., 2014), mass transfer (Nicol

& Joubert, 2013), conversion (Bistan et al., 2012) and kinetics (Boahene et al., 2013). Furthermore, many studies on hydrodynamics of TBRs (i.e., flow distribution, liquid and gas holdup, pressure drop, liquid velocities and gas velocities) were performed in the literature (Van der Merwe et al., 2007; Boyer & Fanget, 2002; Al-Dahhan et al., 1997; Schubert et al., 2008; Sederman & Gladden, 2005; Sundaresan 2013; Honda et al., 2014; Janecki et al., 2014). Hydrodynamics of TBRs affect heat and mass transfer and as a result, it can influence reactor performance (Sundaresan, 2013). In general, as with any other packed-bed type reactor, these studies require various measurement techniques to probe and visualize the phenomena occurring inside the reactor (Salleh, 2014). However, in the literature, there are still lacking techniques related to the measurements of local liquid and gas velocities, flow regime identification, phase holdups distribution, liquid flow distribution and identification of maldistribution. Therefore, the focus of this research is to address such shortcomings, to develop techniques and perform investigations related to local liquid and gas velocities, flow regime identification, phase holdups and liquid distribution and identification of maldistribution.

The four types of flow regimes were observed in TBRs which are trickle flow regime, pulse flow regime, spray flow regime, and bubbly flow regime. The prediction of the flow conditions at different flow regime transitions occur is of a great importance for the reaction, design and scale-up purposes. The liquid and gas flow rate are primary factor in determining the flow regimes. Additional factors include the inlet distributor, the reactor's dimensions, the particle's size and the shape of the packing, methods used, and the thermo-physical properties of the gas and liquid phases (Ranade et al, 2011).

The trickle flow regime occurs at low gas and liquid flow rates. The gas-liquid interaction is small and liquid flows in the forms of either films or rivulets over the packed particles. Meanwhile, pulse flow regimes are observed at moderate flow rates of gas and liquid. Two other additional flow regimes (spray and bubbly) may occur at higher gas and liquid flow rates. These flow regimes are less commonly used in practical industries. Figure 1.2 illustrates a sample diagram of the flow regimes map of TBRs.

Interestingly, most industrial processes utilize a trickle flow, particularly hydrogenation. Still other utilizes a pulsing flow (hydrotreating process) due to the energetic interactions between the phases (Al-Naimi et al., 2011). Others are often operated close to a flow transition boundary (between the trickle and the pulse flow regimes). The transition regime condition improves the mass transfer rate, the catalyst utilization, and the production capacity (Ranade et al., 2011).

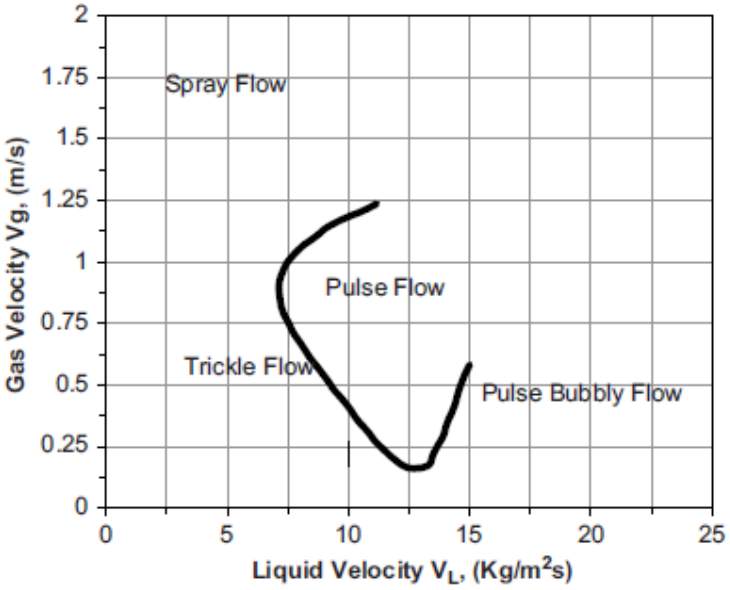

Figure 1.2. A Sample of Flow Regime Map (Taken from Sie & Krishna, 1998)

1.2 MOTIVATION

Some of the trickle bed reactor (TBR) hydrodynamic parameters can be categorized as pressure drop, phase holdup, phase velocities, flow regime, and others. The local parameter such as liquid and gas velocities, and local liquid holdup behavior in TBRs are very complex. Boyer & Fanget., 2002, has presented two groups of techniques to measure hydrodynamic parameters. The non-intrusive techniques delivers global parameters, cross-section-averaged and/or local data, meanwhile intrusive probes are dedicated to local measurements. Intrusive technique is when the probes are inside the reactor whereas non-intrusive technique is when the probes are totally outside and do not disturb or interfere with the process. Example of intrusive techniques is wire mesh sensor (WMS) or any conductance based techniques where the probes are inside the reactor. Meanwhile, the example of non-intrusive techniques are mostly radiation based (Gamma-ray Densitometry, Gamma-ray Computed tomography, X-ray Tomography, and Nuclear Magnetic Resonance Imaging). Magnetic-field gradient techniques is an example of non-intrusive technique which is not radiation based.

The wire mesh sensor (WMS) is used not only to study liquid saturation (fraction of the liquid volume in the void volume of the bed) and its distribution, but also local liquid velocity distribution (Schubert, 2010). The finding of WMS is be useful for better understanding of the liquid distribution inside the reactor. However, one of the disadvantages of the WMS is that it could affect the flow. This is because WMS has to be inserted in the middle of the packed bed in the reactor. The flow of the liquid will be obstructed by the wire mesh. The intrusive effect on gas-liquid flow has been studied by

Wangjiraniran et al., (2003). They found that the accuracy of the measurement is affected by the WMS.

Several studies using non-intrusive (optical and radiation based) techniques were performed to measure the local liquid velocity in packed bed type reactors such as, for example, fluid velocity by Laser Doppler Velocimetry (LDV), (Johnston et al., 1975; Dancey et al., 2000) and Particle Image Velocimetry (PIV), (Lee & Lee, 2009; Patil & Liburdy, 2013). Particle tracking velocimetry (PTV) also has been used to measure the velocity field and the velocity distribution (Moroni & Cushman, 2001). Unfortunately, none of these techniques LDV, PIV and PTV applied in TBRs. Furthermore, LDV provides only a point velocity measurement. Meanwhile PIV suffered from background noise, producing poor quality data. However, recently combination techniques of Digital Imaging Radiography (DIR) and Particle Tracking Velocimetry (PTV) have been used by Salleh, 2014, to obtain the local liquid velocity in a vertical 2D panel of small diameter (4.5 cm) TBR. Unfortunately, the DIR & PTV techniques can only be used for the limited size of the column.

The nuclear magnetic resonance imaging (MRI) is the most reliable technique to determine the liquid distribution and local liquid velocity. Unfortunately, the previous work on TBRs usually applied to small columns (less than 5.08 cm) and the techniques are expensive for regular use and cumbersome (Boyer & Fanget, 2002). Furthermore, the technique is not suitable for an industrial practice by many researchers (Schubert, et al., 2010).

The determination of flow regimes is incredibly important because other hydrodynamic parameters, especially the mass transfer rates, are affected by different

hydrodynamics in each regime (Urseanu, et al., 2005). Previous studies investigated by a single-phase pressure transmitter to measure pressure fluctuations time series in the middle of the bed (Horowitz, et al., 1997). Al-Naimi, et al., 2011 used two-phase pressure drop data in the bed to identify the flow regime. The data from the pressure measurement were analysed with calculating standard deviation, Fourier power spectrum and Hurst exponent to determine flow regimes. Unfortunately, the determination flow regime by pressure can only be determined at the wall of the reactor. The data did not represent the whole reactors. It could be suitable for small diameter reactors and is applicable to small diameter reactors.

Conductimetric probes are used to identify the flow regime transition in the TBR (Muzen & Cassanello, 2007). It is an intrusive techniques that capable to identify the flow regime by analyzing the conductivity data from the probes. However, the probes are not applicable industrial practice whereas, the probes are affected by the flow distribution, and special liquid need to be used to detect different conductivity.

Earlier studies on liquid flow maldistribution have been done by using tracer techniques (Hanratty & Dudukovic, 1992). It is a successful technique in order to identify the flow maldistribution. However, a special type of tracers should be used. Conductance technique has been applied by Tsochatzidis et al., 2002 to investigate the liquid maldistribution. A different type of distributor such as a uniform, half-blocked and a quarter-blocked have been used to study the flow maldistribution. The conductance techniques are able to detect the maldistribution. Unfortunately, this technique needs a special conductivity liquid and the accuracy also depend on the size of the probe per size of the reactor.

As a result, a new method that is comparable to the established technique should be considered. The point and intrusive technique that combines with non-invasive technique is more appropriate for better understanding of the hydrodynamics of TBRs.

1.3 RESEARCH OBJECTIVES

The overall objectives of this work are to develop a new, point measurement that uses optical fiber probes to measure the local liquid and gas velocity, holdup and their time series. In addition, a non-invasive technique which is Gamma-Ray Densitometry (GRD) will be implemented to measure flow regime identification as well as other hydrodynamic parameters. The detailed objectives can be grouped as follows:

1. Developing a new Two Tip Optical Fiber Probe (TTOFP) for hydrodynamics measurement of local velocities, holdups and their time series at various radial, and axial locations. This includes angular. Validating the results of TTOFP with those obtained by Gamma Ray Densitometry (GRD), Digital Imaging Radiography (DIR) for 2D plane and a known velocity experiment for TTOFP.
2. Investigating the effect of superficial liquid and gas velocities on the local liquid and gas velocities and holdups in radial and axial positions.
3. Implementing a non-invasive measurement technique based on Gamma Ray Densitometry (GRD). Which can be used in pilot plant and industrial scales and/or using industrial operating conditions. This includes:
    - Implementing GRD to investigate the flow regime identification using different superficial liquid and gas velocities radially and axially.

- Implementing GRD to investigate the radial profiles of the line averaged phase holdups with different liquid and gas flow rates.
- Implementing GRD on identifying gross maldistribution with different types of inlet distributors along the bed height.

1.4 DISSERTATION ORGANIZATION

This dissertation structured in the following manner.

- Section 1 presents the introduction which consists of the scope, motivation, and objectives and thesis structure.
- Paper I which is related to flow regime identification using on-line gamma ray densitometer for trickle bed reactors.
- Paper II which is related to novel measurement technique based on optical probe to measure local flow dynamics in packed bed reactors.
- Paper III which is related to overall distribution identification and effect of inlet distributor on the phase holdup in a trickle bed reactor using gamma ray densitometry (GRD).
- Section 2 summarizes the conclusions drawn from the entire study. Recommendations for future work on the hydrodynamic study of TBRs are also discussed.

REFERENCES

Al-Dahhan, M. H., Larachi, F., Dudukovic, M. P., & Laurent, A. (1997). High-Pressure Trickle-Bed Reactors: A Review. *Industrial and Engineering Chemistry Research, 36*(8), 3292-3314.

Al-Naimi, S. A., Al-Sudani, F. T. J., & Halabia, E. K. (2011). Hydrodynamics and flow regime transition study of trickle bed reactor at elevated temperature and pressure. *Chemical Engineering Research and Design, 89*(7), 930-939.

Bistan, M., Tišler, T., & Pintar, A. (2012). Conversion and estrogenicity of 17β-estradiol during photolytic/photocatalytic oxidation and catalytic wet-air oxidation. *Acta Chimica Slovenica, 59*(2), 389-397.

Boahene, P. E., Soni, K. K., Dalai, A. K., & Adjaye, J. (2013). Hydroprocessing of heavy gas oils using FeW/SBA-15 catalysts: Experimentals, optimization of metals loading, and kinetics study. *Catalysis Today, 207*, 101-111.

Boyer, C., & Fanget, B. (2002). Measurement of liquid flow distribution in trickle bed reactor of large diameter with a new gamma-ray tomographic system. *Chemical Engineering Science, 57*(7), 1079-1089.

Burkhardt, M., & Busch, G. (2013). Methanation of Hydrogen and Carbon Dioxide. *Applied Energy, 111*, 74-79.

Dancey, C. L., Balakrishnan, M., Diplas, P., & Papanicolaou, A. N. (2000). The spatial inhomogeneity of turbulence above a fully rough, packed bed in open channel flow. *Experiments in Fluids, 29*(4), 402-410.

Duduković, M. P., Larachi, F., & Mills, P. L. (2002). Multiphase catalytic reactors: A perspective on current knowledge and future trends. *Catalysis Reviews - Science and Engineering, 44*(1), 123-246.

Giri, A. K., & Majumder, S. K. (2014). Pressure drop and its reduction of gas-non-newtonian liquid flow in downflow trickle bed reactor (DTBR). *Chemical Engineering Research and Design, 92*(1), 34-42.

Gunjal, P. R., & Ranade, V. V. (2007). Modeling of laboratory and commercial scale hydro-processing reactors using CFD. *Chemical Engineering Science, 62*(18-20), 5512-5526.

Haase, S., Weiss, M., Langsch, R., Bauer, T., & Lange, R. (2013). Hydrodynamics and mass transfer in three-phase composite minichannel fixed-bed reactors. *Chemical Engineering Science, 94*, 224-236.

Hanratty, P. J., & Duduković, M. P. (1992). Detection of flow maldistribution in trickle-bed reactors via tracers. *Chemical Engineering Science, 47*(12), 3003-3014.

Honda, G. S., Gase, P., Hickman, D. A., & Varma, A. (2014). Hydrodynamics of trickle bed reactors with catalyst support particle size distributions. *Industrial and Engineering Chemistry Research, 53*(22), 9027-9034.

Horowitz, G. I., Cukierman, A. L., & Cassanello, M. C. (1997). Flow regime transition in trickle beds packed with particles of different wetting characteristics - check-up on new tools. *Chemical Engineering Science, 52*(21-22), 3747-3755.

Huerta, I., Biasi, P., García-Serna, J., Cocero, M. J., Mikkola, J. -., & Salmi, T. (2014). Effect of low hydrogen to palladium molar ratios in the direct synthesis of H2O2 in water in a trickle bed reactor. *Catalysis Today.* Available online 28 May 2014.

Janecki, D., Burghardt, A., & Bartelmus, G. (2014). Influence of the porosity profile and sets of ergun constants on the main hydrodynamic parameters in the trickle-bed reactors. *Chemical Engineering Journal, 237*, 176-188.

Johnston, W., Dybbs, A., & Edwards, R. (1975). Measurement of fluid velocity inside porous media with a laser anemometer. *Physics of Fluids, 18*(7), 913-914.

Kaplan, R., Erjavec, B., Senila, M., & Pintar, A. (2014). Catalytic wet air oxidation of bisphenol A solution in a batch-recycle trickle-bed reactor over titanate nanotube-based catalysts. *Environmental Science and Pollution Research.* Article in Press. Available online 28 May 2014.

Lee, J. -., & Lee, S. -. (2009). Flow visualization in the scaled-up pebble bed of high temperature gas-cooled reactor using particle image velocimetry method. *Journal of Engineering for Gas Turbines and Power, 131*(6)

Lei, Y., Liu, H., Shen, Z., & Wang, W. (2013). Development of a trickle bed reactor of electro-fenton process for wastewater treatment. *Journal of Hazardous Materials, 261*, 570-576.

Lopes, R. J. G., & Quinta-Ferreira, R. M. (2010). Numerical studies of catalyst wetting and total organic carbon reaction on environmentally based trickle-bed reactors. *Industrial and Engineering Chemistry Research, 49*(21), 10730-10743.

Matsunaga, Y., Yamada, H., & Tagawa, T. (2009). Comparison between upflow reactor and trickle-bed reactor in gas-liquid-liquid-solid four-phase reaction. *Journal of Chemical Engineering of Japan, 42*(SUPPL. 1), 125-129.

Mederos, F., Ancheyta, J., & Chen, J. (2009). Review on criteria to ensure ideal behaviors in trickle-bed reactors. Applied Catalysis A: General, 355, 1.

Moroni, M., & Cushman, J. H. (2001). Three-dimensional particle tracking velocimetry studies of the transition from pore dispersion to fickian dispersion for homogeneous porous media. *Water Resources Research, 37*(4), 873-884.

Muzen, A., & Cassanello, M. C. (2007). Flow regime transition in a trickle bed with structured packing examined with conductimetric probes. *Chemical Engineering Science, 62*(5), 1494-1503.

Nicol, W., & Joubert, R. (2013). Liquid-solid mass transfer distributions in trickle bed reactors. *Chemical Engineering Journal, 230*, 361-366.

Nigam, K. D. P., Saroha, A. K., Kundu, A., & Pant, H. J. (2001). Radioisotope tracer study in trickle bed reactors. *Canadian Journal of Chemical Engineering, 79*(6), 860-865.

Patil, V. A., & Liburdy, J. A. (2013). Flow structures and their contribution to turbulent dispersion in a randomly packed porous bed based on particle image velocimetry measurements. *Physics of Fluids, 25*(11).

Pushnov, A. S. (2006). Calculation of average bed porosity. *Chemical agnd Petroleum Engineering, 42*(1-2), 14-17.

Ranade, V. V., Chaudhari R. V., and Gunjal, P. R. (2011). Trickle Bed Reactors, Elsevier, Amsterdam, Pages 25-75.

Salleh, K. A. M., (2014). "Local liquid velocity measurement of trickle bed reactor using digitial industrial X-ray radiography", Doctoral Dissertations, Missouri University of Science and Technology, Rolla, Missouri, USA.

Schubert, M., Hessel, G., Zippe, C., Lange, R., & Hampel, U. (2008). Liquid flow texture analysis in trickle bed reactors using high-resolution gamma ray tomography. *Chemical Engineering Journal, 140*(1-3), 332-340.

Schubert, M., Khetan, A., da Silva, M. J., & Kryk, H. (2010). Spatially resolved inline measurement of liquid velocity in trickle bed reactors. *Chemical Engineering Journal, 158*(3), 623-632.

Sederman, A. J., & Gladden, L. F. (2005). Transition for pulsing flow in trickle-bed reactors studied using MRI. *AIChE Journal, 51*(2), 615-621.

Sie S.T., Krishna R., Process development and scale up: III. Scale up and scale down of trickle bed process, Rev. Chem. Eng. 149(3), 203-252, 1998.

Shen, Y., Maamor, A., Abu-Dharieh, J., Thompson, J. M., Kalirai, B., Stitt, E. H., & Rooney, D. W. (2014). Moving from batch to continuous operation for the liquid phase dehydrogenation of tetrahydrocarbazole. *Organic Process Research and Development, 18*(3), 392-401.

Sundaresan, S. (2013). Role of hydrodynamics on chemical reactor performance. *Current Opinion in Chemical Engineering, 2*(3), 325-330.

Tsochatzidis, N. A., Karabelas, A. J., Giakoumakis, D., & Huff, G. A. (2002). An investigation of liquid maldistribution in trickle beds. *Chemical Engineering Science, 57*(17), 3543-3555.

Urseanu, M. I., Boelhouwer, J. G., Bosman, H. J. M., Schroijen, J. C., & Kwant, G. (2005). Estimation of trickle-to-pulse flow regime transition and pressure drop in high-pressure trickle bed reactors with organic liquids. *Chemical Engineering Journal, 111*(1), 5-11.

Van der Merwe, W., Nicol, W., & de Beer, F. (2007). Three-dimensional analysis of trickle flow hydrodynamics: Computed tomography image acquisition and processing. *Chemical Engineering Science, 62*(24), 7233-7244.

Wangjiraniran, W., Motegi, Y., Richter, S., Kikura, H., Aritomi, M., & Yamamoto, K. (2003). Intrusive effect of wire mesh tomography on gas-liquid flow measurement. *Journal of Nuclear Science and Technology, 40*(11), 932-940.

Wenmakers, P. W. A. M., Van Der Schaaf, J., Kuster, B. F. M., & Schouten, J. C. (2010). Comparative modeling study on the performance of solid foam as a structured catalyst support in multiphase reactors. *Industrial and Engineering Chemistry Research, 49*(11), 5353-5366.

PAPER

I. FLOW REGIME IDENTIFICATION USING ON-LINE GAMMA-RAY DENSITOMETRY FOR TRICKLE BED REACTORS (TBRs)

Mohd Fitri Abdul Rahman, Vineet Alexander and Muthanna H. Al Dahhan

Department of Chemical and Biochemical Engineering, Missouri University of Science and Technology, 110 Bertelsmeyer Hall, 1101 N. State Street, Rolla, MO 65409, USA

ABSTRACT

Flow regime identification of Trickle Bed Reactor (TBR) is one of the critical parameters to identify the good distribution of liquid and gas. Many techniques have been developed by previous researchers to measure this parameter. Unfortunately, most of the techniques require probes intervention in the reactor which affects the flow distributions of gas and liquid. Gamma-ray densitometry is a non-invasive technique which can be used for laboratory, pilot plant and industrial scales reactors. This work measures the flow regime identification by Gamma-ray Densitometry measurement techniques. The experiment was performed on 0.14 m diameter reactor made of Plexiglas filled with 3 mm glass bead which acts as the solid. Water is the liquid phase while the air is in the gas phase. The superficial velocities for both gas and liquid were in the range 0.03 m/s to 0.27 m/s and 0.004 m/s to 0.014 m/s respectively.

Keywords Trickle bed reactor; Gamma-ray Densitometry; Flow Regimes Identification

1. INTRODUCTION

Trickle bed reactors (TBRs) are widely used in petroleum, petrochemical and chemical industry, wastewater treatment and biochemical processing (Ranade et al., 2011). TBRs is a packed bed in which gas and liquid reactants flow concurrently downward. When gas and liquid flow over the fixed bed, complex interactions between the flowing gas and liquid and stationary particles are encountered in TBRs, lead to different regimes. Flow regime represents the flow pattern of liquid and gas which depends on gas and liquid flow rates, physical properties and bed characteristics (Al-Naimi et al., 2011; Al-Dahhan et al., 1997). Various flow regimes exist in trickle bed reactors such as trickling, pulse, spray and bubbling regimes (Ng, 1986; Al-Dahhan et al., 1997; Attou et al., 1999, Ranade et al., 2011).

The trickle flow regime occurs at low gas and liquid flow rates. An increase in the liquid and gas mass flow rates leads to pulsing flow regime. In industries, TBRs are usually operated in a trickle, transition, and pulse flow regime (Satterfield, 1975; Saroha & Nigam, 1996; Attou & Ferschneider, 1999; Al-Naimi et al., 2011; Al-Dahhan et al., 1998), and it is based on the literature reported correlations and data which have uncertainty due to the different conditions used in the lab as compared to those in industrial applications.

Liquid distribution, pressure drop, liquid holdup, catalyst contacting, catalyst utilization heat and mass transfer and other hydrodynamic parameters vary with flow regime type since the phases interaction and flow structure change with the flow regime (Latifi et al., 1992; Al-Dahhan et al., 1998). Therefore, it is important to define which flow regime the reactor is operating at for a given set of conditions and the desired

reaction and kinetics. Several techniques have been developed and implemented to improve the measurement of flow regimes and their transition. Hence, studies in the literature have been conducted on identifying flow regimes using laboratory scales reactors where the facilitations are not related to industrial processes. Most of the studies used visual observations to monitor the flow regimes (Ranade et al., 2011). Also measuring time series pressure drop or pressure signals at the wall and statistically analyzing them regarding mean, variance, and standard deviation have been used in the literature (Horowitz et. Al, 1997; Urseanu et al., 2004 and Al-Naimi et al., 2011). Table 1.1 summarize some studies on flow regime identification with the techniques used.

An extensive study has been done on pressure drop in TBRs. Pressure drop is one of the critical parameters on hydrodynamics. The pressure drop represents the energy dissipated to offset the resistance to fluid motion through the reactor bed. It is important in determining energy losses, the sizing of the compression and pumping devices, and very often, in assessing the liquid holdup, the external wetting efficiency, the interfacial mass transfer coefficients level, among other aspects (Wammes et al., 1991; Larachi et al., 1991, 2000; Al-Dahhan & Dudukovic, 1994; Latifi et al., 1999; Narasimhan et al., 2002; Cai & Resetarits, 2011).

Horowitz et al., 1997 has developed a method for identification of flow regime from pressure fluctuation time series. Setra C206 pressure transmitter, located 40 cm above the column bottom is used to measure the pressure fluctuation. The measurement time was10s with a sampling rate of 100 Hz.

Table 1. Summary some Studies on the Flow Regime with the Techniques Used.

Author	Reactor Conditions	Techniques used	Indicator used and comments
Al-Naimi et al., 2011	Stainless steel TBR. 0.05 m ID Total Length 1.25m. Alumina Sphere, 0.00016m diameter. Air-water and air-acetone systems.	Conductance and Pressure Drop Measurement	A sudden transient in the standard deviation of pressure drop signals value was observed for the transition from a trickle to pulse regime. Lopes & Quinta-Ferreira, 2010 reported conductance technique did not give sharp boundary at which the transition observed. Compared with correlation
Munteanu & Larachi, 2009	Transparent TBR. 1.6 cm ID Total Length 28 cm. Glass bead, 1 mm diameter Air-water and phenylacetylene-kerosene/hydrogen systems.	Magnetic emulation of micro and macrogravity	Magnetic fields were found to displace the transition boundary from a trickle to pulse flow. Proposed a correlation for the bubble flow to pulse transition based on the gas-to-liquid Reynolds number ratio. Unfortunately, their technique applied on a small scale reactor.
Horowitz et al., 1997	Acrylic Column, 7.1 cm ID, 135cm long and packed with alumina spheres (2-5mm diameter) Gas-Liquid-Solid system Liquid: Water and Foaming solution Gas: Air	Visual inspection Pressure Measurement.	Standard deviation, Fourier power spectrum, Hurst exponent and correlation dimension of the attractor describing the system dynamics. The transition regime observed by a sharp increase of standard deviation plot of pressure measurement data. Correlation dimension increases with an increase in liquid flow rate.

Table 1. Summary some Studies on the Flow Regime with the Techniques Used. (Continued).

			No clear indication of using correlation dimension due to limited error on low signal/noise ratio. No correlation comparison
Urseanu et al., 2004	Steel Column, 0.051m diameter and 1.2 m height. Cumene-Hydrogen System.	Pressure Measurement Acoustic Signal Measurement	Pulses regime indicated by broad peaks in the signals of acoustic measurement. The simple correlation was developed and compared with Trickle Bed Simulator of University Laval.
Muzen and Cassanello, 2007	Square acrylic column (4cm x 4cm) Structure packed of plastic sheets. Gas-Liquid-Solid system. Air and Pottasium Chloride (Liquid).	Conductimeter	Standard Deviation and Kolmogorov Entropy (KE). KE significantly decrease for intermediate liquid velocities and increase again for larger liquid velocities. No correlation comparison.
Latifi et al., 1992	Trickle bed 5cm ID 5 mm glass bed Gas-Liquid-Solid System Gas: Nitrogen Liquid: Electrolyte Solution	Microelectrode	Compared with literature in the form of the variation of $(L/G)\lambda\psi$ as a function of G/λ. The agreement is quite satisfactory.Compared visually observed and microelectrode technique.Detailed pulse regime distribution was not reported. (Lopes & Quinta-Ferreira, 2010)
Anadon et al., 2008	Cylindrical Column 70cm length and ID 43 mm. Packed with γ-Al2O3 packing 3mm diameter. Air-Water system.	MRI	MRI compared with pressure drop and conductance measurement. The transition regime indicated by isolated local pulsing events on the MRI images.No correlation.

The raw data of time series have been plotted and quickly determined the trickle, transition and pulse regime without any data analysis from the signals (Figure 1). However, further analysis also has been conducted by the authors with standard deviation plot, power spectrum, and correlation dimension calculation.

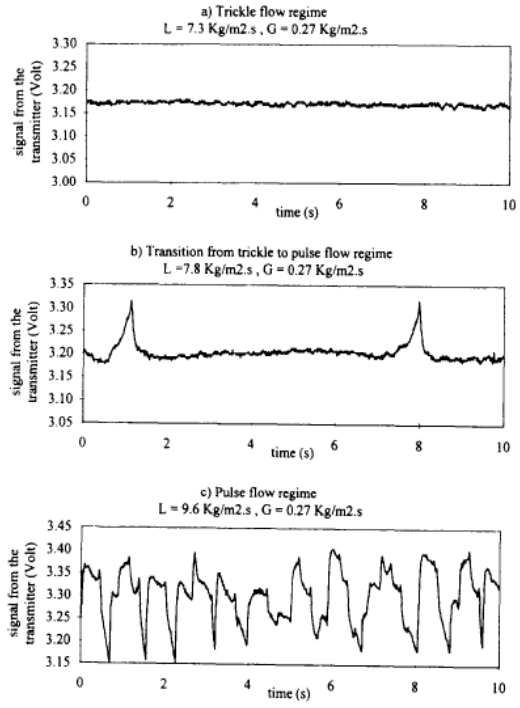

Figure 1. Typical Results of Pressure Fluctuation Time Series without any Data Analysis (Taken from Horowitz et al., 1997)

Correlation dimension is a parameter that describes the dynamics of the systems after all transients die out by introducing an attractor. An attractor is a zero-volume set in phase system to which a dissipative system converges as time tends to infinity. To calculate the correlation dimension, a method suggested by (Grassberger and Procaccia1983) was applied. The procedure involves correlation dimension is evaluated from the scaling region in a logarithmic plot of the correlation integral vs. the size of a sphere in the embedding space (Grassberger and Procacia, 1983). The author concluded

correlation dimension increases as an increase in the liquid flow rate but gave no clear-cut criterion for identifying flow regime.

Furthermore, the finding of Horowitz et al., 1997 was repeated by Urseanu et al., 2004 which measured the two-phase pressure drop for flow regime identification for high-pressure TBR (0.051 m reactor diameter and packing with 3 mm glass bead). They have also plotted standard deviation versus superficial liquid velocity (U_l) which showed a characteristic shape, increased proportionally with U_l.

The regime transition was approximately determined using the inflection point from each standard deviation curve, and they have also backed-up the finding by a parallel set of experiments using acoustic signal measurements. Acoustic signals were recorded using Ultra probe 2000, with a frequency of 1000 Hz. From the data, the standard deviation was calculated and plotted. The experiment was done with one operating pressure 0.2MPa and U_g = 0.2 m/s. They found a similar trend between the standard deviation from pressure drop and acoustic signal data.

Unfortunately, the measurement of pressure drop was obtained only at the wall of the reactor. The measurement could be reliable only for small TBRs, but it will not represent the bigger size of the reactor. Many researchers have identified the flow regimes by the sudden change from the standard deviation plotted over the U_l (Horowitz et al., 1997; Urseanu et al., 2005; Muzen & Cassanello, 2007; and Al-Naimi et al., 2011). Unfortunately, the finding was only a rough estimation of the time series analysis. Further analysis on time series is needed. Also, comparison with other techniques needs to be performed to better understanding the differential pressure drop and other hydrodynamics properties.

Tjugum et al., (2002) demonstrated the use of multibeam gamma-ray densitometry for flow regime identification in the pipe (76.2 mm inner diameter). They plotted average intensity distribution and compared with the theoretical calculation of Gas Volume Fraction (GVF). The expression formula of GVF is given by transmitted intensity, water cut, and calibration of pipes with gas, oil, and water. However, they assumed oil/water/gas mixture is homogeneous. They have successfully identified several flow regimes occur in the pipe with different liquid and gas flow rates. Unfortunately, limited reference on gamma-ray densitometry conducted on the packed bed with air-water-solid systems.

Usually, the industrial scale TBRs are large in diameters (2-6m diameter) and operated at high pressures and temperature. Hence, monitoring the flow regimes is the most cumbersome. Therefore, there is a need to develop techniques involving non-invasive approaches that can be applied in the laboratory, pilot plant and industrial reactors. There is also need to develop a technique for flow regime diagnosis that is non-invasive, which are implemented on industrial scale columns without upsetting the operation, and that provides reliable information.

One of the techniques of non-invasive is Gamma Ray Densitometry (GRD). GRD is used extensively in industry for applications such as level control, density measurement, and weight measurements in conveyors (Charlton 1984; Johansen & Jackson 2004; Zain et al. 2008). GRD can also be permanent installed permanently on the respective unit operation or portable. Zain et al. (2008), used a portable gamma-ray densitometry to inspect column for any malfunction regarding mechanical or process in industries. Many companies used GRD as one of the Non-Destructive Testing (NDT)

technique for diagnostic inspection of column or pipe for example Tower Scan company (www.towerscan.com), Plant Assessment Technology Group, Nuclear Malaysia and Tracerco Company (www.tracerco.com).

Accordingly, in this work, gamma-ray densitometry (GRD) based technique has been developed, validated and implemented as a non-invasive technique capable of identifying the flow regimes and their transition in the operated lab, pilot plant and industrial scales trickle bed reactors.

2. EXPERIMENTAL WORK

2.1. TRICKLE BED REACTOR EXPERIMENTAL SETUP

Figure 2 shows the experimental setup which consisting of 0.14 m diameter and 2.13 m height Plexiglas column packed with 3 mm diameter glass beads. The height of the packing bed is 1.83 m. The top section of the column has a shower head for the liquid phase of 0.013 m diameter and two gas inlet for the gas phase of 0.0064 m diameter. The shower head inlet consists of 22 holes of 0.003 m (1/8 inches). Meanwhile, the distributor has two sizes of holes of 0.009 m (3/8 inches) diameter and 0.003 m (1/8 inches) respectively. The twos size of the distributor to get a better initial distribution of gas and liquid.

Deionized water with a temperature of about 70^{o}F was used as the liquid phase, and the inlet pressure was maintained at 20 psi. Dry air supplied by high pressure and the high capacity compressor was used as the gas phase. The water is circulated to the column through flow downward and their water collecting tank (The water motor pump used model 503186, 3E-12NT from Little Giant Pump Company, Oklahoma, USA, with

maximum flow rate 500GPH). Valves controlled both liquid and gas flow rates and measured by two types of Rotameters (Dwyer Instruments, USA, Model RMC-102-SSV and RMC-106-SSV flowmeter range 10-100 SCFH air and 100-1000 SCFH air for the gas flow meter and liquid flowmeter model FL-75E from Omega flow rate range 1.5-15GPM).

The superficial liquid flow rates used were in the range of 0.004 – 0.016 m/s and the superficial gas flow rates were in the range 0.03 – 0.27 m/s covering flow regime through pulsing flow regime.

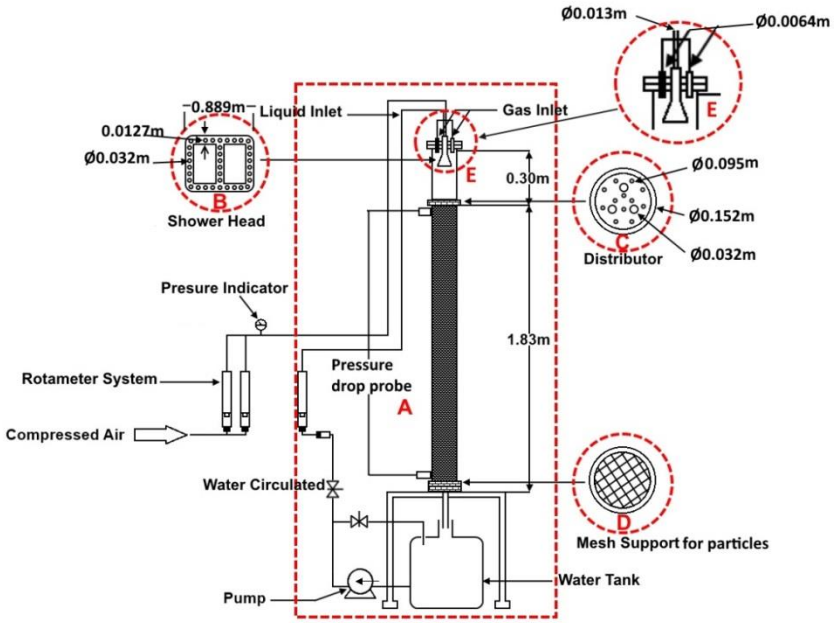

Figure 2. Trickle Bed Reactor Experimental Setup (A: Pressure drop probe, B: Shower Head C: Distributor, D: Mesh Support E: Inlet)

As mentioned earlier the trickle bed reactor was mounted inside the structure of the GRD technique to perform measurement at various height and radial location as

illustrated in Figure3. A pressure drop transducers (Omega Pressure Transducer PX409 015DWUV) also installed and used to measure the change in pressure between the bed.

2.2 GAMMA RAY DENSITOMETRY (GRD) TECHNIQUE

The newly developed GRD technique consist of a radioactive collimated sealed source of Cs-137 of initial activity 250 mCi on Jun 12, 2012, and a 0.0508 m collimated detector which mounted on the opposite side on the flexible structure. The structure of GRD allows the source/detector to move and to be rotated at various angles.

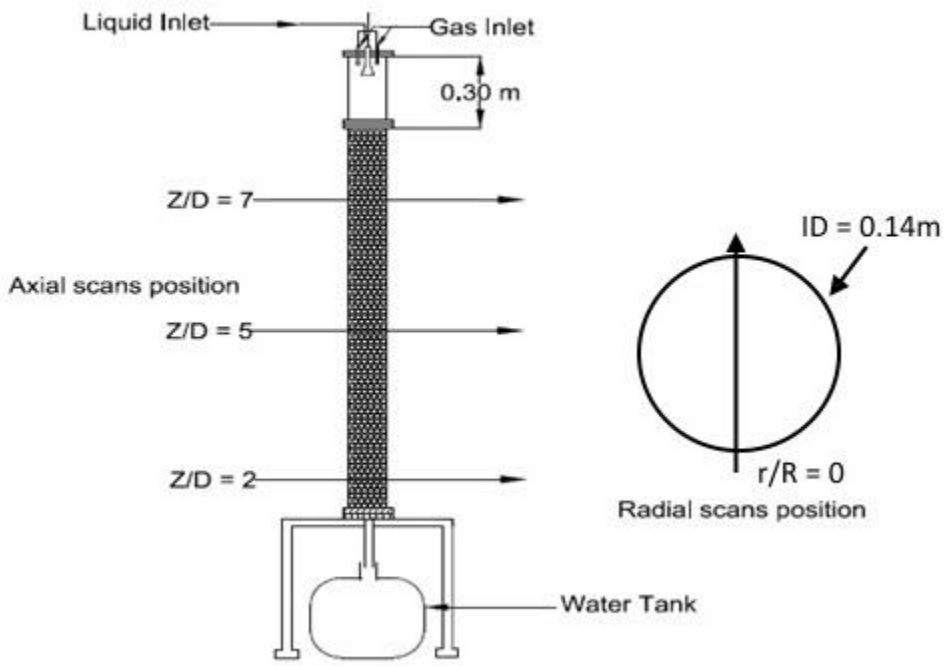

Figure 3. Scan Positions in Trickle Bed Reactor

The sealed sources collimator has a hole of 0.001 m while the detector collimator has an aperture of 0.005 m wide and 0.2 m tall. It is evident that the alignment of the holes of the source and the detector is a critical step in implementing our GRD technique.

Therefore, a laser-based light technique with a demo detector has been guided to achieve proper alignment and to maintain during the experiments. A series of counts it measures by demo detector to make sure the highest counts should be recorded with the particular position of the alignment. Then, the alignment will be fixed with guided laser beam. Couples of check and balance of the source/detector positions done during before and after experiments.

The radioactive source transmitted a focused beam through the column and process material, to the detector. The amount the radiation (counts) receives by the detector changes consequently as the density of the material in the column changes. The amount of the radiation (counts) that reaches the detector through the process material is reflective of the phases and collective densities of the materials along the radiation line. Hence, these counts or the radiation received by the detector reflects the flow along the radiation line. The photon beam of γ-rays coming from the radioactive sealed source is made such that it provides a point beam, which is custom made by Tracer Co Company (Pasadena, Texas) to enhance the resolution of our measurements.

The major advantages of GRD that make it attractive for industrial use are,

1. Non-invasive.
2. High integrity.
3. High reliability and low maintenance.
4. Low installation costs

The current GRD system in the lab can measure the flow regime identification and also the radial diameter profile of solids, gas, and liquid hold-up and it can be used as reduced tomography technique.

2.3. GRD SIGNALS AND THEIR ANALYSIS FOR FLOW REGIME IDENTIFICATION

Figure 4 shows the time series of the photon counts for a baseline condition when the reactor is packed with glass beads particles without flowing of gas and liquid phase. While Figure 5 shows the time series of the photon count at a selected condition of 0.01 m/s superficial liquid velocity and 0.06 m/s superficial gas velocity. The photon count measured for varying flow rate will be due gas-liquid, solids, and column. The variation of photon count will be only due to the gas-liquid movement as the photon attenuation of solids (packed bed), and column is fixed. Hence, the GRD fluctuation at varying flow rate translates the phenomena of gas-liquid flow pattern at a various flow rate over the catalyst bed. There are different methods to analyze the time series and in this study, the following methods are implemented.

1. TIME SERIES ANALYSIS
    - A. Mean and Standard Deviation
    - B. Autocorrelation.
2. FREQUENCY DOMAIN ANALYSIS
    - A. Spectral Analysis
3. STATE SPACE ANALYSIS
    - A. Kolmogorov Entropy.

3. RESULTS AND DISCUSSION

3.1 RESULTS OF STATISTICAL ANALYSIS

Statistical quantities of GRD signals can be obtained only for gas-liquid flow rates, and it can be done by subtracting the statistical quantities measured at operating condition with the baseline conditions. The baseline condition is defined for the scanning state for fixed solid bed without any flow conditions. In this case, the attenuation is due to solids (catalyst) and due to column wall. The baseline attenuation is always fixed as the catalyst is non-porous and immovable and same goes for the column wall. So simple subtraction of statistical quantities is undergone to see the statistical prints observed for various flow rate which is the representation gas-liquid flow distribution variation or transition or operation at different flow regime. The statistical quantities measured are a standard deviation and mean.

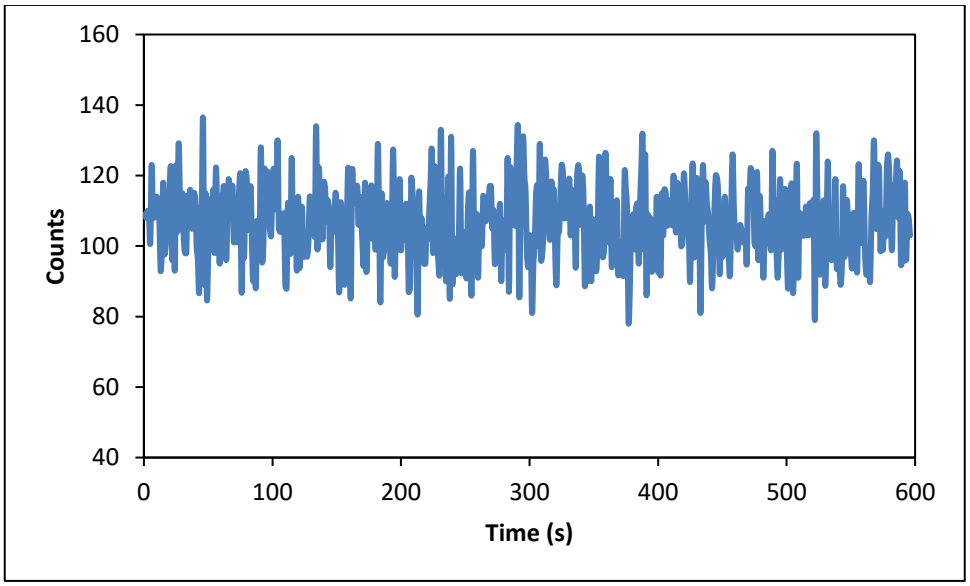

Figure 4. Time Series Signals of the Photon Count Baseline of the Condition of the TBR Packed with the Particles without Flowing of Gas and Liquid.

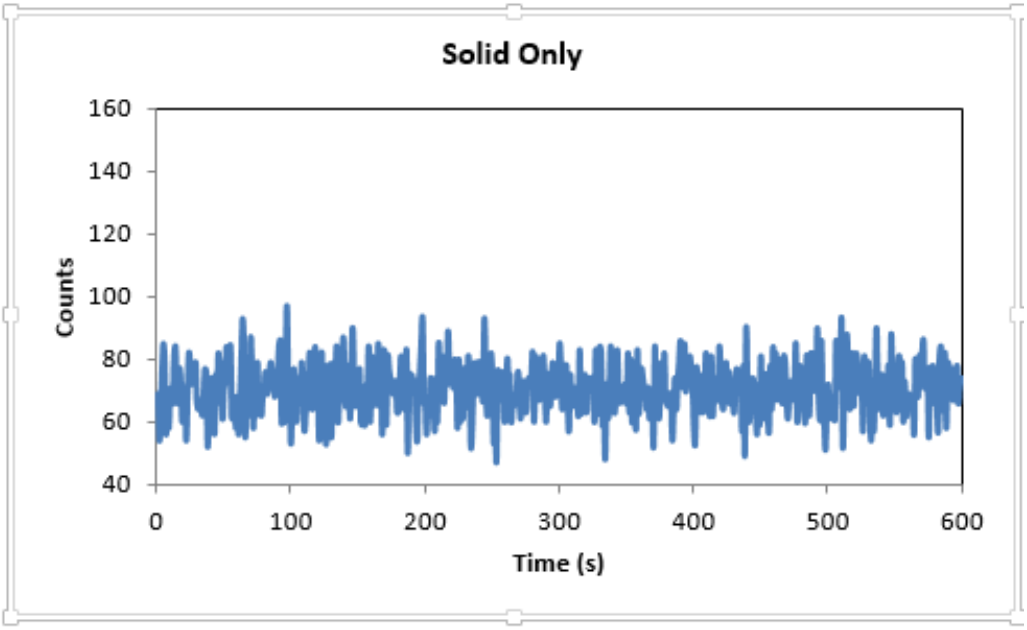

Figure 5. Time Series Signals of the Photon Counts at Ul = 0.01 m/s and Ug = 0.06 m/s at Z/D = 5 and r/R = 0.

The standard deviation (σ) measures the amount of dispersion around the mean. The formula for σ is as follows;

$$\sigma = \sqrt{\frac{\sum_{i=1}^{N}(x_i - \bar{x})^2}{(N-1)}} \quad (1)$$

Where N is total number of data point, x_i is the measured signals and $\bar{x}$ is the mean. The general time series mean as follow;

$$\mu = \frac{\sum_{i=1}^{N} x_i}{N} \quad (2)$$

The data can be analyzed with a mean and standard deviation of the attenuation of the signal only due to gas-liquid flow or the process condition. The overall mean for the process can be written as follows:

$$\mu = \mu_{\boldsymbol{b}} - (\mu_c)_i \quad (3)$$

Where $\mu_{\boldsymbol{b}}$ mean for time series of baseline data (only solid) and μ_c for mean of time series with different flow rates of liquid. This can be done because the mean of base line condition which is fixed is embedded in the mean of flow rate condition.

Similarly, the standard deviation for process conditions is the difference of standard deviation of baseline data to standard deviation plot for the time series at different superficial liquid velocities;

$$\sigma = \sigma_b - (\sigma_c)_i \quad (4)$$

Where σ_b is the standard deviation of baseline data and σ_c is the standard deviation of time series data with different superficial liquid and gas velocities. The subtraction of time series of baseline data is implemented in this research from the static scans of the TBR. The photon attenuation counts obtained from this method represents only the dynamic or static liquid behavior with different superficial liquid and gas velocities.

Figure 6 and 7 show the results of GRD for the mean and standard deviation with varying superficial liquid velocity U_l. The mean and standard deviation increase with increasing superficial liquid velocity. Flow regime transition can be observed at the inflection point where there is a sudden variation of the slope The patterns of the curves were similar at the different level of axial position with similar results of inflection points

which are the point of transition from a trickle to pulse flow. It shows that the flow behavior or gas-liquid flow is quite similar at these axial locations and the center of the bed. It can also be inferred that there is no maldistribution of liquid at the center of the bed along the axial height. The transition superficial liquid velocity is found to in the range of 0.1 to 0.12m/sec for the fixed superficial gas velocity of 0.09 m/sec

Figure 8 shows the standard deviation plot at Z/D=5 and r/R=0 for varying superficial liquid velocity and keeping three fixed superficial gas velocity (0.03m/sec, 0.12 m/sec, 0.18m/sec). It was observed the similar trend of transition regime, trickle, and pulse regimes. The transition range is found to superficial liquid velocity (0.1-0.12m/sec) for all the cases. There is one interesting observation that the standard deviation values are more for higher gas flow rate in trickle regime and vice versa in pulse regime. It can be attributed to the fact the at higher gas- higher liquid flow rate the system is in more ordered form compared to the case when high liquid and low gas flow rate. The results are in good agreement with Horowitz et al., (1997), Urseanu et al., (2005), and Al-Naimi et al., (2011), despite different techniques such as pressure drop fluctuations data and acoustic signals. The measurements were taken in a time series as similar to the GRD technique. Van Ommen et al., (2011) suggested that any change in the standard deviation of time series data (regardless of any techniques of measurement) was often used to identify the flow regime. The comparison was made with pressure drop measurement on the plotted standard deviation in Figure 9. The pressure drop measurement determines the global phenomena which is the results of overall prevailing microscopic phenomena of the bed. It shows similar transition regime for overall and line average measurement using Gamma-Ray Densitometry (GRD).

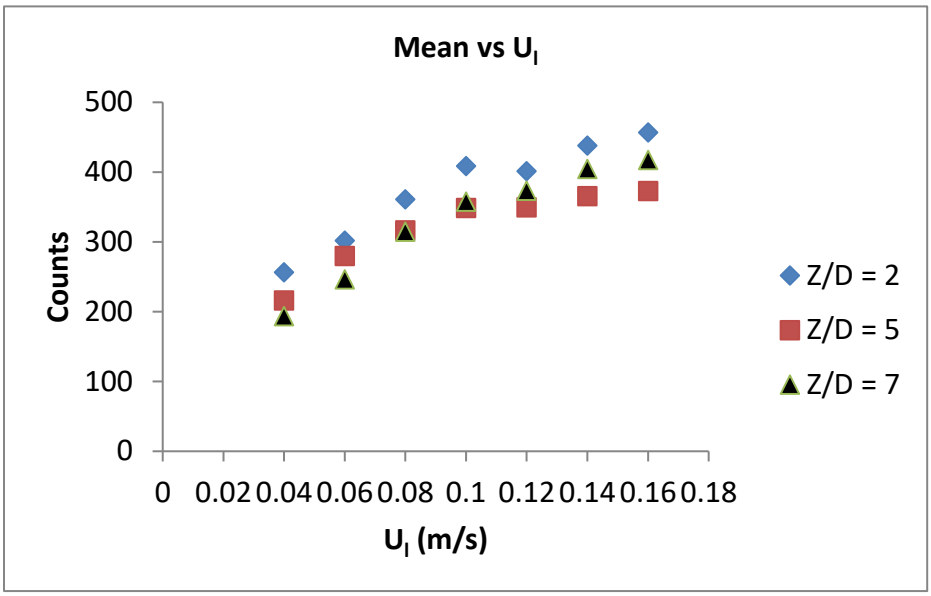

Figure 6. Average Count (Mean) of GRD for TBR with Different Superficial Liquid Flow Rate at Z/D = 2 at Ug = 0.09 m/s at the middle scans of the TBR

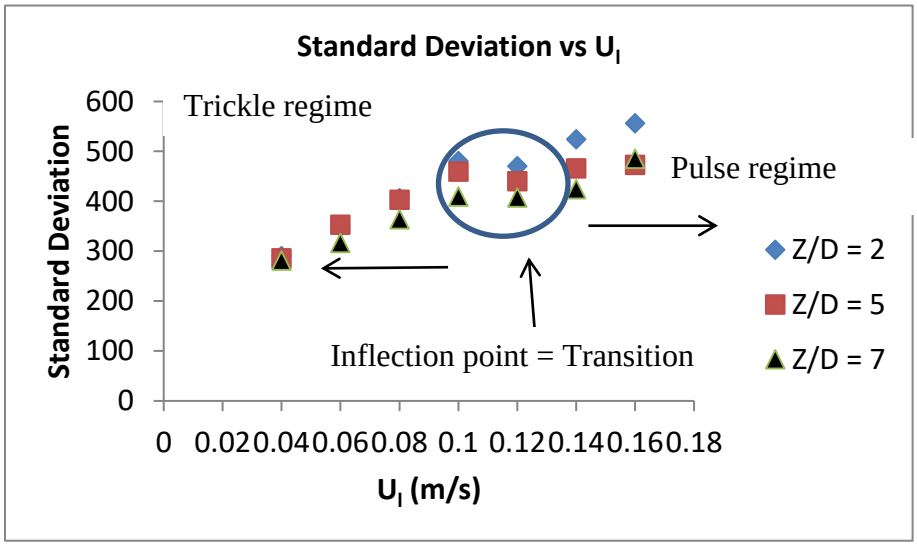

Figure 7. Standard Deviation of GRD Counts for TBR with Different Superficial Liquid Flow Rate at Z/D = 2 at Ug = 0.09 m/s at the middle scans of the TBR.

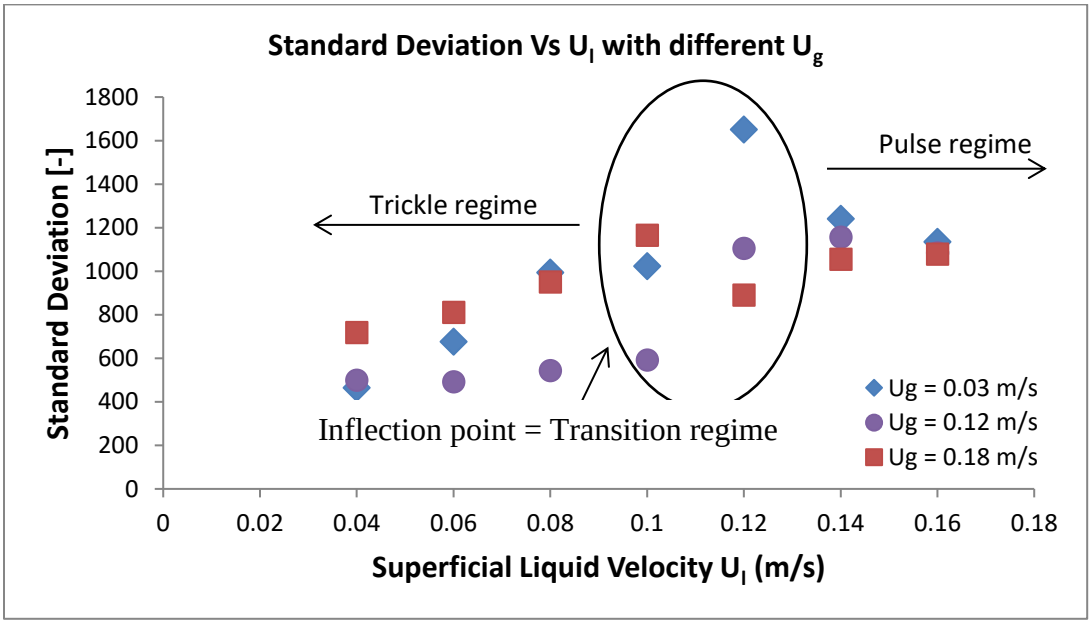

Figure 8. Standard Deviation versus Different Superficial Liquid and Gas Velocities at Z/D = 5 and r/R = 0.

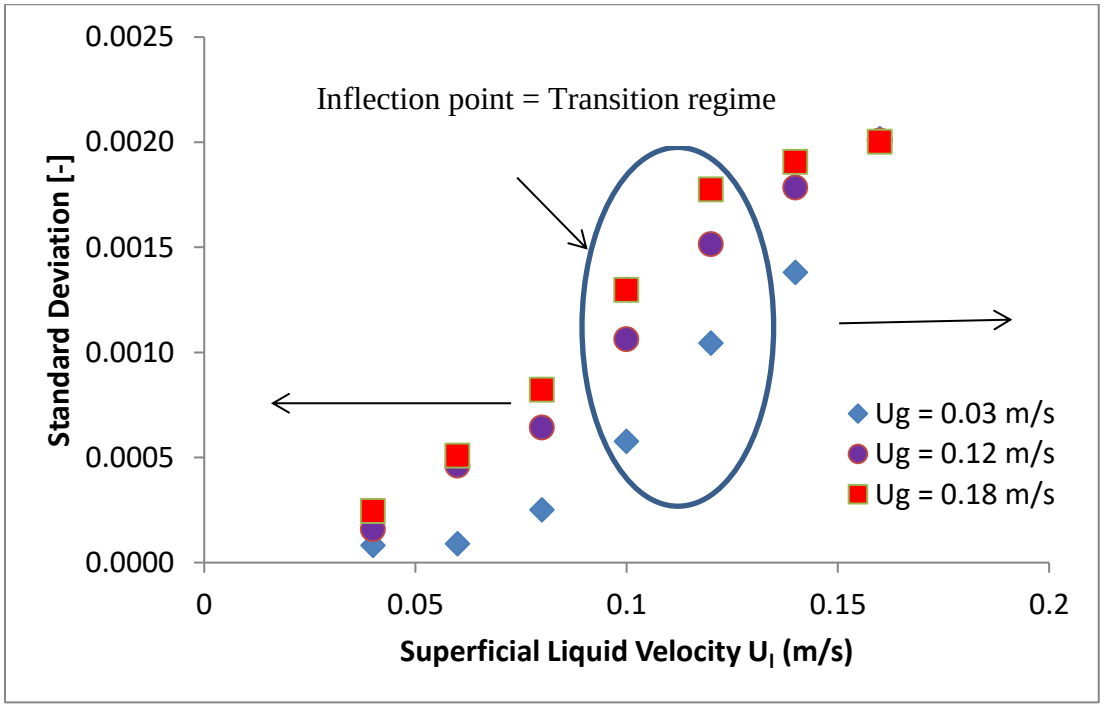

Figure 9. Flow Regime Identification Using Pressure Drop Measurement with different Ug at Z/D = 5 and r/R =0.

There is one disadvantage of using time series method that is the measurement technique may not be able to capture different phenomena occurring at different time scale. There were some losses of information in the time series of data from the GRD because many factors affected the flow such as the type of packing, the size of packing and superficial liquid and gas velocities which generate information at different time scales. Hence, further analysis by changing the time series domain to frequency domain analysis was implemented.

3.2. RESULT OF SPECTRAL ANLAYSIS

The spectral analysis converts the time domain based signal to frequency domain, and it describes the distribution of power contained in a signal over frequency. The spectral analysis is performed using Fourier transformation F(x).

Fourier transform of a time series x(t) is as follows:

$$F(x) = \int_{-\infty}^{+\infty} x(t) \exp(-j2\pi f.t)\, dt \tag{5}$$

Where, *f*, is frequency. The power spectral density (PSD), φ_{xx}, is the square of the magnitude of the continuous Fourier transform which represents as follow,

$$\varphi_{xx} = F(x).F^{*}(x) \tag{6}$$

Where *F*(x)* is the complex conjugate of Fourier transform.

Shaikh and Al-Dahhan (2013) developed flow regime identifier based on analysis of PSD (φ_{xx}) plot. They said the power law fall of the signal at higher flow rate is the indicator

of flow regime change. Figure 10 shows the plot of PSD for varying liquid flow rate at fixed gas velocity 0.09 m/sec at Z/D=5 and r/R=0. It is seen from Figure 10, power law fall is observed at U_l = 0.012 m/s and it is the indicator of the pulse flow regime. This can be also explained phenomenologically, as at trickle flow the gas will be in continuous phase and liquid will also be fairly in continuous phase with film over the solids and rare occurrences of small droplets in bulk phase. The PSD for this state will be kind homogenous across all frequency range as the GRD signal attenuation is only due to stationary solid (nonporous) and the liquid film. This is observed in figure 10a and 10b. In pulse flow, the gas phase is continuous with liquid phase is in semi-continuous state with high interaction. In this case the PSD can show non homogenous behavior like drop due to high interaction of liquid and generating different powers of signal at different frequency scale. This is observed in figure 10c and 10d with the power law fall in signal. This fall may be due to the high interaction of liquid phase. Hence, the power law fall may be the rough indicator demarking the trickle and pulse flow regime. In figure 10c where the first fall is observed can be the indicator of pulse flow which is 0.012 m/sec.

3.3 RESULT OF AUTOCORRELATION

Autocorrelation is the cross-correlation of a signal with itself. It is the similarity between observations as a function of the time lag between them. It is a mathematical tool for finding repeating patterns, such as the presence of a periodic signal obscured by noise, or identifying the missing fundamental frequency in a signal implied by its harmonic frequencies. It is often used in signal processing for analyzing functions or series of values, such as time domain signals.

In signal processing, the statistical definition of autocorrelation is often used without the normalization, that is, without subtracting the mean and dividing by the variance. When mean and variance normalize the autocorrelation function, it is sometimes referred to as the autocorrelation coefficient. The autocorrelation was used by Shaikh & Al-Dahhan (2013) to monitor the flow regime in a bubble column online and developed flow regime identifier

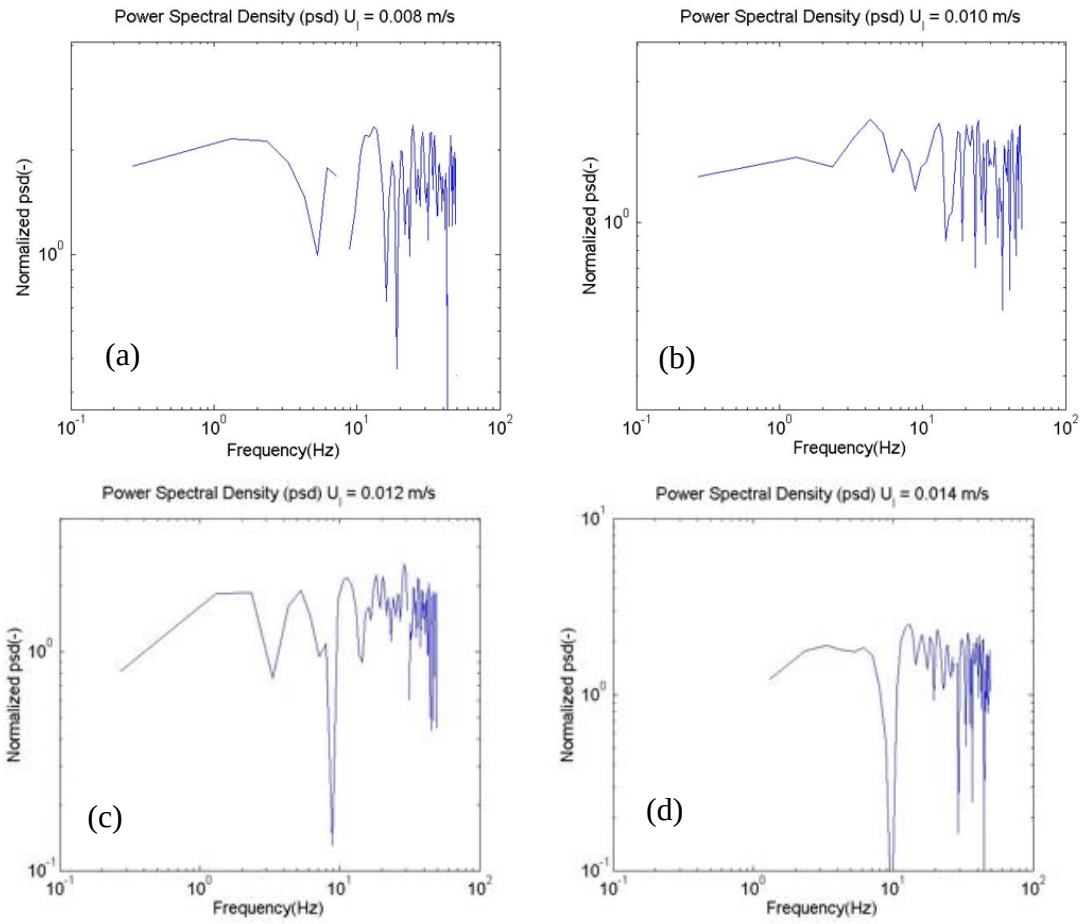

Figure 10. a) PSD for U_l = 0.008 m/s (trickle regime) , (b) U_l = 0.010 m/s (trickle regime), (c) PSD for U_l = 0.010 m/s (pulse regime) and (d) PSD for U_l = 0.014 m/s (pulse regime) all plot with constant Ug = 0.09 m/s with axial at Z/D = 5 and r/R=0.

In signal processing, the statistical definition of autocorrelation is often used without the normalization, that is, without subtracting the mean and dividing by the variance. When mean and variance normalize the autocorrelation function, it is sometimes referred to as the autocorrelation coefficient. The autocorrelation was used by Shaikh & Al-Dahhan (2013) to monitor the flow regime in a bubble column online and developed flow regime identifier based on the exponential type plot for periodic and homogenous conditions. The autocorrelation function in signal processing expresses the linear relationship between signal values at two different times and mathematically it is written as

$$C_{xx}(\tau) = \frac{1}{T}\int_0^T x(t)x(t-\tau).dt \quad (7)$$

where τ is a time lag.

The autocorrelation function is used to estimate how well upcoming values of a signal can be predicted from knowledge of the signal history. The behavior of the autocorrelation curves is a reflection of the nature of the time-series, irrespective of its operating and design conditions (Shaikh & Al-Dahhan 2013). Figure 11 shows the plot of autocorrelation coefficient with the time lag for varying liquid flow rate with a constant gas flow rate of 0.09m/sec at Z/D=5 and r/R=0. In trickle flow, there is inherent periodic nature of liquid due to thin film flow over the catalyst and less occurrence of liquid droplets in bulk flow. Hence the signals can be correlated in this regime. It is seen that the exponential type of plot in figure 11a and 11b in the time lag of 0-2 sec. This exponential correlation is observed due to trickle flow in the system. In pulse flow regime the correlation is difficult due to inherent inhomogeneity created because of the higher interaction of liquid. It is seen in Figure 11c and 11d the exponential nature is distorted,

and it can be attributed to pulse flow regime, and no particular correlation pattern is observed. Hence, Figure 11c and 11d represents pulse flow conditions with transition velocity of 0.012m/sec. Long term processes are not appeared in autocorrelations cure, so time lag of 0-2 sec is generally enough to evaluate without any loss in information (Smith,1999).

3.4 RESULT OF KOLMOGOROV ENTROPY (KE)

Kolmogorov Entropy is one of the chaotic analysis technique which can be implemented on time series of GRD photon count fluctuation. Kolmogorov entropy is state space analysis and measures the level of disorder in a chaotic system. In a classical system, KE is a measure of the degree of 'chaos' inherent in the dynamics of the system (Pechukas, 1982). Multiphase flow in TBR is a chaotic system, and the varying degree of chaos are observed at various flow regimes. This criterion is utilized to demarcate different regime in a TBR. Kolmogorov Entropy is a quantitative measure of the rate of information loss of the system dynamics due different level of disorder in the system.

KE values of a periodic non-chaotic system are zero, for the random chaotic system it's a finite positive quantity, and for complete disorder or non-deterministic system, its value is Infinite. The KE also quantifies the degree of unpredictability of the system. The method used in this study to evaluate KE is the approach of Schouten: maximum likelihood estimation of Entropy (Schouten et al., 1994) and MATLAB program is developed at multiphase Engineering and applications laboratory (mReal) on the basis of the same. This method is used due to its successful implementation on pressure fluctuation to identify flow to identify flow regime (Nedeltchev et al., 2011).

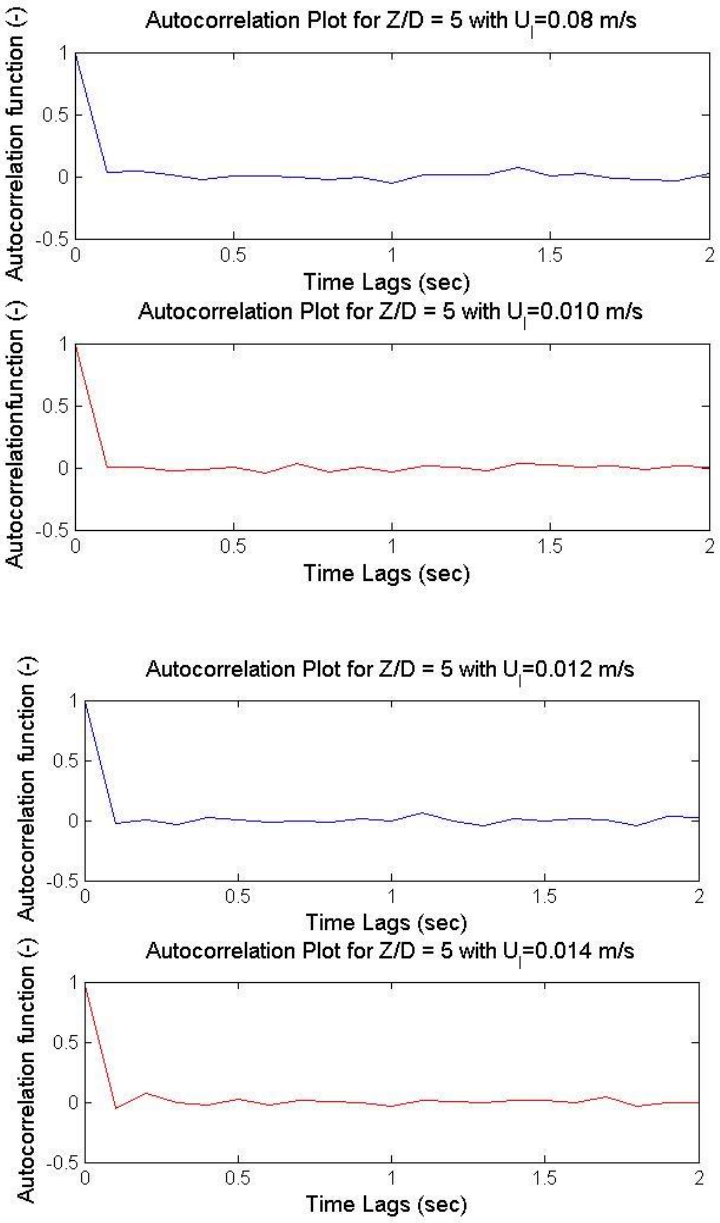

Figure 11. Results of Autocorrelation for Z/D =5 and r/R=0 with different Ul with constant Ug = 0.09 m/s

Figure 12 shows the results of Kolmogorov Entropy calculation at Z/D=5 and r/R=0, for fixed superficial gas velocity of 0.09cm/sec and varying superficial liquid velocity. The maximum peaks observed in the plots are the point of instability, and the minimum is the point of stability, the point of stability are transition point of flow regime

(Toukan, 2016). At low flow rate, the system is in trickle flow and on increasing liquid flow rate the system disorder is increased hence the KE values too. The KE reaches the first peak value at 0.08m/sec at this point the system in trickle flow at most random or chaotic state. On further increasing the liquid velocity the system reorganizes itself in trickle flow and disorder reduces in this same regime and reaches the minimum point at 0.012 m/sec. At this point, the system is in trickle flow, but it's in the most organized state. Further increase in liquid velocity increases the KE value and hence the disorder and jumps to pulse flow regime. Again the same trend is noted in pulse flow regime. The transition velocity from trickle flow to pulse flow is 0.012m/sec. This observation is in agreement with all the other analysis reported in this study.

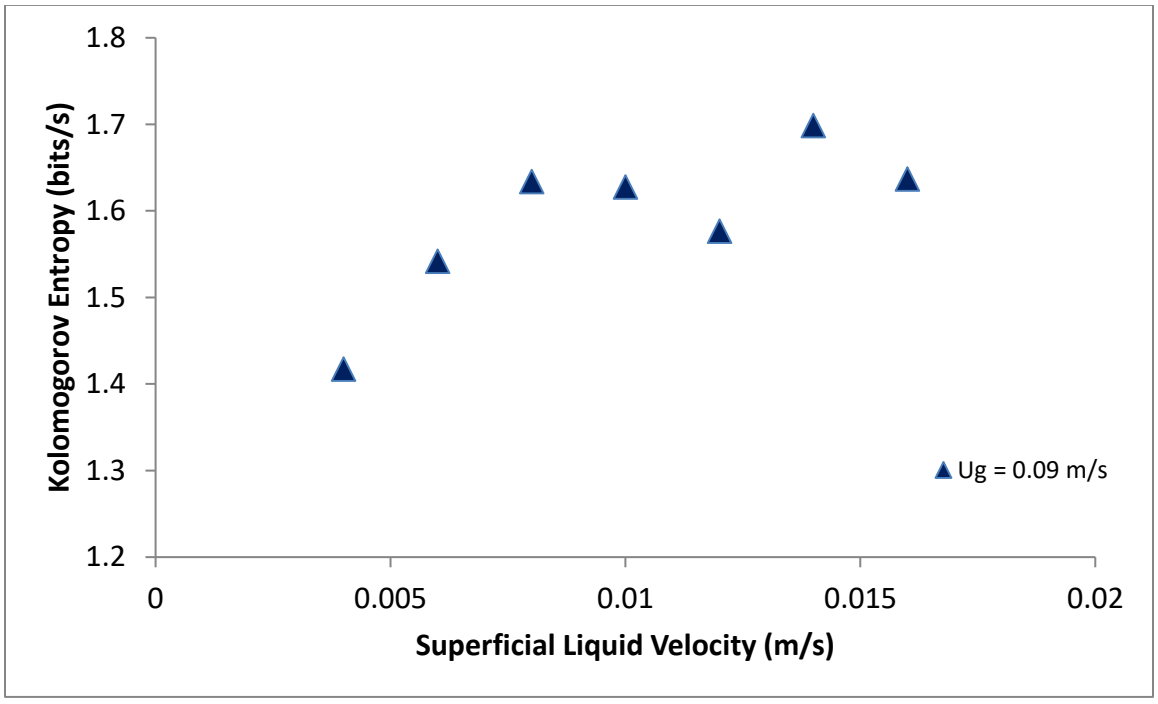

Figure 12. Superficial Liquid Velocity versus Kolmogorov Entropy at Different Ug, Z/D = 5 and r/R = 0.

4. REMARKS

Identification of flow regime is made on a TBR based on the photon count signal obtained from non-invasive GRD technique. The time series data obtained from GRD is subjected to statistical analysis by measuring standard deviation (SD) and mean. The slope change in mean and SD plot with varying liquid flow rates and at different constant gas flow rate is used to demarcate the regimes. The transition region is identified, and it is found to same for all the axial measurement at the center of the reactor. It shows the flow distribution is quite uniform along the axial length at the center of the reactor. Pressure drop measurement also indicated similar transition trend which indicates the overall and line average phenomena at the center of the reactor are behaving in a similar manner.

To accurately pinpoint the flow regime transition point, the GRD signal obtained at the middle of the reactor (Z/D=5, r/R=0) is tested on another time domain (Autocorrelation), frequency domain (Spectral Analysis) and state space (Kolmogorov Entropy). The identified flow regimes are a trickle and pulse flow. Autocorrelation showed that in trickle flow the signals could be correlated, and there is no identifiable correlation exists in pulse flow. The spectral analysis identified the flow regime based on power law fall. Kolmogorov entropy which is state space analysis distinguished flow regime based on the trend of change in disorder or randomness in the system. All the analysis are successful in identifying flow regime and are in agreement with each other. This finding shows that the GRD is capable of determining flow regime in all three domain of analysis which time, frequency and state space. This information is vital for industrial purpose, as GRD can be successfully implemented at industrial scale and flow analysis in any domain can make regime identification.

ACKNOWLEDGEMENT

The author acknowledge the Ministry of Science, Technology and Innovation Malaysia (MOSTI) for sponsoring the primary author's study within the Chemical and Biochemical Engineering Department at Missouri University of Science and Technology. Also, the primary author would like to acknowledge the fund by professor Al-Dahhan, Multiphase Reactor Engineering Laboratory (mREAL) to support experimental work.

REFERENCES

AL-DAHHAN, M. H., KEMOUN, A., & CARTOLANO, A. R. (2006). Phase distribution in an upflow monolith reactor using computed tomography. *AIChE Journal, 52*(2), 745-753.

Al-NAIMI, S. A., Al-SUDANI, F. T. J., & HALABIA, E. K. (2011). Hydrodynamics and Flow Regime Transition Study of Trickle Bed Reactor at Elevated Temperature and Pressure. *Chemical Engineering Research and Design, 89*(7), 930-939.

ATTOU, A., & FERSCHNEIDER, G. (1999). A Two-Fluid Model for Flow Regime Transition in Gas-Liquid Trickle-Bed Reactors. *Chemical Engineering Science, 54*(21), 5031-5037.

AYDIN, B., & LARACHI, F. (2005). Trickle Bed Hydrodynamics and Flow Regime Transition at Elevated Temperature for a Newtonian and a Non-Newtonian Liquid. *Chemical Engineering Science, 60*(23), 6687-6701.

CHARLTON, J. S. (1984). Radioisotope Techniques for Problem-Solving in The Chemical Industry. *Proceedings of the Institution of Mechanical Engineers.Part A.Power and Process Engineering, 198*(5), 81-88.

CHEN, J., RADOS, N., AL-DAHHAN, M. H., DUDUKOVIĆ, M. P., NGUYEN, D., & PARIMI, K. (2001). Particle Motion in Packed/Ebullated Beds by CT And CARPT. *AIChE Journal, 47*(5), 994-1004.

COTTIS R.A., Homborg A. M., and Mol J.M.C., (2015), The Relationship between Spectral and Wavelet Techniques for Noise Analysis., Electrochimica Acta. (Article in Press)

ELPERIN, T. AND M. KLOCHKO (2002). Flow Regime Identification in a Two-Phase Flow using Wavelet Transform. *Experiments in Fluids* **32**(6): 674-682.

GLADDEN, L. F., & SEDERMAN, A. J. (2013). Recent Advances in Flow MRI. *Journal of Magnetic Resonance*(229), 2-11

HOROWITZ, G. I., CUKIERMAN, A. L., & CASSANELLO, M. C. (1997). Flow RegimeTransition in Trickle Beds Packed with Particles of Different Wetting Characteristics - Check- up on New Tools. *Chemical Engineering Science, 52*(21-22), 3747-3755.

JOHANSEN G. A., & JACKSON P., (2004). Radioisotope Gauges for Industrial Process Measurements, John Wiley & Sons, Ltd., p. 244.

LARACHI, F., ILIUTA, I., AL-DAHHAN, M. A., & DUDUKOVIC, M. P. (1999). Discriminating trickle-flow hydrodynamic models: Some recommendations. *Industrial and Engineering Chemistry Research, 39*(2), 554-556.

LI, W. -L., ZHONG, W. -Q., JIN, B. -S., XIAO, R., & HE, T. –T., (2013). Flow Regime Identification in a Three-Phase Bubble Column Based on Statistical, Hurst, Hilbert-Huang Transform and Shannon Entropy Analysis. *Chemical Engineering Science, 102*, 474-485.

LIM, M. H. M., SEDERMAN, A. J., GLADDEN, L. F., & STITT, E. H. (2004). New insights to a trickle and pulse flow hydrodynamics in trickle-bed reactors using MRI. *Chemical Engineering Science, 59*(22-23), 5403-5410.

LU, X. AND H. LI (1999). Wavelet Analysis Of Pressure Fluctuation Signals In A Bubbling Fluidized Bed. *Chemical Engineering Journal* **75**(2): 113-119.

MUZEN, A., & CASSANELLO, M. C. (2007). Flow Regime Transition in a Trickle Bed with Structured Packing Examined with Conductimetric Probes. *Chemical Engineering Science, 62*(5), 1494-1503.

NEDELTCHEV, S., Shaikh, A., & Al-Dahhan. (2011). Flow Regime Identification in a Bubble Column via Nuclear Ga ge Densitometry and Chaos Analysis. *Chemical Engineering Technology*, 34, No. 2, 255-233

NG, K. M. (1986). Model for Flow Regime Transitions in Cocurrent Down-Flow Trickle-Bed Reactors. *AIChE Journal, 32*(1), 115-122.

PECHUKAS, P. (1982). Kolmogorov entropy and "quantum chaos". *Journal of Physical Chemistry, 86*(12), 2239-2243.

RANADE, V. V., CHAUDHARI, R. V., & GUNJAL, P. R., (2011). *Trickle Bed Reactors*. Amsterdam, Elsevier**:** 211-256.

ROY, S. (2006). Phase Distribution and Performance Studies of Gas-Liquid Monolith Reactor. *Ph.D. Dissertation,* Washington University, St. Louis, Missouri. 172-173.

SANKEY, M. H., HOLLAND, D. J., SEDERMAN, A. J., & GLADDEN, L. F. (2009). Magnetic Resonance Velocity Imaging of Liquid and Gas Two-Phase Flow in Packed Beds. *Journal of Magnetic Resonance, 196*, 142-148.

SAROHA, A. K., & NIGAM, K. D. P. (1996). Trickle Bed Reactors. *Reviews in Chemical Engineering, 12*(3-4), 207-347.

SATTERFIELD, C. N. (1975). Trickle-Bed Reactors. *AIChE, 21*(2), 209-228.

SEDERMAN, A. J., & GLADDEN, L. F. (2001). Magnetic Resonance Imaging as a Quantitative Probe of Gas-Liquid Distribution and Wetting Efficiency in Trickle-Bed Reactors. *Chemical Engineering Science* (56), 2615-2628.

SHAIKH, A., & AL-DAHHAN, M. (2013). A New Method for Online Flow Regime Monitoring in Bubble Column Reactors via Nuclear Gauge Densitometry. *Chemical Engineering Science, 89*, 120-132.

SULLIVAN, C. J., GARNER, S. E., & BUTTERFIELD, K. B. (2004). Wavelet Analysis of Gamma-Ray Spectra. Paper presented at the *IEEE Nuclear Science Symposium Conference Record,1* 281-286.

SIMS W. B., GASKEY S. W., & Luss D. (1994). Effect of Flow Regime and Liquid Velocity on Conversion in Trickle-Bed Reactor. *Industrial Engineering Chemical Resource,* 33, 2530- 2539

SMITH, STEVEN (1999). Digital signal processing. California Technical Publishing, San Diego, California.

TOUKAN, ALI (2016). Hydrodynamic of Co-current Gas Liquid Upflow in a Moving Packed Bed Reactor with Porous Catalysts. Master Theses, Missouri Science and Technology University, Rolla, MO, USA.

TJUGUM, S. A., HJERTAKE, B. T., & JOHANSEN, G. A. (2002). Multiphase Flow Regime Identification by Multibeam Gamma-Ray Densitometry. *Measurement Science and Technology, 13*(8), 1319-1326.

URSEANU, M. I., BOELHOUWER, J. G., BOSMAN, H. J. M., SCHROIJEN, J. C., & KWANT, G. (2005). Estimation of Trickle-to-Pulse Flow Regime Transition and Pressure Drop in High-Pressure Trickle Bed Reactors with Organic Liquids. *Chemical Engineering Journal, 111*(1), 5-11.

VAN OMMEN, J. R., SASIC, S., VAN DER SCHAAF, J., GHEORGHIU, S., JOHNSSON, F., & COPPENS, M. -. (2011). Time-Series Analysis of Pressure Fluctuations in Gas-Solid Fluidized Beds - A Review. *International Journal of Multiphase Flow, 37*(5), 403-428.

WANG, J., ZHANG, W., FENG, L., & GU, X. (2006). Wavelets Analysis of Pressure Fluctuation in Agitated Fluidized Bed. *Huagong Xuebao/Journal of Chemical Industry and Engineering (China), 57*(12), 2854-2859.

ZAIN, R. M., RAHMAN, M. F. A., HASAN, N. P. M., & ABDULLAH, J (2008). "Gamma-Ray Transmission Scans of Naphtha Splitter Column: A Case Study." *AIP Conference Proceedings* 1017(1): 210-214.

II. NOVEL MEASUREMENT TECHNIQUE BASED ON OPTICAL PROBE TO MEASURE LOCAL FLOW DYNAMICS IN PACKED BED REACTORS

Vineet Alexander, Mohd Fitri Abdul Rahman,and Muthanna H. Al Dahhan

Department of Chemical and Biochemical Engineering, Missouri University of Science and Technology, 110 Bertelsmeyer Hall, 1101 N. State Street, Rolla, MO 65409, USA

ABSTRACT

In this work a novel experimental technique called Two-Tips Optical Probe (TTOP) is developed and implemented on a trickle bed reactor (TBR). This technique identifies local flow dynamic parameters such as local liquid and gas velocities, local liquid and gas saturations in void space of packed bed packing. This measurement technique is validated with X-Ray Digital Industrial Radiography (DIR) and known velocity experiment. The TBR used in this study is made up of Plexiglas column of diameter 0.14m and filled with 3 mm glass bead packing. Water and air are the phases with the superficial velocity of liquid from 0.004 m/sec to 0.016 m/sec and fixed superficial velocity of the gas at 0.09 m/sec. Local hydrodynamic parameters are evaluated using TTOP at these conditions.

Keywords: Trickle bed reactor; optical fiber probe;

1. INTRODUCTION

Packed bed reactors (PBR) are widely used in industries such as petroleum, petrochemical, chemicals and biochemical industries. Especially, Trickle bed reactors (TBR), which are concurrent downflow of gas-liquid over the fixed-bed catalyst and is one of the main reactor of choice for various industrial appli- cations (Al-Dahhan & Dudukovi´c (1994),Al-Dahhan et al. (1997),Burkhardt & Busch (2013),Zehraoui et al. (2013),Meng et al. (2013)). PBR flow patterns are highly complex due to three phase interaction and results in different flow regime at various operating conditions. In general, most of the industrial applications are run at the trickle or pulse flow regime. Although these flow regimes are based on the overall flow pattern, it may not be the case at different local positions inside the void space of the catalyst packing. The flow behavior in local regions directly impacts the overall performance of these reactors, and it can be categorized based on the contact pattern of phases with the catalyst at these locations. The contact pattern can be defined as fully wetted, partial and dry wetting of catalyst and it directly depends on operating conditions and design of the reactor. For liquid limiting reactions fully wetting of catalyst is desired ((Al-Dahhan et al., 1997)), otherwise for the exothermic process, it can result in undesirable conditions like hot spots and catalyst agglomeration.

Identification and quantification of the local hydrodynamic parameter are highly essential for better understanding the behavior of these reactors. The local flow distribution or saturation of phases and their respective local ve- locities at void space of catalyst packing quantifies the local flow dynamics. Many researchers have put the effort over the years to understand the com- plex hydrodynamics of these reactors, but most of

the research focus was on overall hydrodynamics, such as overall liquid and gas holdups, pressure drop, flow regimes, catalyst wetting effectiveness, mass transfer, and heat transfer (Al- Dahhan et al. (1997),Sederman & Gladden (2001),Schubert et al. (2010b)).There are limited studies observed for local measurements, and it is mainly due to lack of reliable and low-cost techniques that can measure them locally at desired locations (Boyer & Fanget (2002),Schubert et al. (2010a),Anuar Mohd Salleh et al. (2015)). While some attempts were made at evaluating local liq- uid velocities (Sederman & Gladden (2005),Schubert et al. (2010b),Mohammed et al. (2013),Mohd Salleh et al. (2014)) , and the local gas dynamics (Collins et al. (2017)) for packed bed systems. For local liquid velocities, some measure- ment techniques have been explored and reported in the literature for packed bed systems. These measurement techniques can be classified based on radi- ation and non-radiation. The radiation-based technique such as MRI and X- Ray Radiography are non-invasive and are capable of scanning opaque systems. Non-Radiation based techniques include light-based imaging technique such as Particle Image Velocimetry (PIV), and other non-radiation based techniques are mostly intrusive such as Wire Mesh Sensors and Conductivity probes. The detailed application of optical probe sensors in multiphase reactors has been reviewed by (Li et al. (2012)).

Mohd Salleh (2014) developed X-Ray Digital Industrial Radiography (DIR) and Particle Tracing Velocimetry (PTV) technique and implemented on a 4.5cm internal diameter (ID) and 40cm height trickle bed reactor to measure local liquid velocity. DIR consists of X-Ray source and a complementary metal oxide semiconductor (CMOS) digital detector. Tracking particles of size 106 − 125um diameter is fed and particle tracking is done by the developed algorithm from DIR images and measured local liquid

velocity. They observed the local liquid velocity could reach from 35 to 50 times the overall superficial liquid velocity. Scalability of this technique is not being studied yet, and it is only implemented at lab scale level.

Gladden et al. (2003) and Sederman & Gladden (2001) used Magnetic Resonance Imaging (MRI) and performed 3-D flow study in two phase(solid-liquid) and three phase(gas-solid-liquid) packed bed reactor of internal diameter 43 mm and 700 mm long PolyTetraFluroEthylene (PTFE) tube. They generated image size 45mm X 45mm and observed the local liquid velocity can go up to 5 times superficial liquid velocity for single phase (only liquid) flow and for two- phase (gas-liquid) flow it can go up to 50 times superficial liquid velocity. MRI is a reliable noninvasive technique with high speed and temporal resolution but it is highly expensive to implement at large diameter reactors, and mostly it applied to small scale columns less than 2 inches.

Schubert et al. (2010a) and Mohammed et al. (2013) developed wire mesh sensors (WMS). The whole assembly of WMS contains wires meshes at two planes with a distance of 6.0mm. The wire mesh has 16 stainless steel wires of 0.2mm diameter and detects the liquid flow pattern based on the electrical permittivity of passing fluid. They implemented this on TBR having internal diameter 100mm and packed with 2.5mm spherical alumina catalyst till height of 135.5cm. The time difference of flow sensing between the sensors and the distance between the two planes are used to measure the liquid interstitial velocity, based on the assumption that the trickling liquid follows a straight line between the sensors. They observed the liquid interstitial velocity increases with increasing liquid mass flow rate. The issues with WMS is that it is highly intrusive as the sensors occupy the significant amount of cross-sectional area and can drastically

alter the flow pattern and the assumption to neglect tortuosity factor causes serious restrictions on derived interstitial liquid velocity.

The literature shows very promising experimental techniques to measure local hydrodynamics in three phase systems but all focus on measuring liquid dynamics. There is still a lot of knowledge gap in this area especially dealing with large scale or even industrial scale reactor. The objective of this work is to develop and validate a measurement technique called two-tip optical probe which can measure and quantify the local flow dynamics of both gas and liquid phase in packed bed reactors and its implementation on TBR to measure local liquid and gas velocities and their respective local saturation's at void space of catalyst bed. The data based on these local hydrodynamic parameters yields benchmark data for the reactor, pellet or multi-scale models, scale-up, and CFD validation and helps in better comprehension of flow structure through the bed at various local locations for packed bed reactor.

2. TWO TIP OPTICAL PROBE

Measurement technique based on optical probes called four-point optical probe are extensively used for gas-liquid systems (Xue et al. (2008), Youssef & Al-Dahhan (2009),Kagumba & Al-Dahhan (2015)). Four point optical probes characterizes the bubble dynamics like bubble chord length, bubble rise velocity, bubble interfacial area (Xue et al. (2003)). The orientation of the four-point optical probe to obtain bubble characteristics makes it impossible to place it in the packed bed systems. Hence, a concept based on two tips is devised, in which a two fiber optical cables are placed parallel to each other at 1mm distance. When this assembly is placed inside the packed

bed, then both tips face towards the diametrically opposite side. This orientation of two-tip optical probe makes it possible to place these probe at desired local locations. The algorithms are developed to quantify the local flow dynamics from its time series data.

2.1 MEASUREMENT PRINCIPLE FOR OPTICAL PROBES

The optical probe used as measurement technique to characterize the gas-liquid flow is due to total internal reflection phenomena encountered at the probe tip when gas medium touches the tip and refraction phenomena when liquid medium touches the probe tip (Xue et al. (2003),Kagumba & Al-Dahhan (2015)). The Refractive index (ni) and critical angle (θc) characterize the total internal reflection phenomena

According to Snells law when light traverse through the interface of different media. The light will bend towards the normal when it enters into optically dense media, and it bends away from normal if it enters optically less dense media. Whereas the normal here is referred to the perpendicular line to the surface. This phenomenon is used to distinguish gas and liquid phase. Figure 1 shows the mathematical form of snell's law.

Hence, if a situation in which n1 > n2, then the light traveling from medium 1 to medium 2 bends towards the interface. The two possible phenomena can occur depending on the critical angle θc as shown in the Figure 2 If the incident light is less than critical angle then refraction occurs (Figure 2a) and otherwise total internal reflection occurs (Figure 2b). If n2 > n1 then the light will completely transmit form medium1 to medium2.

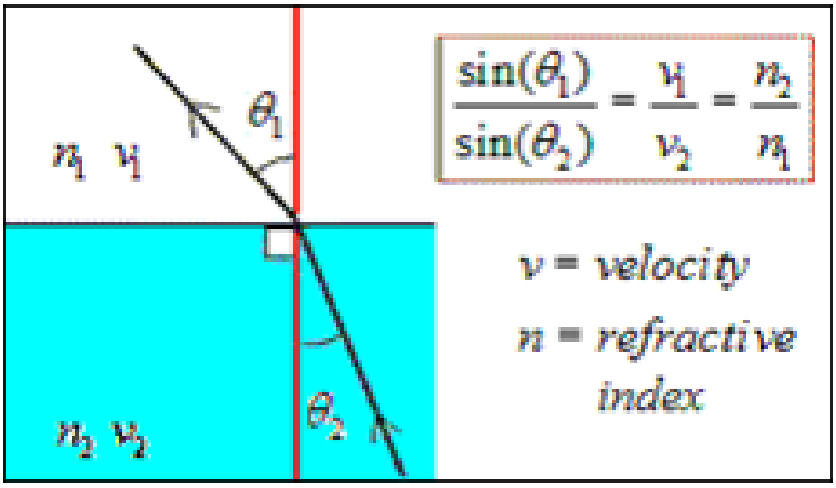

Figure 1. Snell's Law

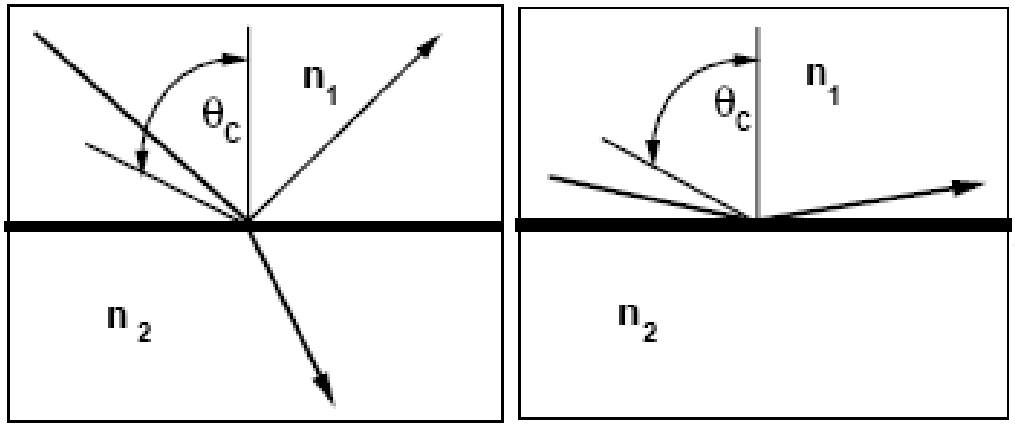

Figure 2. (a) Angle of Incidence is Less Than Critical Angle; Light bends toward interface without total internal reflection (b) Angle of Incidence Greater than Critical Angle; Total Internal Reflection Occurs.

The light inside the core of the fiber propagates through total internal reflection (Figure 3). The light incidents at an angle greater than the critical angle and total internal reflection occurs at either side of the wall through the length of the fiber.

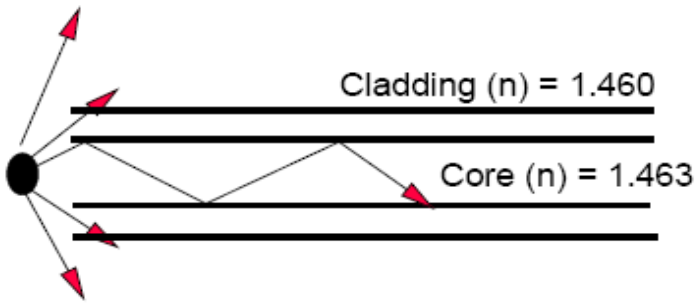

Figure 3. Light Propagation inside the Optical Fiber Probe.

2.2. THE OPTICAL FIBER PROBE TIP BEHAVIOR INSIDE THE GAS-LIQUID SYSTEMS

The optical fiber probe tip is transformed to a conical shaped tip as shown in Figure 4a. This tapered tip facilitates the total internal reflection phenomena. The refractive index of the optical fiber is approximately 1.15, and gas is around 1, and that of is liquid around 1.3-1.5. Hence, with the conical shaped tip, when light touches the gas phase the criteria for total internal reflection satisfies as shown in Figure 4b and when the liquid touches, the criteria for refraction satisfies as illustrated in Figure 4c.

The optical fiber box with data acquisition is used to generate and process the signal Figure 5. A 680nm wavelength of light emitted by Laser Emitting Diode is transmitted through standard fiberglass connectors and relayed to the probe tip and reflected light is detected by a photodiode. The photodiode signals are translated into voltage signals which were collected by data acquisition board (United Electronics Industries, PowerDAQ PD-2MFS-8-1M/12) at a sampling frequency of 40 kHz. When the tip is in the presence of gas, most of the light internally reflects and travels back up the fiber. When the tip is in the presence of a liquid, most of the light refracts out into the liquid, and little light travels back up the fiber. The light traveling back up the fiber re-

enters the coupler, which sends a percentage usually 50% of this reflected light down the other leg of the coupler to a photodiode. The photodiode then converts the quanta of light into a voltage signal. The Figure 6 shows how a single probe responds to a bubble striking and leaving in a gas-liquid system. In the Figure 6, (A) and (E) shows the probe response inside the water, (C) shows the response inside the gas, (D) and (E) shows the gas bubble entering and leaving the tip, basically it defines gas-liquid interface.

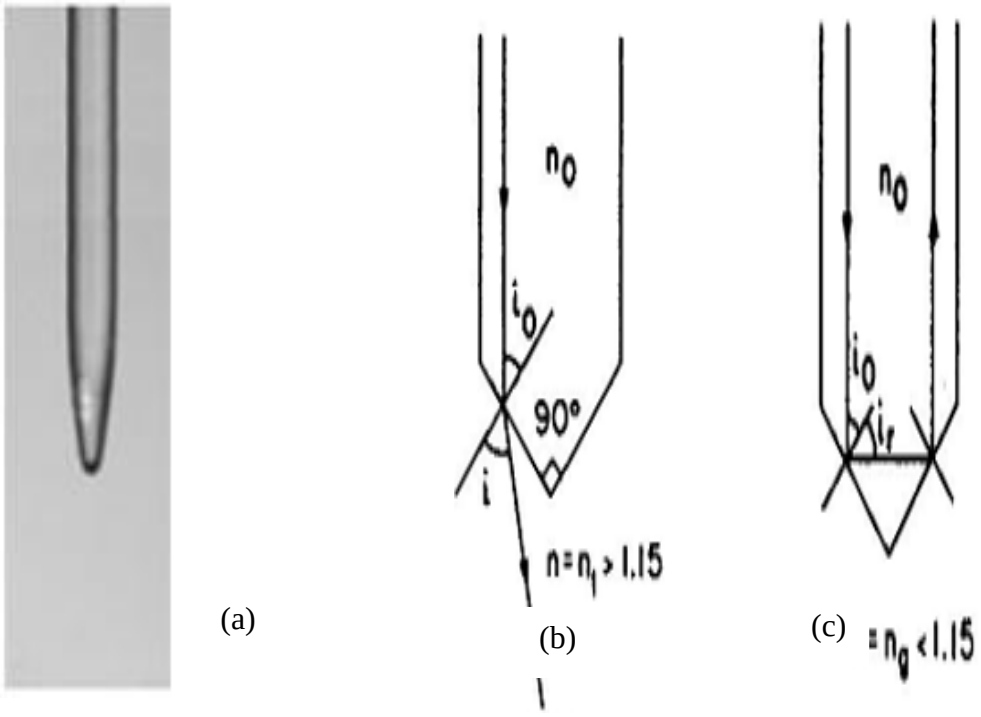

Figure 4. (a) Optical fiber probe tip made into conical shape (b) Refraction phenomena gas touches the probe tip (c) Reflection phenomena when liquid touches the probe tip. (Xue et al. (2003))

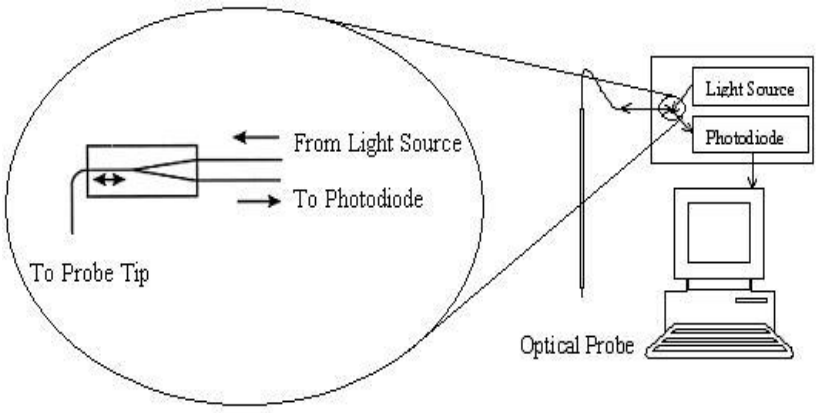

Figure 5. Schematic of Optical Fiber Box (Kagumba & Al-Dahhan (2015))

A 680 nm wavelength of light emitted by Laser Emitting Diode is transmitted through standard fiberglass connectors and relayed to the probe tip and reflected light is detected by a photodiode. The photodiode signals are translated into voltage signals which were collected by data acquisition board (United Electronics Industries, PowerDAQ PD-2MFS-8-1M/12) at a sampling frequency of 40 kHz. When the tip is in the presence of gas, most of the light internally reflects and travels back up the fiber. When the tip is in the presence of a liquid, most of the light refracts out into the liquid, and little light travels back up the fiber. The light traveling back up the fiber re-enters the coupler, which sends a percentage usually 50% of this reflected light down the other leg of the coupler to a photodiode. The photodiode then converts the quanta of light into a voltage signal. The Figure 6 shows how a single probe responds to a bubble striking and leaving in a gas-liquid system. In the Figure 6, (A) and (E) shows the probe response inside the water, (C) shows the response inside the gas, (D) and (E) shows the gas bubble entering and leaving the tip, basically it defines gas-liquid interface.

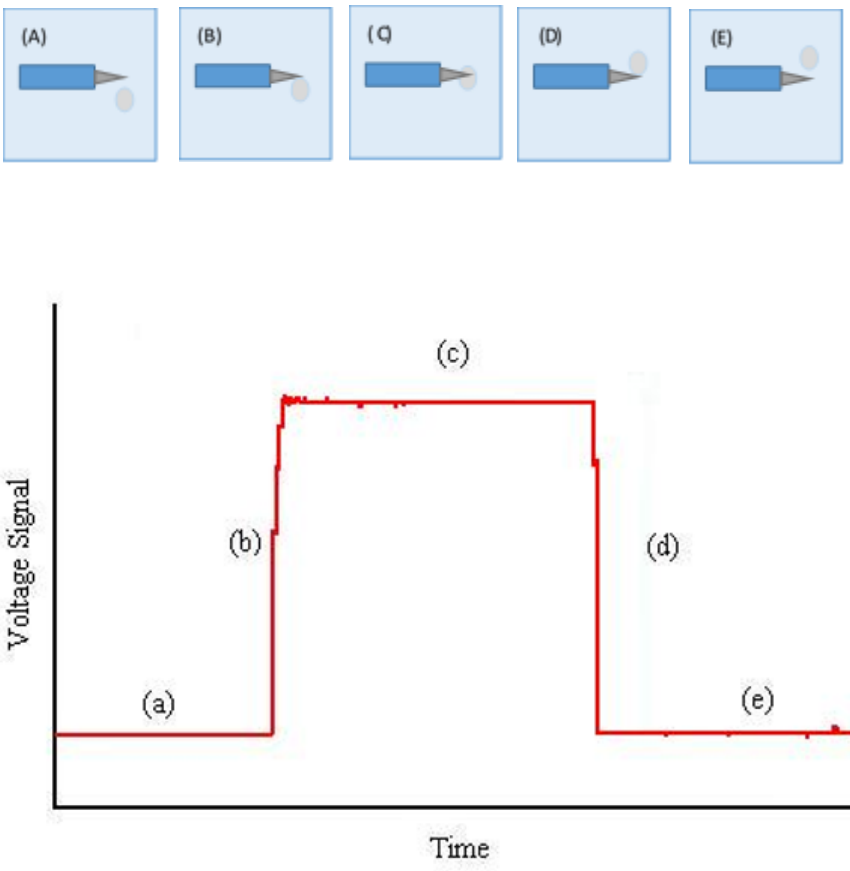

Figure 6. The step response of a bubble striking a single probe tip.

The Figure 6 (a) and (e) shows the probe response inside the water, (c) shows the response inside the gas, (d) and (e) shows the gas bubble entering and leaving the tip, basically it defines gas-liquid interface.

2.3 DESIGN AND FABRICATION OF TWO-TIP OPTICAL PROBE

The fiber optical cable used in this study is made up of quartz glass core with a diameter of 200 µm, with silicon cladding to make total diameter to 380 µm, and a protective layer of Teflon makes overall diameter 600 µm A 200 cm length of fiber optical is taken and peeled from one edge to leave 2 cm quartz glass core A small fire

flame is used to make arc-shaped pointed tip with the length of about 0.02 cm quartz glass The single fiber optic cable is cleaned and then tested with the water and gas environment to make sure to get clear gas and liquid signal. This probe and the technique components are manufactured at multiphase reactors engineering and applications laboratory (mReal) in Missouri University of Science and Technology.

Two fiber optical cable are arranged in geometrical configuration as shown in Figure 7. The fibers are then glued to 1/8 stainless steel tubing for insertion into the reactor.

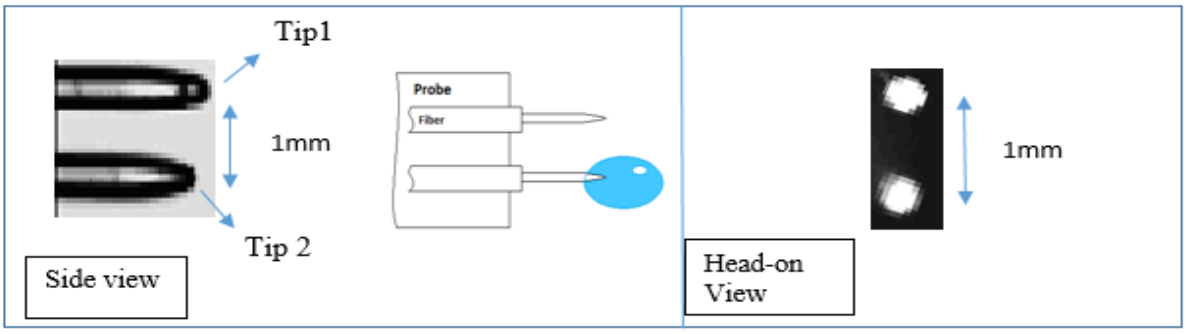

Figure 7. Orientation of Two-Tip Optical Probe

(a) (b)

Figure 8. (a) Two-tip optical probe (b) Placement of two-tip optical probe at local locations inside packed bed

The assembly of two fiber optical cables in this manner is called two-tip fiber optical probe Figure 8a. It can be placed at desired local radial and axial locations inside the packed bed as shown in the Figure 8b.

3. PARAMETERS MEASURED FROM TWO-TIP OPTICAL PROBE

The typical signal obtained from the two-tip optical probe is shown in the Figure 9. The graph depicts the time series signal received from the both the tips. The y-axis is the voltage signal generated and the top band signals having higher voltage represent the time when gas phase was on the tip surface and similarly the bottom band represents the time when the liquid phase was on the tip surface. From the time series signal shown in the Figure 9 different parameters to quantify local flow dynamics are measured using developed algorithm. The parameters measured are as follows.

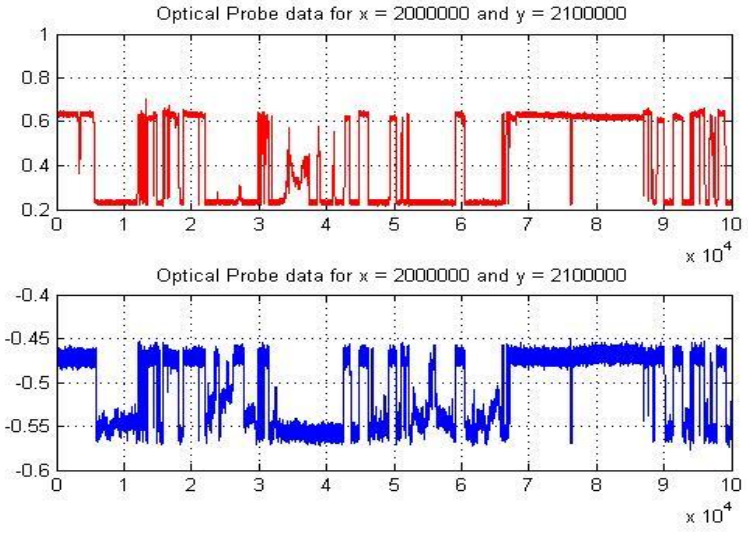

Figure 9. Raw Signal Obtained from Two-Tip Optical Probe

Local Gas Saturation: It is the local gas holdup concerning the gas-liquid mixture present in the catalyst void space for a two-phase flow through packed bed system. It is defined as the fraction of volume occupied by the gas in the catalyst void space where there is flow of gas-liquid phase.

$$\varepsilon_{G,local} = \frac{V_{G,local}}{V_{L,local} + V_{G,local}} \quad (1)$$

The ergodic hypothesis says that the ensemble average is equivalent to time average, spatially volume time average can be replaced by time average holdup. Hence, time average holdup is the ratio of time spent by gas on the probe tip surface by the total measurement time when gas or liquid phase are on the probe tip surface.

$$\varepsilon_{G,local} = \frac{t_G}{t_G + t_L} \quad (2)$$

Local Liquid Saturation: It is the local liquid holdup with respect to gas-liquid mixture within the catalyst void space of packed bed reactor. The summation of local saturation of both phases in the void space should be one as the probe only detects the flow of gas or liquid phase in the measured region. Hence, to obtain local liquid saturation subtract local gas saturation from one.

$$\varepsilon_{L,overall} + \epsilon_{G,overall} = 1$$

$$\varepsilon_{L,overall} = 1 - \epsilon_{G,overall}$$
$$\varepsilon_{L,local} = 1 - \epsilon_{G,local}$$

(3)

Local Gas Velocity: The two-tip optical probe is designed in such a way to obtain local phase velocity. The velocity as by definition is the distance traveled divided by the time taken to travel that much distance. In our case the two tips are placed at a distance of 1 mm and so the only requirement here is to determine the time taken by the bubble to travel this distance between the tips. Figure 10 shows the schematic of probe response to illustrate local velocity calculations.

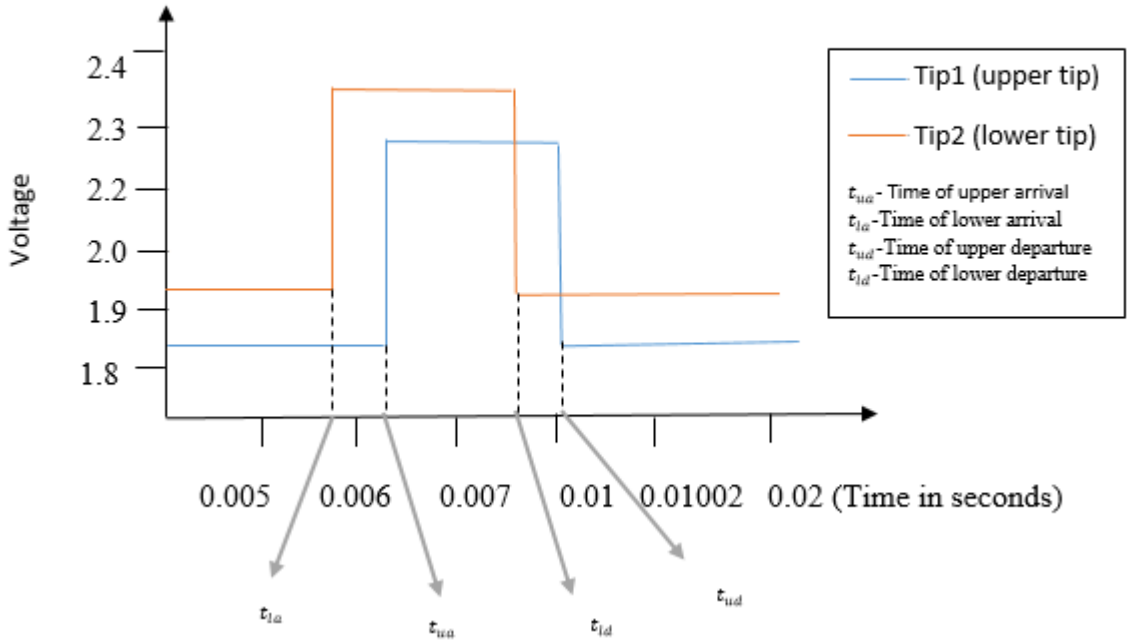

Figure 10. Schematic of Probe Response of Two-Tips of Optical Probe

The two tips are categorized as lower and upper based on their geometrical orientation. In the above case, the tip 2 is the lower as it is placed below tip 1. tla is the time when a bubble first touches the lower probe or tip 2, and tua isthe time at which the same bubble touches the upper probe or tip 1. The time difference (tla-tua or (tua-tla) will give the time taken by the gas bubble to travel 1mm, which is the distance between two tips. Hence the local gas velocity is given as:

$$V_{G,Local} = \frac{1mm}{t_{la} - t_{ua}} \quad (4)$$

For gas-liquid upflow through packed bed (tua − tla) , and for downflow (tla − tua) is used in equation 4. When the gas-liquid flow is in the opposite direction to general flow negative time difference values are observed. The detailed discussion of negative velocities are in Section 7.

Local Liquid Velocity: To measure liquid velocity the time taken by the liquid to travel the distance between two tips is calculated. As the interested measurement zone only has gas and liquid phase. Hence, it means that as soon as the gas departs from the tip, the liquid will arrive or the difference between departure times of gas bubble will give the time taken by the liquid to travel the distance of 1mm. From Figure 10 tld and tud is the time at which the gas bubble departs from the respective tips of the probe. Hence local liquid velocity can be given as:

$$V_{L,Local} = \frac{1mm}{t_{ld} - t_{ud}} \quad (5)$$

Here also if the general direction of gas-liquid phase is upflow then (tud −tld) or in case of downflow (tld − tud) is considered in equation 5.

4. PROCEDURE TO DETERMINE LOCAL HYDRODYNAMIC PARAMETERS FROM TWO-TIP OPTICAL PROBE

4.1 RAW SIGNAL

The total measurement time for one set of experiment is 52 seconds, in this duration approximately 3,000,000 signal data points are generated. It is hard to visualize the whole set of data in one frame. Hence, total data points are split into different frames with each frame containing 100,000 data points. Then the

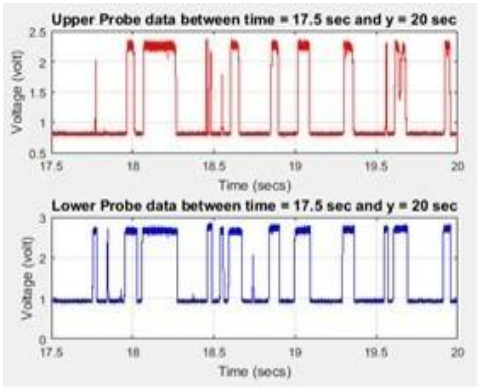

(a)

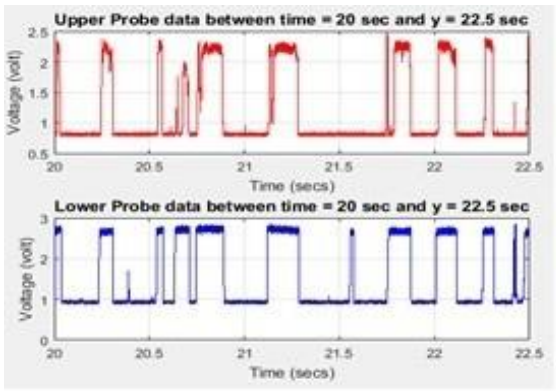

(b)

Figure 11. (a) Raw Time Series Data of The Frame Between 17.5 Sec And 20 Sec (B) Raw Time Series Data of The Frame Between 20 Sec And 22.5 Sec

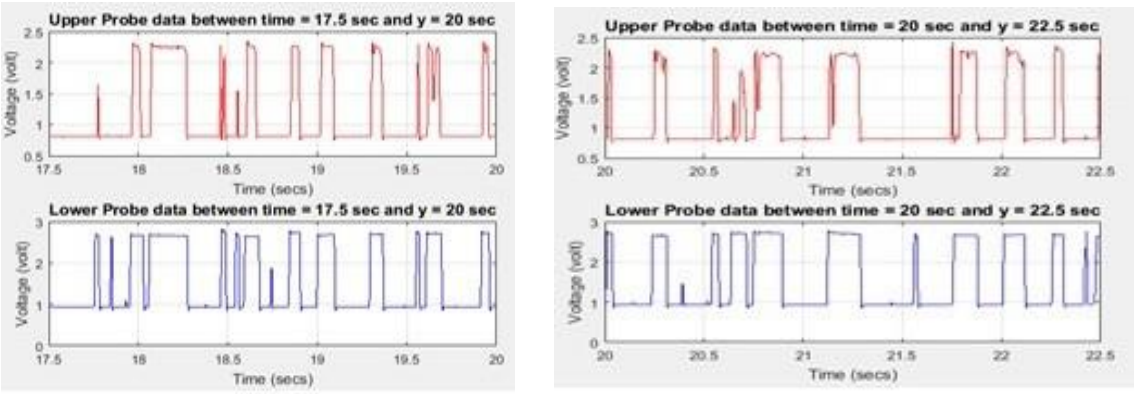

(a) (b)

Figure 12. (a) Filtered Time Series Data of the Frame Between 17.5 Sec And 20 Sec (b) Filtered Time Series Data of the Frame Between 20 Sec And 22.5 Sec

Data points are converted to sampling time based on the sampling frequency, and each frame which is part of one set of measurements will represent different time slots as show in Figure 11.

4.2 FILTERED SIGNAL

The raw signal has noises associated with it as seen in the Figure 11. These noises are mostly due to electronics of data acquisition (DAQ) ports. It is reduced by designing a low pass filter and passing the raw signal through it. Figure 12 shows the filtered signal.

4.3 SMOOTHING OF FILTERED SIGNAL

The filtered signal is smoothed for clear cut demarcation of gas and liquid bands. It is accomplished by assigning a threshold voltage value above which all signals are considered gas phase and below are considered as the liquid phase. The gas phase will be

assigned value one and liquid phase will be assigned value of zero. The histogram plot of raw signal is generated to obtain threshold voltage value. Figure 13 represents the histogram plot of both upper and lower probe signal and each probes signal has two peaks. The peak on the left represents the liquid phase, and the peak on right represents gas phase. These peaks shape varies, and the number of occurrences varies based on the flow conditions. In the case shown in Figure 13 the number of occurrences of the liquid band is more as compared to gas bands. The threshold voltage value is taken as the voltage at which the peak of liquid region drops. In Figure 13a for the upper probe signal the threshold voltage value is 1 and similarly in Figure 13b the threshold voltage value for the lower probe is 1.2. The threshold values are changed from 1 to 1.5 in upper probe signal and 1.1 to 1.5 in lower probe signal and minimal variation in results are seen. For standardization, the voltage at which the first drop for the liquid region is observed is taken as the threshold voltage.

Figure 14 represents the smoothened signal, and all the gas bands are as- signed value of one and liquid bands are allocated value of zero. The smoothened signal will give the exact time when the gas bubble touches the tip of the probe and the exact time when it leaves the tip of the probe.

4.4 DETERMINATION OF LOCAL GAS AND LIQUID SATURATION

The usage of the optical probe in measuring local gas and liquid holdup was done by Wang et al. (2003) in a fluidized bed and Xue et al. (2008) in a bubble column. They all used the ergodic hypothesis to determine the local holdup of phases. According to ergodic hypothesis volume fraction of flowing phases is equivalent to time spent by the

phases in those regions. Hence, the local holdup is measured by dividing the time spent by the gas or liquid phase with total measurement time. In packed bed reactor, the same procedure is applied, but the obtained values are not local holdups but rather local saturations. It is because the tip in the void space of packed bed only senses gas or liquid phase and quantifies the amount of time spent by gas and liquid phase in this regions. The solids are not moved and are not detected by these probes. The wetting factor in local void space is directly proportional to local liquid saturation.

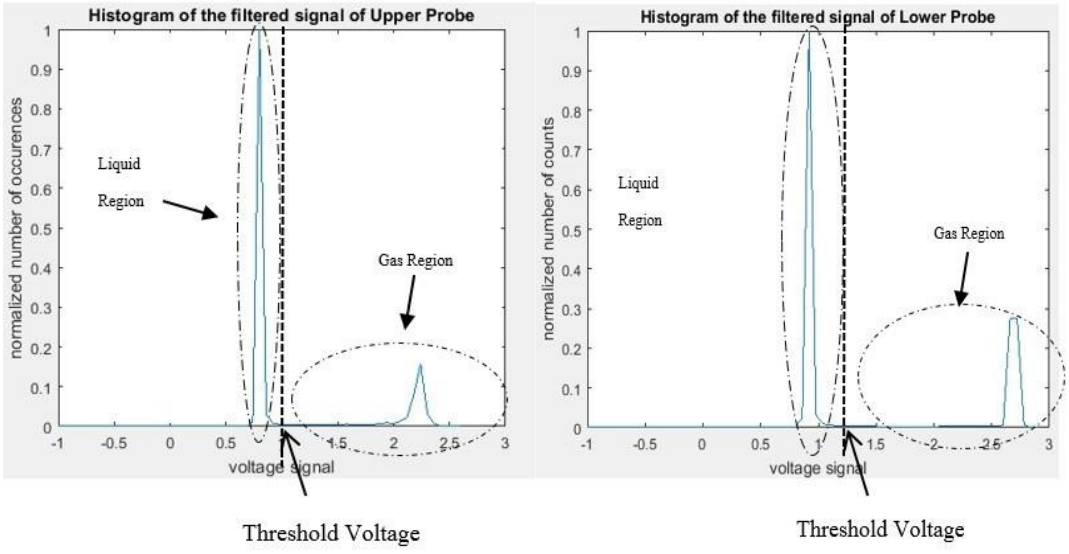

(a) (b)

Figure 13. The histogram plot of raw signal; (a)For the upper probe (b) For the lower probe

The smoothened signal is used to calculate local gas and liquid saturation. The total time is calculated when the signal value is one. This time and the total measurement time is fed to Equation 2 to calculate local gas saturation. Then using local gas saturation in Equation 3 to calculate local liquid saturation.

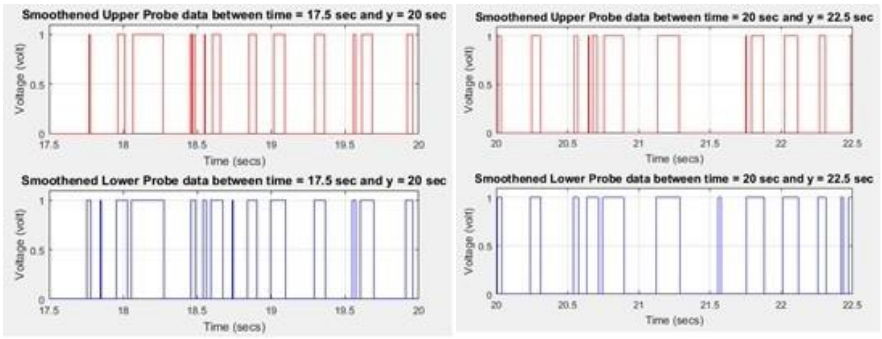

(a) (b)

Figure 14. Smoothed Signal of Filtered Data of Two-Tip Optical Probe; (a) For Time Frame 17.5 Sec To 20 (b) For Time Frame 20 Sec To 22.5

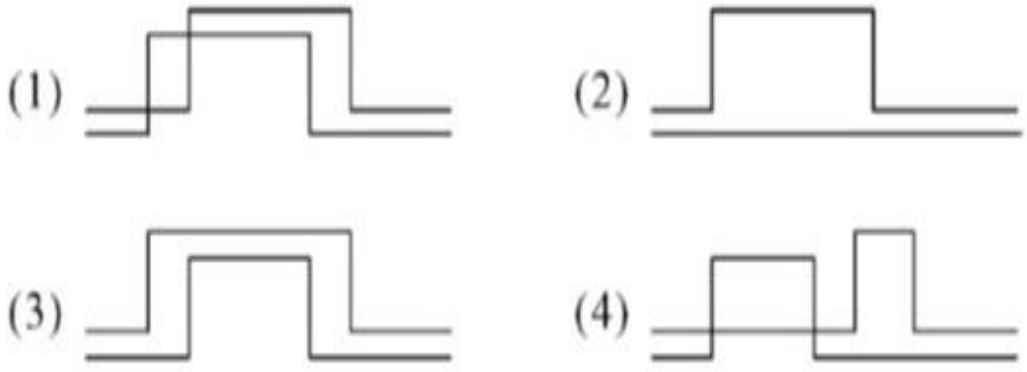

Figure 15. Detected bubbles and validation test: (1) accepted, (2) rejected, (3) rejected, and (4) rejected (Magaud et al. (2001),Aloui & Souhar (1996)

4.5 DETERMINATION OF LOCAL GAS AND LIQUID VELOCITIES

Smoothed data as shown in Figure 14 is used to determine the local velocity parameter of phases, as smoothed data clearly demarcates the gas and liquid region by the voltage value of one and zero. As seen in the equation 4 and 5, to obtain local velocity we need the time of arrivals and time of departures of the bubble in both the tips. To find the

arrival and departure time of bubble an algorithm is developed to track the transition of the voltage value from zero to one in the entire smoothed time series, and this gives us the time of arrival of bubbles. Similarly, the developed algorithm tracks the transition from one to zero to determine the time of departures of bubbles. The complication here is to select the same bubbles which touch both the tips to determine local velocity, as there is the possibility of bubble deviation due to the local force field. Signal selection criteria are to be set to filter out the tracked bubble which can give us the local velocities. In work done on bubble column using the optical probe, Magaud et al. (2001) followed acceptance-rejection algorithm of Aloui & Souhar (1996) on the selection of signals to detect the bubble velocity (Figure 15). The acceptance-rejection algorithm works on the assumption that the bubble chord length is larger than the distance between two tips. This selection criterion may not work in packed bed reactors.

Hence, a new criterion is developed in which all the tracked bubble are filtered out through a condition that the absolute time difference of time of arrivals and time of departures of both the tips shall fall below certain threshold time-limit. This time-limit is determined at the lowest flow rate of phases, all the tracked bubbles at these conditions are visually analyzed and maximum time difference when the same bubble touches both the tips are measured.

This maximum time difference value is the threshold time-limit. The tracked bubble which is not falling in this time-limit is not considered for velocity calculations. It is assumed that the for higher flow rates the same bubble which touch both the tips shall fall below threshold time limit.

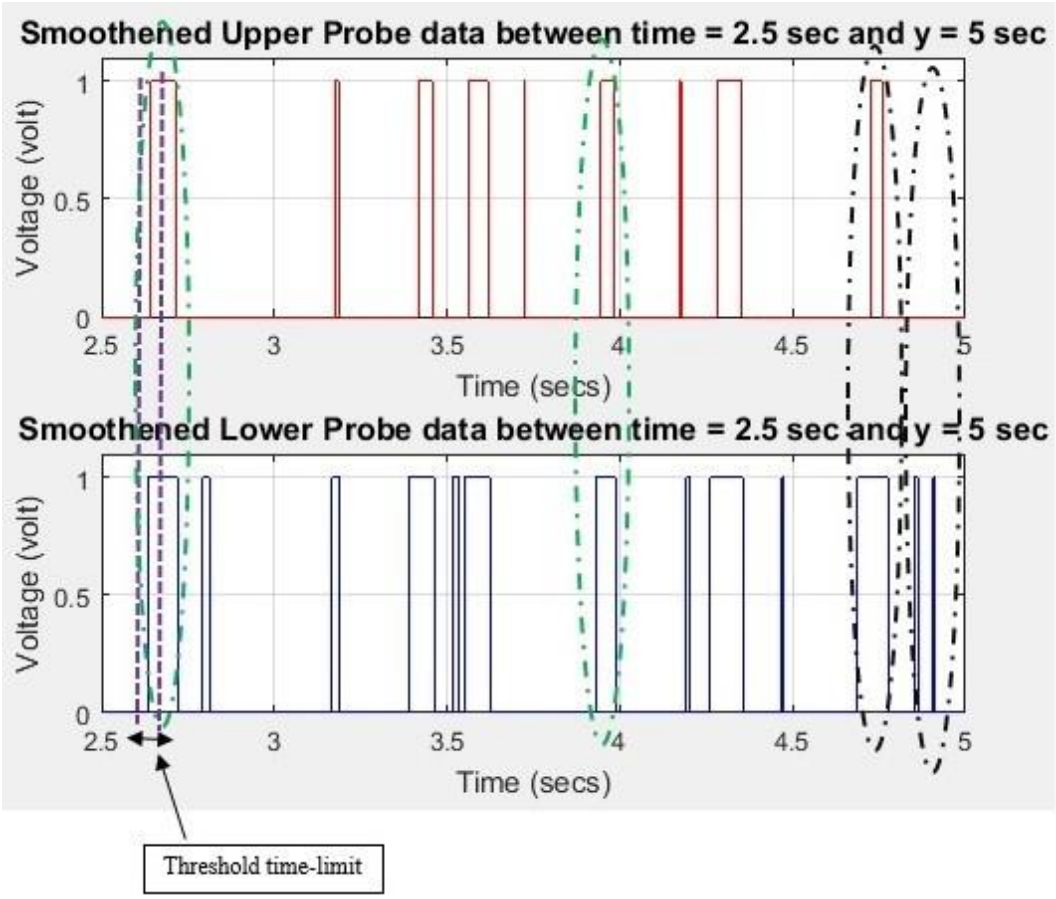

Figure 16. Selection Criteria for Local Gas Velocity Calculation in Two-Tip Optical Probe; Bubbles Similar to Green Circled are Accepted and Bubbles Similar to Black Circled are Rejected

As shown in the Figure 16, the bubble similar to as circled in green is selected to find local gas velocity, as the time difference of arrivals of the same bubble in both the tips falls below the threshold time-limit. Bubbles similar to as circled in black does not satisfy the selection criteria; hence they are rejected from velocity calculations. Similarly, in Figure 17 the bubble similar to as circled in green is selected to find local liquid velocity as the time difference of departures of the same bubble in both the tip falls below the threshold time-limit. Bubbles similar to the black circled one are rejected in this case for failing to match the selection criteria.

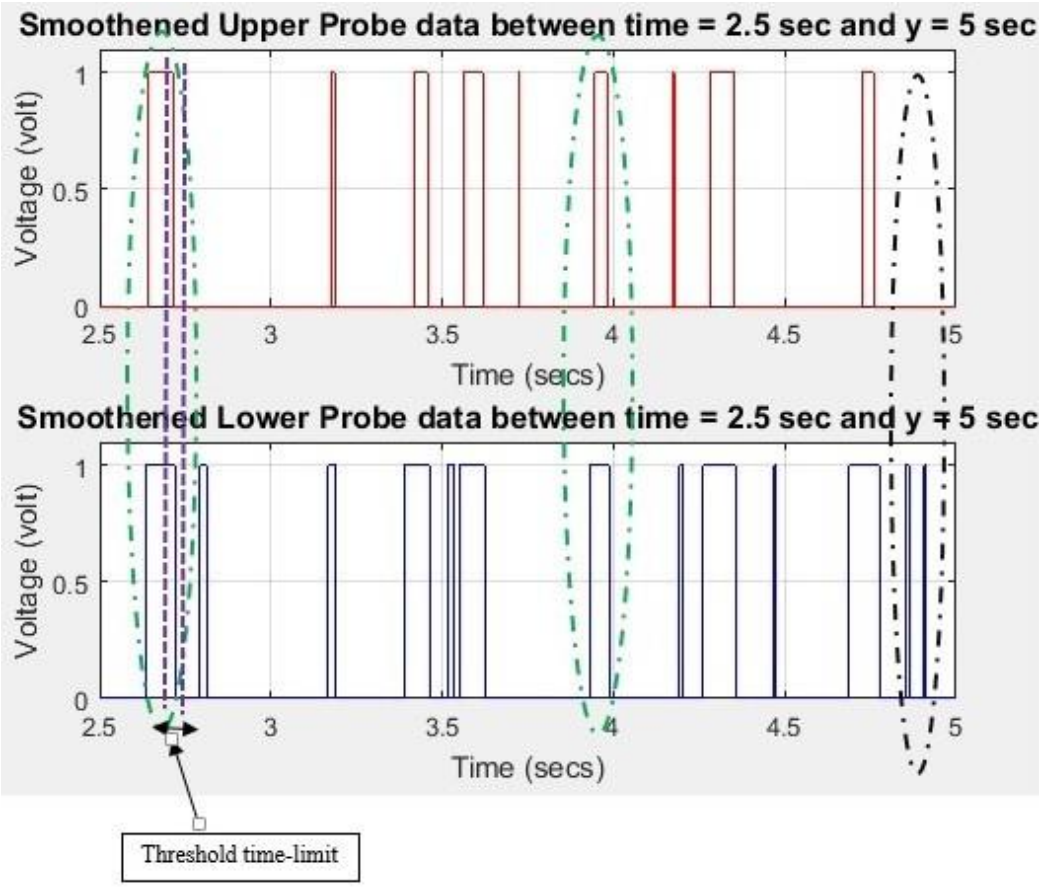

Figure 17. Selection Criteria for Local Liquid Velocity Calculation in Two-Tip Optical Probe; Bubbles Similar to Green Circled are Accepted and Bubbles Similar to Black Circled are Rejected.

Additionally, the developed algorithm will make sure that even under the threshold time-limit conditions no bubbles are repeated. It means all matched bubbles for velocity calculation will have a unique time of arrivals or time of departures, such that no two sets of matched signal have a common time of arrival or departure. Time of arrivals and departures of matched signal obtained after filtering thorough matching conditions is used in equation 4 and equation 5 to get local gas and local liquid velocity respectively.

5. VALIDATION OF TWO-TIP OPTICAL PROBE TECHNIQUE

5.1 VALIDATION WITH X-RAY DIGITAL INDUSTRIAL RADIOGRAPHY TECHNIUQE (DIR) MOHD SALLEH ET AL. (2014), MOHD SALLEH (2014)

A 2inch trickle bed reactor setup packed with 3mm EPS beads was developed by (Mohd Salleh (2014) to determine the local liquid velocity using X-Ray Digital Industrial Radiography Technique, which is the combination of digital industrial radiography (DIR) and particle tracking velocimetry (PTV).

The detailed information of this technique and the procedure to measure local liquid velocity is given in (Mohd Salleh (2014), Anuar Mohd Salleh et al. (2015)). The location for measuring local liquid velocity using optical probes are Z/D=3.3,3.9, and 4.5 as shown in Figure 18. Whereas Z is the axial height from the top of the reactor and D is the diameter of the column. The superficial liquid and gas velocities used in this experiment were 0.003m/s and 0.052m/s respectively.

The axial locations are divided into three smaller locations radially as shown by the blue dashed circle in Figure 19. In these sites, optical probes are placed, and local liquid velocities are measured. The data of X-Ray digital industrial radiography technique is time averaged at these dashed circle locations (Figure 19) to obtain local liquid velocities.

The local velocities data measured from both the techniques are compared and statistically tested using a t-test to check how significantly close or different are two sets of data. The detailed description of statistical testing on this set of data is given Mohd Salleh et al. (2014)

The t-Test is conducted with p-value set at 0.05 ($\alpha = 0.05$), and the results are tabulated in Table 1. If the p-values are less than 0.05 then both set of data different, conversely if the p-value is greater than 0.05 then there is not enough proof statistically to differentiate both sets of data or group. The table 1 shows the p-values are greater than 0.05, which means both the technique data on local liquid velocities are same and falls in same group.

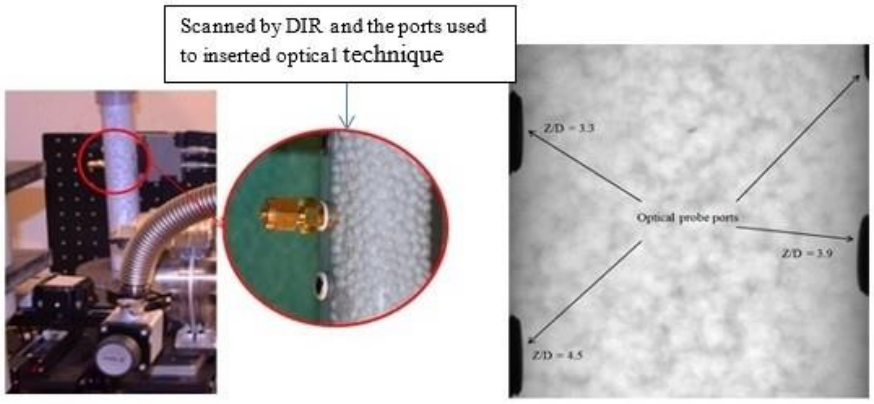

Figure 18. The Two-inch TBR Setup with (a) Fiber Optic Probe and (b) Radiographic Image Port Located at each Z/D Mohd Salleh (2014)

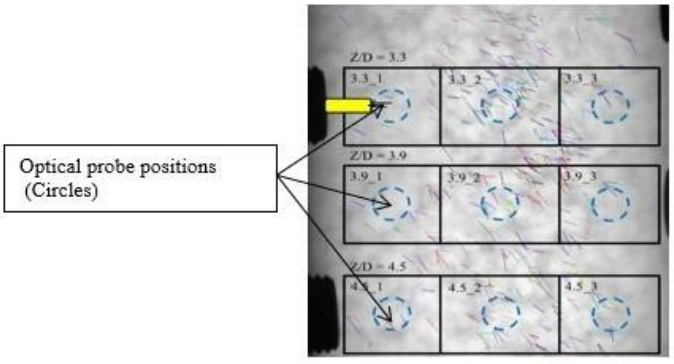

Figure 19. Localized Position of Optical Probe and whole section scanned by DIR (Mohd Salleh (2014))

Table 1 Comparison between Mean, Standard Deviation (σ), Variance (σ2), Degree of Freedom (df), t-Value, and p-Value (α level 0.05) Generated by Statistical Analysis Software (SAS) between the Measured ULL(OP) by Optical Probe (OP) And ULL(DIR) by X-Ray Digital Industrial Radiography (DIR) in a Two-inch TBR (Blue Dashed Circle).(Mohd Salleh (2014))

Location	$ULL(OP)$			$ULL(DIR)$			t-test		
	mean	σ	σ^2	mea	σ	σ^2	df	t	p
	Z/D=3.3								
3.3(1)	7.33	0.1	0.03	5.49	1.64	2.67	3	1.5	0.23
3.3(2)	9.05	0.1	0.03	6.97	4.05	16.4	16	0.84	0.41
3.3(3)	8.50	0.1	0.03	7.46	5.27	27.8	5	0.29	0.78
	Z/D=3.9								
3.9(1)	6.62	0.1	0.01	8.12	0.00	0.00	2	9.02	0.01
3.9(2)	8.90	0.3	0.10	8.04	4.08	16.7	10	0.33	0.75
3.9(3)	8.43	0.1	0.02	7.85	1.97	3.86	6	0.2	0.85
	Z/D=4.5								
4.5(1)	8.47	0.2	0.06	7.45	4.6	21.2	3	0.4	0.72
4.5(2)	6.58	0.2	0.05	9.98	5.06	25.6	7	1.02	0.34
4.5(3)	8.03	0.0	0.00	6.93	2.97	8.82	7	0.84	0.43

5.2 VALIDATION WITH KNOWN LIQUID VELOCITY

A syringe filled with water is attached to a pump. The pump can push the liquid at desired flow rate. The two-tip optical probe is validated using this syringe pump assembly as shown in Figure. The TTOP is placed just below the syringe pump. The pump is set to get three different liquid flow rate of 0.1, 0.2, and 0.3 ml/min. The actual velocity at which water leaves the syringe is calculated from the volumetric flow rate and cross-sectional area. The liquid velocity is also calculated with TTOP and compared with actual liquid velocity as shown in Table 2. The Ula is actual superficial liquid velocity and Ulm are measured liquid velocity using TTOP. The results indicate the measured

velocity from the probe deviates from actual velocity at maximum of around (+10%/ − 10%).

Figure 20. Syringe Pump with Two-Tip Optical Probe

Table 2 Comparison of Actual and Measured Liquid Velocity

Flow Rate (ml/min)	Ula (cm/s)	$Ulm(1)$ (cm/s)	$Ulm(2)$ (cm/s)	$Ulm(3)$ (cm/s)	Mean (cm/s)	Percentage Deviation
0.1	0.05	0.043	0.048	0.047	0.046	-8.02%
0.2	0.11	0.103	0.117	0.123	0.114	3.9%
0.3	0.16	0.169	0.168	0.164	0.167	4.34%

6. EXPERIMENTAL SETUP

The experimental setup shown in Figure 21 consists of Plexiglas column of 0.14 m internal diameter and 1.83m height. The glass beads of 0.003m diameter were randomly packed. Deionized water with a temperature of about 70^{o}F was used as the liquid phase, and the inlet pressure was maintained at 20 psi. Dry air supplied by high pressure and high capacity compressor was used as the gas phase.

The water is circulated to the column from the top and flows downward and then to water collection tank (water motor pump model; 503186, 3E-12NT from Little Giant Pump Company). Valves controlled both liquid and gas flow rates and measured by two types of Rotameters (Dwyer Instruments, USA, Model RMC-102-SSV and RMC-106-SSV flowmeter range 10-100 SCFH air and 100- 1000 SCFH air for the gas flow meter and liquid flowmeter model FL-75E from Omega flow rate range 1.5-15GPM).

The glass beads are used to fill the column to the top which acts as a bed for trickle bed reactor. The optical probes are inserted into the column through 0.635 cm diameter portholes provided along the axial height of the column. The measurements are carried out at the center of the reactor (r/R=0), and three axial locations Z/D= 2, 5, and 7 (Figure 21). Whereas r is the radial position from the center, R is the total radius of the column, Z is the height from the bottom of the reactor, and D is the diameter of the column.

The liquid and gas superficial velocity are 0.09m/sec and 0.004m/s to 0.016m/s and it is seen that this range produce a change of flow regime from trickling to pulse flow. All measurement experiments were replicated three times.

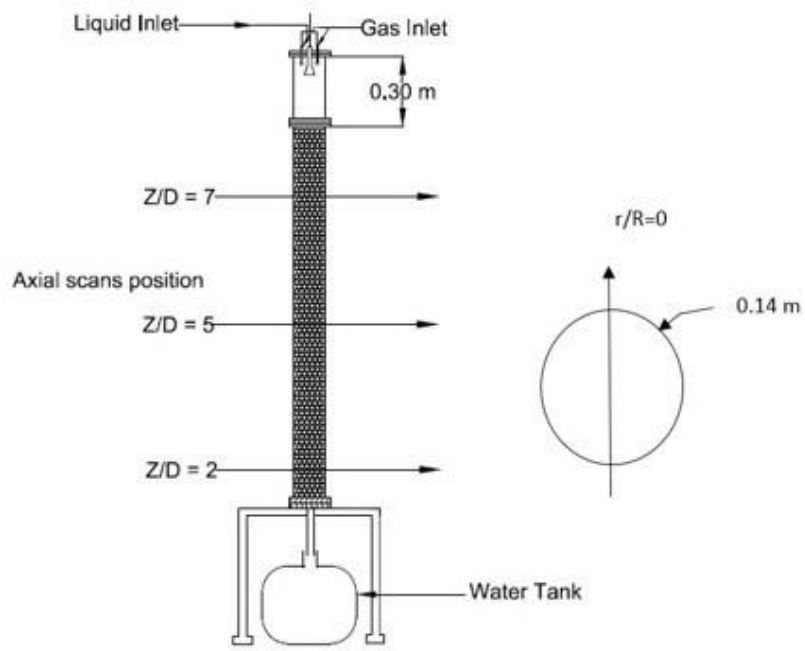

Figure 21. Schematic Diagrams of Optical Probe Measurement Points with Axial and Radial Scan Locations.

7. RESULT OF LOCAL LIQUID AND GAS VELOCITY

Local velocities are measured at various axial positions (Z/D=2, 5, 7) and the center of the bed (r/R=0). As discussed in the Section 4.5 the developed algorithm tracks all the bubble which touches both the tips to find local velocities. In this condition, we observed sometimes getting negative velocities, which indicates that at particular force field in these locations there is a reversal of flow of phase or there is back mixing of phases. The positive velocity indicates that the flow of phases is with the general flow conditions. The zero velocity are also obtained which represents the condition at which either the entire void space is covered with the liquid or gas or bubbles are deviating without touching both the probes simultaneously. Figure 22 shows the number of occurrences of local liquid velocity in terms of positive, negative and zero velocities.

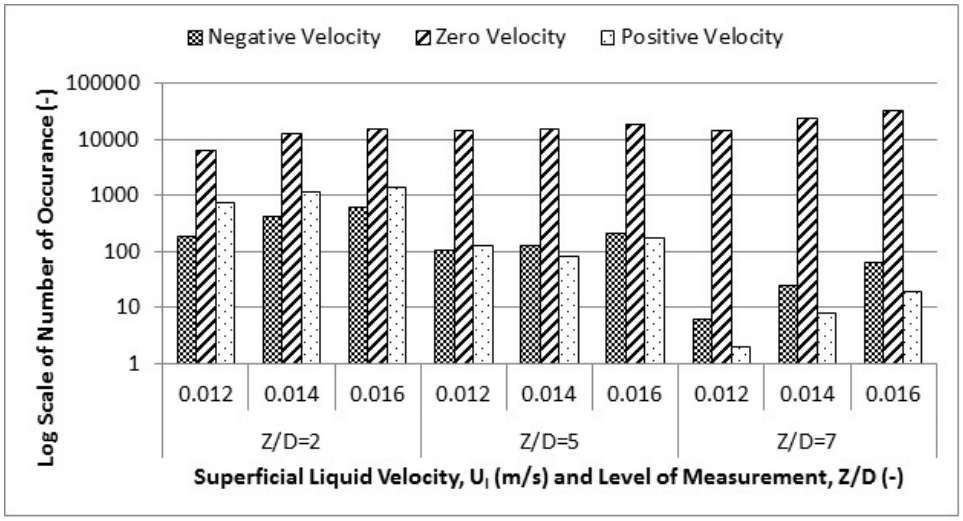

Figure 22. Number of Occurrences Liquid Velocities at Different Axial Locations and Varying Flow Conditions

It is seen at most of the time at all locations and operating conditions the number of occurrences of zero velocity is higher than compared to positive and negative velocity, and the trend is decreasing as we down up the reactor and decreasing the liquid flow rate. It infers that mixing in local areas at the center of the reactor improves as we move down the reactor. Regarding negative velocity the back-mixing was seen less at the top of the reactor and it is seen increasing as we move down the reactor. The possible explanation is the pressure forces arising due to the effect of the distributor, as on moving down the column distributor effects are reduced. The histogram of local liquid velocities are plotted in Figure 23. The results show large distribution in velocity ranges and it shows the complexity or non-homogeneous distribution of measured local liquid velocity observed at local locations. The most dominating positive local liquid velocity is in the range of 0 − 5m/sec at all locations and operating conditions. These findings of local liquid velocity

distribution are in good agreement with techniques such as wire mesh tomography (Schubert et al. (2010b)) and MRI (Sankey et al. (2009)).

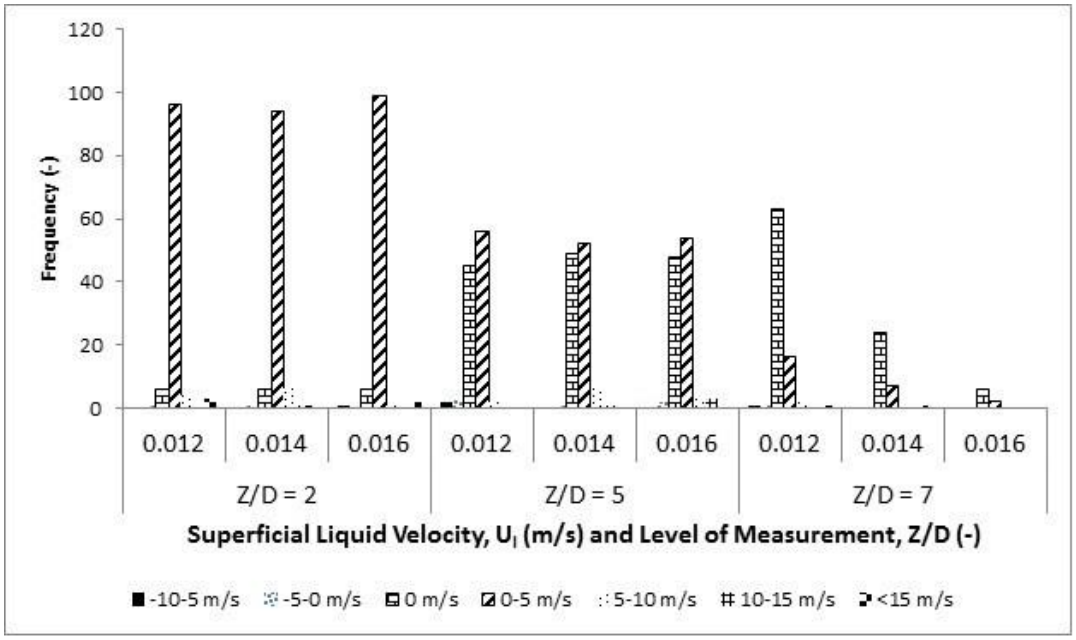

Figure 23. Range of Liquid Velocities at Different Axial Locations and Varying Flow Conditions

Figure 24 shows the number of occurrences of measured local gas velocities. In this case also, we observed occurrences of positive, negative and zeros velocities. The trend is similar to what we have seen in local liquid velocities. The back-mixing is seen to be more at the bottom and explanation is similar to local liquid velocity as the force field dictating the movement of both the phases are same. Figure 25 shows the velocity distribution of local gas velocity. Similar to local liquid velocities the gas phase also shows non-homogeneous gas distributions, with the most dominating positive velocity

range of 0 − 5m/sec. The similar trend is due to the no-slip conditions arising at local void space of packed bed.

8. RESULT OF LOCAL LIQUID AND GAS SATURATIONS

Local liquid and gas saturation's are the local liquid and gas holdup in the local void space of the catalyst bed section. Local saturations give the amount of volume occupied by a gas or liquid phase for a particular period in the local void space of the catalyst packing. These local saturation's values are not equivalent to local holdups of the entire reactor because this does not take solid catalyst into consideration, as to determine local holdups in three phase systems all phases should be taken into considerations. For a two-phase system of gas- liquid, local saturation measured from optical probes (Kagumba & Al-Dahhan (2015), Xue et al. (2008)) are equivalent to local holdups. The measurement principle to determine local saturation's are discussed in section 4.4. The two tips generate two local saturation value at each local locations. The average values of two tips are taken and plotted.

Figure 26 shows the local liquid saturation values at the various axial location and varying liquid flow rate. Liquid saturation value of 0.55 means on an average 55 percent volume of the local void space is occupied by the liquid and 45 percent volume is occupied by gas during the measurement time. It is seen that the values of liquid saturations are increasing on increasing the liquid flow rate. It means the wetting of catalyst at these local location increases with increasing liquid flow rate. The center location (r/R=0) seems to have good distribution of liquid and gas along the axial direction as local liquid saturation's are not much varying along the axial length at these

flow conditions. Local gas saturation's are obtained by subtracting local liquid saturation from one. Figure 27 shows the local gas saturation plot at similar condition.

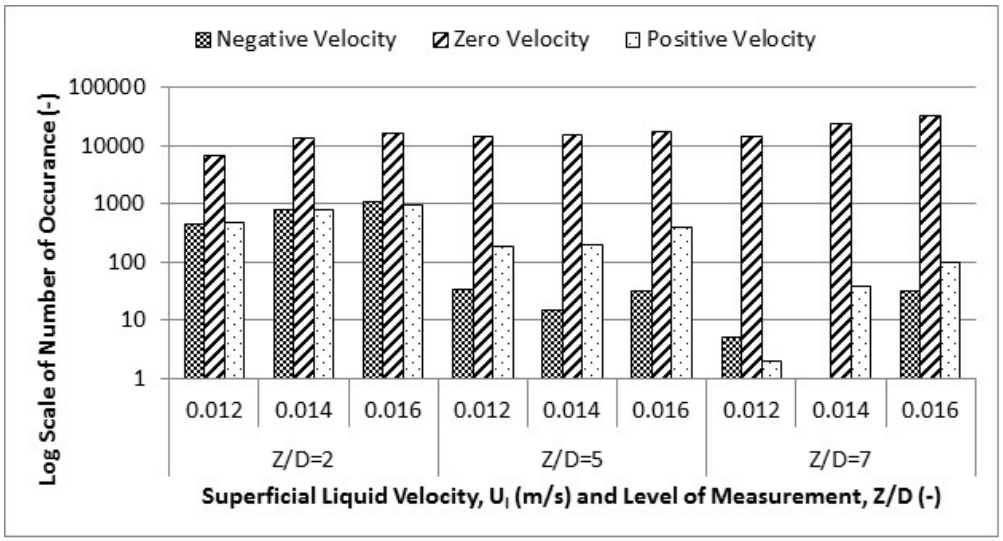

Figure 24. Number of Occurrences Gas Velocities at Different Axial Locations and Varying Flow Conditions

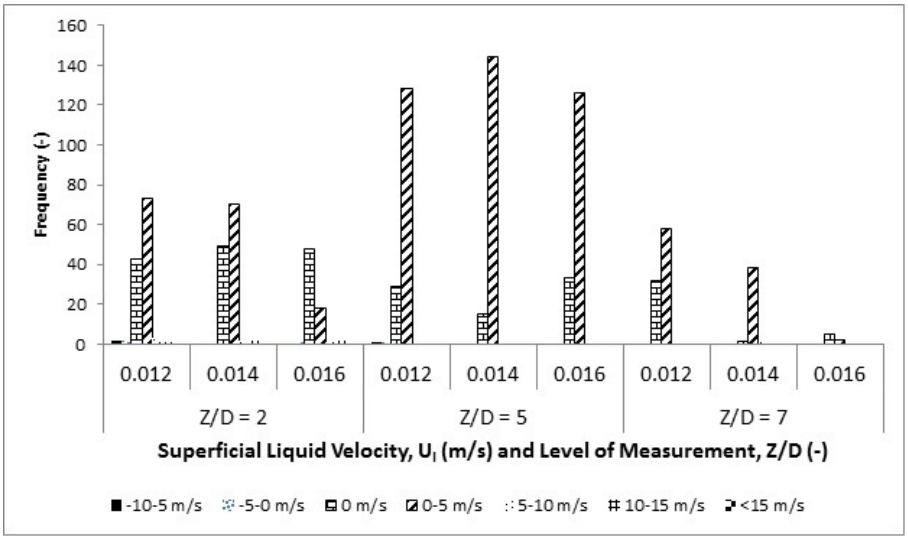

Figure 25. Range of Gas Velocities at Different Axial Locations and Varying Flow Conditions

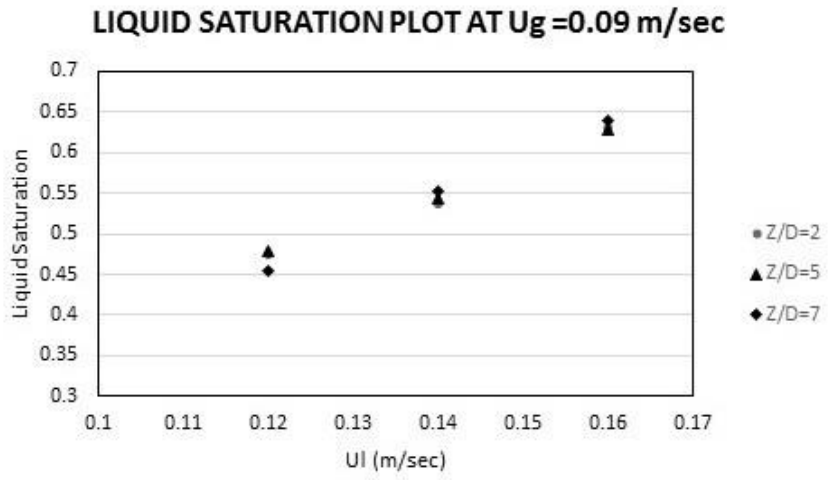

Figure 26. Liquid Saturation Values at Different Axial Location and Varying Liquid Flow Condition

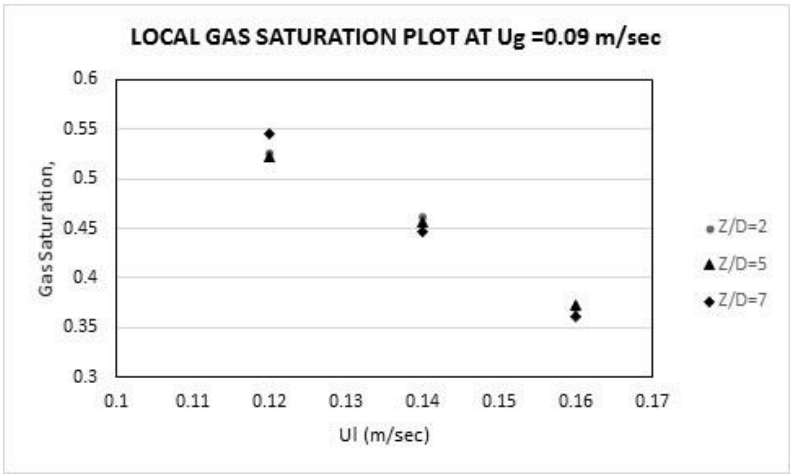

Figure 27. Gas Saturation Values at Different Axial Location and Varying Liquid Flow Condition

9. REMARKS

Two-tip optical probe measurement technique is developed to quantify the local flow dynamics in packed bed reactors. It is implemented on a trickle bed reactor and

successfully measured the local liquid and gas velocities and saturations using developed algorithms. This technique is validated with Industrial X-Ray Digital Radiography Technique (DIR) (Mohd Salleh et al. (2014)). The local liquid flow dynamics measured using the two-tip optical probe in a trickle bed reactor are in good agreement with experiments by Schubert et al. (2010b) and Sankey et al. (2009). For the first time that local flow dynamics of both gas and liquid phase have been investigated for packed bed reactor.

ACKNOWLEDGEMENT

The authors acknowledge the Kuwait Institute of Scientific Research (KISR) and Malaysian Ministry Of Science and Technology (MOSTI) for the financial support. Sincere appreciation to Dean Lenz from the Chemical and Biochemical Engineering Department, Missouri University of Science and Technology for design and installation of the experimental setup. Also, authors are thankful to the fund provided by Prof. Al-Dahhan to support this experimental work.

REFERENCES

Al-Dahhan, M. H., & Dudukovi´c, M. P. (1994). Pressure drop and liquid holdup in high pressure trickle-bed reactors. *Chemical Engineering Science*, *49*, 5681–5698.

Al-Dahhan, M. H., Larachi, F., Dudukovic, M. P., & Laurent, A. (1997). High-Pressure Trickle-Bed Reactors: A Review. *Industrial and Engineering Chemistry Research*, *36*, 3292–3314.

Aloui, F., & Souhar, M. (1996). Experimental study of a two-phase bubbly flow in a flat duct symmetric sudden expansion - Part II: Liquid and bubble velocities, bubble sizes. *International Journal of Multiphase Flow* , *22* , 849–861. URL:

Anuar Mohd Salleh, K., Koo Lee, H., & Al-Dahhan, M. H. (2015). Studying local liquid velocity in liquid-solid packed bed using the newly developed X- ray DIR technique. *Flow Measurement and Instrumentation*, *42* , 1–5.

Boyer, C., & Fanget, B. (2002). Measurement of liquid flow distribution in trickle bed reactor of large diameter with a new gamma-ray tomographic system. *Chemical Engineering Science*, *57*, 1079–1089.

Burkhardt, M., & Busch, G. (2013). Methanation of hydrogen and carbondioxide. *Applied Energy*, *111* , 74–79.

Collins, J. H. P., Sederman, A. J., Gladden, L. F., Afeworki, M., Douglas Kushnerick, J., & Thomann, H. (2017). Characterising gas behaviour during gasliquid co-current up-flow in packed beds using magnetic resonance imaging. *Chemical Engineering Science*, *157*, 2–14.

Gladden, L. F., Lim, M. H. M., Mantle, M. D., Sederman, A. J., & Stitt, E. H. (2003). MRI visualisation of two-phase flow in structured supports and trickle- bed reactors. *Catalysis Today*, *79-80* , 203–210.

Kagumba, M., & Al-Dahhan, M. H. (2015). Impact of internals size and con- figuration on bubble dynamics in bubble columns for alternative clean fuels production. *Industrial and Engineering Chemistry Research*, *54*, 1359–1372.

Li, X., Yang, C., Yang, S., & Li, G. (2012). Fiber-optical sensors: Basics and applications in multiphase reactors. *Sensors (Switzerland)*, *12*, 12519–12544.

Magaud, F., Souhar, M., Wild, G., & Boisson, N. (2001). Experimental study of bubble column hydrodynamics. *Chemical Engineering Science*, *56* , 4597– 4607.

Meng, Y.-L., Tian, S.-J., Li, S.-F., Wang, B.-Y., & Zhang, M.-H. (2013). Trans-esterification of rapeseed oil for biodiesel production in trickle-bed reactors packed with heterogeneous Ca/Al composite oxide-based alkaline catalyst. *Bioresource Technology*, *136*, 730–734.

Mohammed, I., Bauer, T., Schubert, M., & Lange, R. (2013). Hydrodynamic multiplicity in a tubular reactor with solid foam packings. *Chemical Engineering Journal*, *231* , 334–344.

Mohd Salleh, K. A. (2014). *Local liquid velocity measurement of trickle bed reactor using digital industrial X-ray radiography* . Ph.D. thesis Missouri Uni- versity of Science and Technology.

Mohd Salleh, K. A., Rahman, M. F. A., Lee, H. K., & Al Dahhan, M. H. (2014). X-ray Digital Industrial Radiography (DIR) for local liquid velocity (VLL) measurement in trickle bed reactors (TBRs): Validation of the technique. *Review of Scientific Instruments*, *85* .

Sankey, M., Holland, D., Sederman, A., & Gladden, L. (2009). Magnetic res- onance velocity imaging of liquid and gas two-phase flow in packed beds. *Journal of Magnetic Resonance*, *196* .

Schubert, M., Khetan, A., da Silva, M. J., & Kryk, H. (2010a). Spatially resolved inline measurement of liquid velocity in trickle bed reactors. *Chemical Engineering Journal*, *158* , 623–632.

Schubert, M., Kryk, H., & Hampel, U. (2010b). Slow-mode gas/liquid- induced periodic hydrodynamics in trickling packed beds derived from direct measurement of cross-sectional distributed local capacitances. *Chemical Engineering and Processing: Process Intensification*, *49*, 1107–1121.

Sederman, A. J., & Gladden, L. F. (2001). Magnetic resonance imaging as a quantitative probe of gas-liquid distribution and wetting efficiency in trickle- bed reactors. *Chemical Engineering Science*, *56*, 2615–2628.

Sederman, A. J., & Gladden, L. F. (2005). Transition fo pulsing flow in trickle- bed reactors studied using MRI. *AIChE Journal*, *51* , 615–621.

Wang, T., Wang, J., Yang, W., & Jin, Y. (2003). Experimental study on bubble behavior in gas-liquid-solid three-phase circulating fluidized beds. *Powder Technology, 137*, 83–90.

Xue, J., Al-Dahhan, M., Dudukovic, M. P., & Mudde, R. F. (2003). Bubble dynamics measurements using four-point optical probe. *Canadian Journal of Chemical Engineering* , *81* , 375–381.

Xue, J., Al-Dahhan, M., Dudukovic, M. P., & Mudde, R. F. (2008). Bubble velocity, size, and interfacial area measurements in a bubble column by four- point optical probe. *AIChE Journal* , *54* , 350–363.

Youssef, A. A., & Al-Dahhan, M. H. (2009). Impact of internals on the gas holdup and bubble properties of a bubble column. *Industrial and Engineering Chemistry Research*, *48*, 8007–8013.

Zehraoui, A., Hassan, A. A., & Sorial, G. A. (2013). Biological treatment of n-hexane and methanol in trickle bed air biofilters under acidic conditions. *Biochemical Engineering Journal*, *77* , 129–135.

III. OVERALL DISTRIBUTION IDENTIFICATION AND EFFECT OF INLET DISTRIBUTOR ON THE PHASE HOLDUP IN A TRICKLE BED REACTOR USING GAMMA-RAY DENSITOMETRY (GRD)

Mohd Fitri Abdul Rahman, Vineet Alexander and Muthanna H. Al Dahhan

Department of Chemical and Biochemical Engineering, Missouri University of Science and Technology, 110 Bertelsmeyer Hall, 1101 N. State Street, Rolla, MO 65409, USA

ABSTRACT

Local liquid and gas maldistribution and their holdups in a packed column are difficult to identify due to multiphase properties and other design factors. Good liquid and gas flow distribution important to get high performance of Trickle Bed Reactor (TBR). Gross maldistribution indicates some faulty or bad flow distribution of liquid and gas. In this work, gross maldistribution of phases has been identified using Gamma Ray Densitometry (GRD) technique with three types of inlet distributors (single inlet towards the wall, single inlet at the center, and proper shower) by measuring line average diameter profile of phases (liquid, gas, and solids) holdups. Gamma-ray densitometry is a non-invasive technique which can be implemented at the laboratory, pilot plant and industrial scales reactors. Experiments were performed on 0.14 m diameter reactor made of Plexiglas filled with 0.003 m glass bead which acts as the solid. The superficial velocities for both gas and liquid were in the range of 0.03 m/s to 0.27 m/s and 0.004 m/s to 0.014 m/s respectively. Proper shower distributor showed early liquid spreading in comparison to other distributors. The effect of superficial gas velocity on liquid spread

was seen to be non-significant, and liquid distribution is found to be almost uniform at the center region of the catalyst bed

Keywords: Maldistribution, Trickle Bed Reactor (TBR), Gamma-Ray Densitometry (GRD)

1. INTRODUCTION

Maldistribution or inhomogeneous flow, in general, can be termed as improper flow distribution of phases along the catalyst bed in Trickle-Bed Reactors (TBRs) . In trickle bed reactor, liquid maldistribution can be classified into two categories: gross maldistribution and local maldistribution. Improper liquid distribution at the inlet causes gross maldistribution which can be minimized by proper design of the distributor. On the other hand, local maldistribution may occur due to various factors such as properties of particles (size, shape, surface roughness, etc.), the arrangement of particles, packing density, and properties of the gas and liquid phases.

Liquid distribution in (TBRs) can significantly influence its performance. Poor liquid distribution can lead to significant gas or liquid pockets, resulting in a reduced overall external mass transfer of gas or liquid reactants to the catalyst surface and lower the reactor performance. If the reaction is exothermic and comprises volatile liquid components, then the gas phase reactions in the non-wetted region can cause the formation of local hot spots leading to catalyst deactivation. Therefore, uniform distribution of the liquid at the inlet as well as in the bed is essential for achieving better performance of the reactor. There are many factors which can result in maldistribution of phases; some of them are partial wetting, flow rates of liquid and gas, non-uniform

distributor, etc. Ideal inlet distributor should dispense the liquid phase uniformly at the top of the column thus facilitating the uniformity of liquid distribution in the remainder of the bed. Proper distribution at the inlet of the bed is one of the effective ways to minimize adverse effects of the liquid maldistribution. Despite uniform distribution at the inlet, liquid maldistribution may occur along the length of the column because of other factors such as packing characteristics and bed tilt. In such cases, redistribution of liquid after a certain height of the bed is necessary to control the liquid maldistribution. It is important to note that the porous bed of catalyst particles facilitates liquid distribution. A significant portion of the bed near the liquid inlet may remain unwetted if proper distributor at the inlet is not used.

Alvarez et al. (2007) reviewed the critical role of internals including reactor inlet that could provide the initial distribution of the reactants and protection against fouling and maldistribution. Mederos et al. (2009) showed the effect of column diameter on maldistribution by reporting that in reactors larger than 0.0254 m diameter observed a significant liquid maldistribution. Various distributor designs used in the industrial TBRs are thoroughly reviewed by Maiti & Nigam, (2007).

Studies reveal that if the liquid is introduced non-uniformly at the top of the bed, the flow distribution is not likely to improve down the bed even for the conditions of the high gas velocity (Maiti & Nigam (2007); LLlamas et al. (2008)). The flow distribution is distinctly different for the various types of inlet distributor and improves when going from the point, line, multipoint, to the uniform distributor (Ravindra et al. (1997); Marcandelli et al. (2000)). Point and Line distributor by its geometry give maldistribution at the inlet. The studies using these types of inlets are much needed to get a real insight

into the effect of the non-uniform distributor, and it can provide the prediction capabilities of the hydrodynamic models (Boyer et al. (2005)) to help examine the effect of various operating parameters on the resulting flow distribution. There are extensive studies on distributor technologies (Bazer-Bachi et al. (2013)). Table 1 lists a selected summary of the studies on maldistribution and inlet distributor in TBRs. Many experimental techniques have been developed to study the effect of the inlet distributors and to identify any maldistribution. The techniques are Gamma-Ray Computed Tomography (CT), Tracer, Nuclear Magnetic Resonance (NMR), Wire Mesh, Conductance, and Pressure Transducers. These techniques can easily identify any maldistribution. Furthermore, CFD simulation has been conducted to verify the findings and to examine the flow distribution (Atta et al. (2010)). Tsochatzidis et al. (2002) had investigated the effect of a different kind of inlet distributor on liquid maldistribution using pressure drop and conductance probe. Three distinct types of distributors were used such as uniform, half-blocked and quarter-blocked. The main conclusion is that high maldistribution at inlet results in lower pressure drop. Also, they found the uneven liquid distribution is associated with the higher holdup values. However, the uniform radial liquid distribution tends to be reduced with increasing flow rates.

Llamas et al. (2009) have developed the wire mesh tomography sensors for the study of liquid maldistribution in TBRs. One of the experiments was to investigate the dispersion of the liquid saturation at the central zone of the reactor. It showed the ability of the catalyst to spread the liquid in the radial direction. Maldistribution was easily visualized with different types of the liquid distributor.

Recently, Bazmi et al. (2013) studied the flow maldistribution in dense and sock loaded trilobe catalyst TBR with experimentation data from the liquid collector and modeling using Neural Networks. The experiment setup consists of 0.14 m ID column and the adjustable height of column varies from 0.1 m to 1 m. The liquid collector used was divided into seven compartments with an equal surface area. The flow rate through each chamber was determined by averaging the flux of the outlet liquid in a specific amount time. Maldistribution coefficient (Mf) was used and is defined according to Marcandelli et al. (2000). Results showed that by increasing the gas and liquid ow rates, the liquid spreading quality was improved and in good agreement with the Artificial Neural Network (ANN) model predictions. draining to the reactor volume.

Meanwhile, the study of liquid spreading from a single point source has been done by Boyer et al. (2005) using CT technique and liquid collecting device. The experimental data was used to validate the CFD model. The findings are that the liquid spreading is more in pre-wetted bed, and it reduces when the gas flow rate is increased. but the effect of the liquid flow rate and different packing characteristics failed to appear. However, the Computed Tomography (CT) can quantify the liquid spreading in pre-wetted and non-pre-wetted beds for various gas and liquid flow rates. Schubert et al. (2008) also studied liquid spreading with high-resolution CT. They used a Cs-137 radiator with 662 KeV photon energy and approximately 160 GBq activity. Boyer et al. (2005) used a similar CT radioactive source but with activity 11.1GBq. They found liquid spreading with packing length was clearly observed in the glass packing, while in the catalyst packing it is hard to distinguish between high and low dynamics liquid containing zones.

Table 1 A selected summary of investigations of local maldistribution in TBRs

References	Techniques	Key Findings
Tsochatzidis et al. (2002)	Pressure drop measurement & local conductance probe.	The bed length is required to establish uniform radial distribution tends to be reduced with increasing flow rates. Uneven liquid distribution is associated with higher holdup values.
Atta et al., (2007)	CFD model using porous media flow concept.	The increase in flow rates improves the liquid distribution. The CFD-based porous model can forecast the reactor maldistribution.
Llamas et al., (2008)	Wire Mesh Tomography. A different type of liquid distributor was used.	Maldistribution is easily visualized at a cross-sectional area of the reactor.
Bazmi et al., (2013)	Liquid Collector and Modeling Artificial Neural Network.	Increasing the gas and liquid flow rates caused the liquid spreading quality is improved Increasing of the bed height would result in better liquid spreading up to the certain level. At this level, the liquid redistributor is needed for avoiding the channeling flow in bed

In general, liquid maldistribution directly affects the performance due to improper contacting of gas-liquid phases over catalyst surface and channeling of the flow. Gravity-

driven nature of liquid flow offers relatively few degrees of freedom to tune/manipulate the liquid distribution.

However, detailed studies are still lacking on identifying liquid maldistribution using a technique that can be implemented on a large scale and opaque systems.

Therefore, in this work, GRD technique has been implemented to identify the liquid maldistribution in a 0.1524 m TBR. It is also used to investigate the effect of inlet distributor on the liquid distribution via line averaged phase holdup along the bed diameter and along the length of the catalyst bed.

2. EXPERIMENAL SETUP

Figure 1 shows schematic of the trickle bed reactor (TBR) used in this study. The TBR is placed in between Cs-137 gamma source and thallium activated sodium iodide NaI (Tl) scintillation detector.

The experiment was conducted on 0.14 m (ID) Plexiglas column, randomly packed with 0.003 m glass beads to a bed height of 1.83 m. The GRD scanning was carried out at different radial (r/R= - 0.80, 0.60, -0.40,-0.20, 0, 0.20, 0.40, 0.60, 0.80) and three axial positions (Z/D= 2, 5, and 7), whereas r is the distance from center to the scanning location and R is the radius of the column.

The Z is the distance from the bottom of the column to scanning location and D is the diameter of the column. The operating condition used for this study are at superficial liquid (0.004 m/s to 0.014 m/s) and superficial gas velocity (0.03 m/s to 0.27 m/s).

.

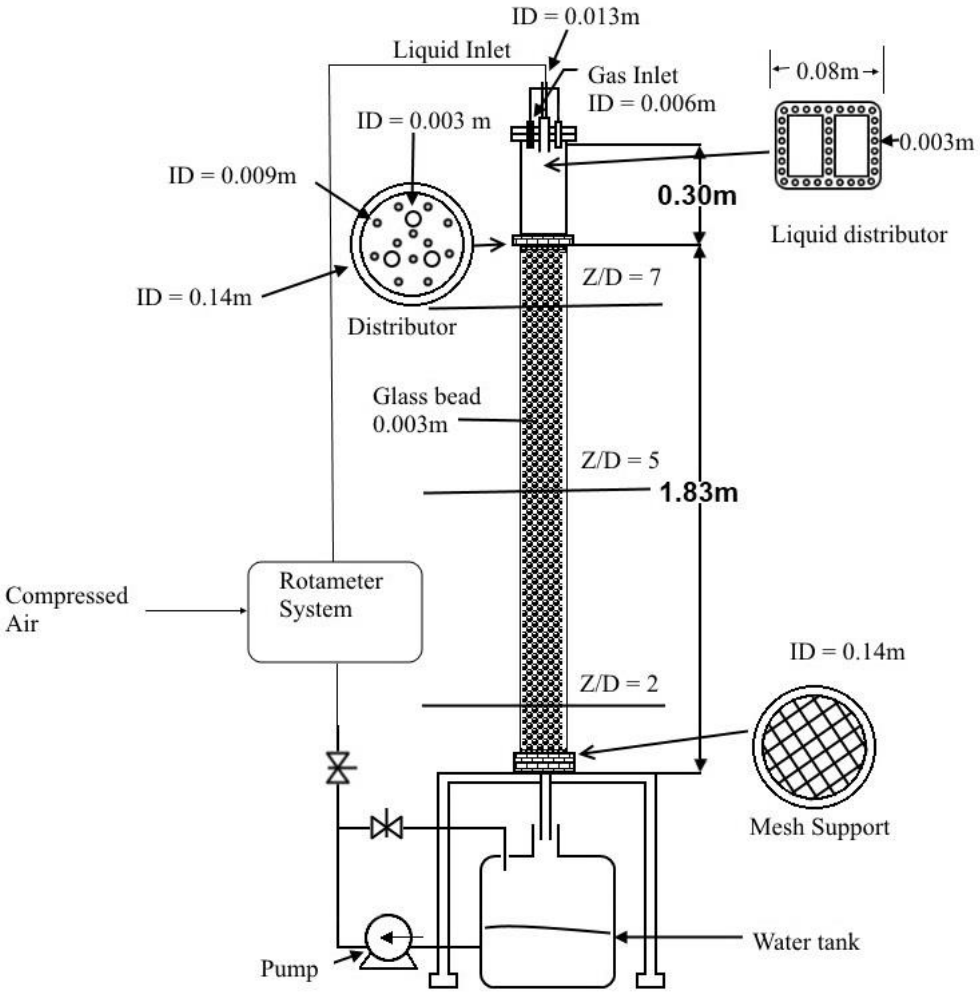

Figure 1. Experimental setup

Three kinds of inlet distributors are used in this study; they are listed as follows:

1. Single inlet near to the wall of the column. (Fig. 2)
2. Single inlet at the center of the column. (Fig. 3)
3. Proper Shower Inlet. (Fig. 4)

The inlet distributors showed in Figure 2, and Figure 3 are used to create maldistribution at the inlet. These distributors are made of brass and having Internal

Diameter (ID) of 0.025 m. The length of these inlet distributors is made in such a way that it touches the top portion of the bed. This is necessary to ensure the liquid flow is continuous and does not get affected by gas flow rate.

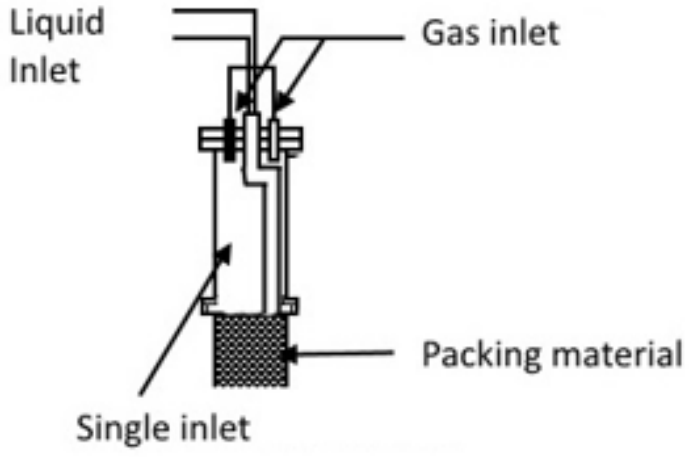

Figure 2. Single Inlet Near The Wall

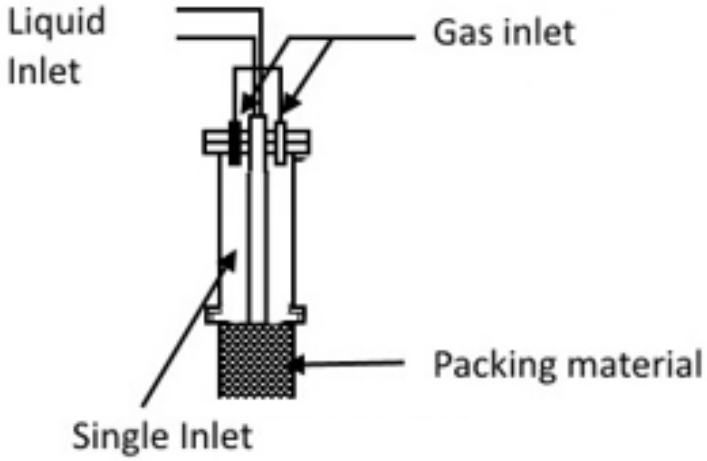

Figure 3. Single Inlet/Distributor At The Center Of The Column

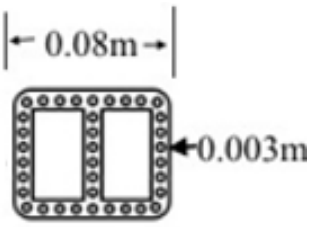

Figure 4. Proper Shower Inlet/Distributor

The inlet distributor shown in Figure 4 is used to create a better distribution of liquid at the inlet compared to other two kinds of distributor. This is an eight shape distributor with equally spaced inlet holes to distribute liquid evenly at the inlet of the bed.

3. METHOD OF ANALYSIS

The Gamma source of Cs-137 will eject gamma rays, and a detector which is placed in a straight line will detect the photon counts emitted by gamma ray source. The amount of photon count received is evaluated using software called ProSpect from Canberra (www.canberra.com). The data from the GRD experiment are analyzed using Microsoft Excel and MATLAB software.

The photon attenuation was measured at different radial and axial position through the reactor. Based on Beer Lamberts Law, the intensity of photon attenuation that is transmitted through a homogenous material is expressed as follows:

$$T = \frac{I}{I_o} = e^{-\mu\rho l} \quad (1)$$

Where T is the transmission ratio, Io, is the incident radiation, I is detected radiation, μ is the mass attenuation coefficient,ρ is the medium density, and l is the path length through the medium.

The measured ln (Io/I) (called A, for simplicity) is equal to the integral sum of the attenuation through the material along the beam path.

$$A = ln\left(\frac{I}{I_o}\right) = \mu\rho l \tag{2}$$

The index i denotes the line scan and if the medium is made of three materials with mass attenuation coefficients μ_g, μ_l, and μ_s, densities ρ_g, ρ_l, *and* ρ_s, and thicknesses l_g, l_l, and l_s, for the gas, liquid, and solid phases, respectively, then the total attenuation $A_{gls,i}$ is,

$$A_{gls,i} = \mu_g\rho_g l_{g,i} + \mu_l\rho_l l_{l,i} + \mu_s\rho_s l_{s,i} \tag{3}$$

L_i is the total length of the pixel through which gamma ray beam passes is,

$$L = l_g + l_l + l_s, \quad l_{g,i} = \varepsilon_g L_{g,i}, \; l_{g,i} = \varepsilon_l L_{l,i}, \quad l_{s,i} = \varepsilon_s L_{s,i} \tag{4}$$

Where, $\varepsilon_g, \varepsilon_l$, and ε_s are the line average holdups (volumetric fractions) for the gas, liquid and solid phases, respectively. Since the summation of the holdups equal unity (i.e.$\varepsilon_g + \varepsilon_l + \varepsilon_s = 1$) in each line scan i, the attenuation of GRD scan for three-phase system (Equation 3) can be written as shown in Equation 5.

$$A_{gls,i} = ln\left(\frac{I_o}{I_{gls}}\right) = \left[\mu_g\rho_g\varepsilon_{g,i} + \mu_l\rho_l(1 - \varepsilon_{g,i} - \varepsilon_{s,i}) + \mu_s\rho_s\varepsilon_{s,i}\right]L_i \tag{5}$$

3.1 EXPERIMENTAL DETERMINATION OF PHASE HOLDUPS

The formula used to measure holdup distribution is similar as (Chen et al. (2001)). The procedure of various scans is as follows:

1. Scanning empty column to get background count.

   In this case, GRD scan is conducted on an empty column. The photon attenuation will occur only due to the wall and will remain constant for another kind of scanning. So the photon count measured in this case is considered as I_o.

This value of I_o is used in other scans to find A as mentioned in equation (2).

2. Scanning TBR column filled with water.

In this case, TBR is scanned with water filled in it. This will give attenuation ($A_{l,i}$) due to liquid only.

$$A_{l,i} = ln\left(\frac{I_o}{I_l}\right) = \mu_l \rho_l L_{l,i} \tag{6}$$

3. Scanning TBR only filled with random packing glass beads of 0.003 m diameter.

In this case attenuation ($A_{g,s}$) is due to gas and solids.

$$A_{gs,i} = ln\left(\frac{I_o}{I_{gs}}\right) = \left[\mu_g \rho_g\left(1 - \varepsilon_{s,i}\right) + \mu_s \rho_s \varepsilon_{s,i}\right] L_i \tag{7}$$

4. Scanning TBR filled with solid and liquid phase.

In this case, the attenuation ($A_{l,s}$) is due to solid catalyst and liquid filled in the void space of catalyst packing.

$$A_{ls,i} = ln\left(\frac{I_o}{I_{ls}}\right) = \left[\mu_l \rho_l\left(1 - \varepsilon_{s,i}\right) + \mu_s \rho_s \varepsilon_{s,i}\right] L_i \tag{8}$$

Since $\rho_g << \rho_l$ or ρ_s, and μ_g, μ_l, and μ_g, are of the same order of magnitude, the attenuation caused by the gas phase is negligible. Hence, combining Equation 6, 7, and Equation 8 yields the solid holdup in line *i*,

$$\varepsilon_{s,i} = 1 - \frac{(A_{ls,i} - A_{gs,i})}{A_{l,i}} \tag{9}$$

This solid holdup is fixed for all the cases for the line (i), as the solids are not moving in the catalyst packing for the various operating condition.

5. Scanning TBR for varying gas and liquid flow rates.

In this case, the attenuation is due to the all the three phase. The attenuation

(A_{gls}) is similar to equation 5.

By solving equation 5, 6, and 8, estimation of gas holdup ($\varepsilon_{g,i}$) can be obtained as follows,

$$\varepsilon_{g,i} = \frac{(A_{ls,i} - A_{gls,i})}{A_{l,i}} \tag{10}$$

Thus, liquid holdup (ε_l) in line *i* is calculated as follows.

$$\varepsilon_{l,i} = 1 - \varepsilon_{g,i} - \varepsilon_{s,i} \tag{11}$$

The above equations are modified from gamma-ray computed tomography instrument which used similar types of source and used by Al-Dahhan et al. (2006), Roy (2006). Also, the principles of attenuation of gamma-ray are the same, but in computed tomography, they are scanned in the whole cross-section with denoted the index of ij, while the GRD is an only a line scans of i index.

4. RESULT AND DISCUSSION

In this study, three different kinds of inlet distributor are used to investigate the gross maldistribution in TBR. Line average phase holdups are measured at the various radial and axial locations using GRD to see the impact of distributors on overall maldistribution. All the measurements are conducted on a pre-wetted catalyst bed.

4.1 PHASE HOLDUP WITH SINGLE INLET NEAR TO COLUMN WALL

This experiment was conducted to create apparent maldistribution of liquid in the system. In industries, this kind of distributor is not used, but this study is done to tests GRD capability to detect any maldistribution in the system and to provide data for better hydrodynamic models. In this study, both visual observation and GRD results are taken,

to see the extent of maldistribution in the system. Sample GRD results of radial phase holdup distribution at U_g = 0.03 m/s and U_l = 0.004 m/s is shown here. The liquid is more towards the side where inlet distributor is located and is clearly visible in Figure 5.

The liquid starts to spread evenly only in between Z/D=7 and Z/D=5. GRD result is compared with visual observation to see the capability of GRD to measure maldistribution. In the Figure 6, the liquid holdup at Z/D=7 is seen to be higher toward one side, which was expected from visual observation and even measured by GRD also. The liquid spreads better on moving down the reactor and Z/D=5, which is the middle of the reactor the spread is somewhat even. There is slight maldistribution seen at the bottom of the column. It can be attributed to the fact that, there is a catalyst structure at the base, which is tightly packed and creates lots of resistance to the fluid flow path, and in this area fluid flow is mostly gravity driven.

Figure 7. Showed the effect of different gas velocity on liquid holdup at Z/D=5. In all the cases, maldistribution was evident. Increasing superficial gas velocity is not improving the liquid distribution at this location for this kind of distributor.

Figure 5. Liquid Distribution for Single Inlet Near the Wall Column

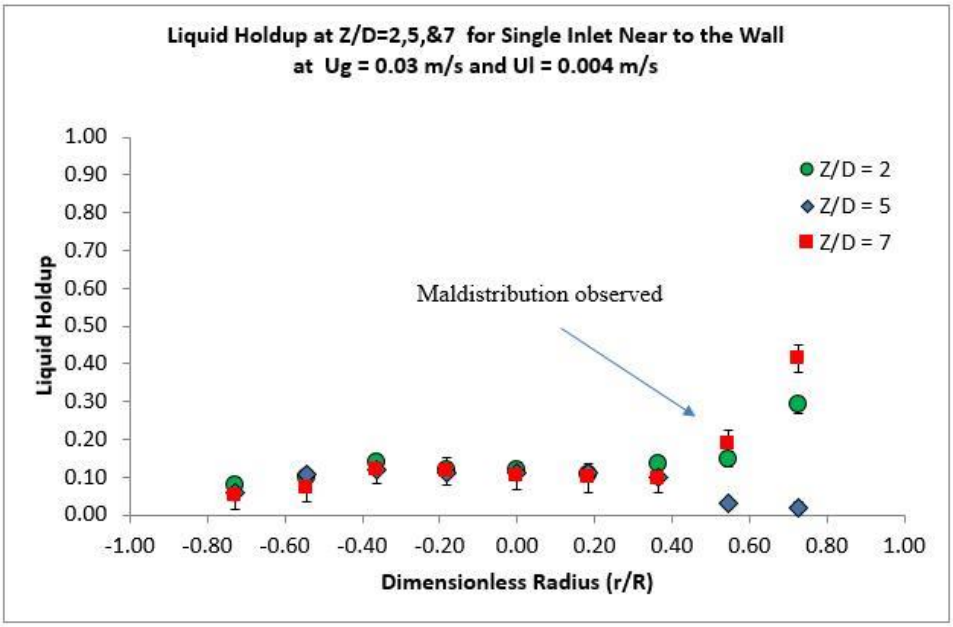

Figure 6. Liquid Holdup for Single Inlet Near The Wall in TBR Of 0.14m Internal Diameter (ID)

4.2 PHASE HOLDUP WITH SINGLE INLET IN THE CENTER

From the previous section, it can be seen that the GRD is capable of identifying phase maldistribution. In this case, a point inlet distributor at the center of the reactor is used, and average line holdup of phases is measured using GRD. The sample results are shown for U_g = 0.03 m/s and U_l = 0.004 m/s at three different axial position.

The visual observation revealed that the liquid starts spreading at approximate 0.15 m from the top of the column and spreads almost evenly by reaching Z/D =7 (Figure 8). Liquid holdup and gas holdup measured from GRD showed that there is an almost uniform distribution at all the measured axial position, of which the best distribution is seen in the middle of the reactor (Z/D=5). This can be seen in Figure 8 and Figure 9.

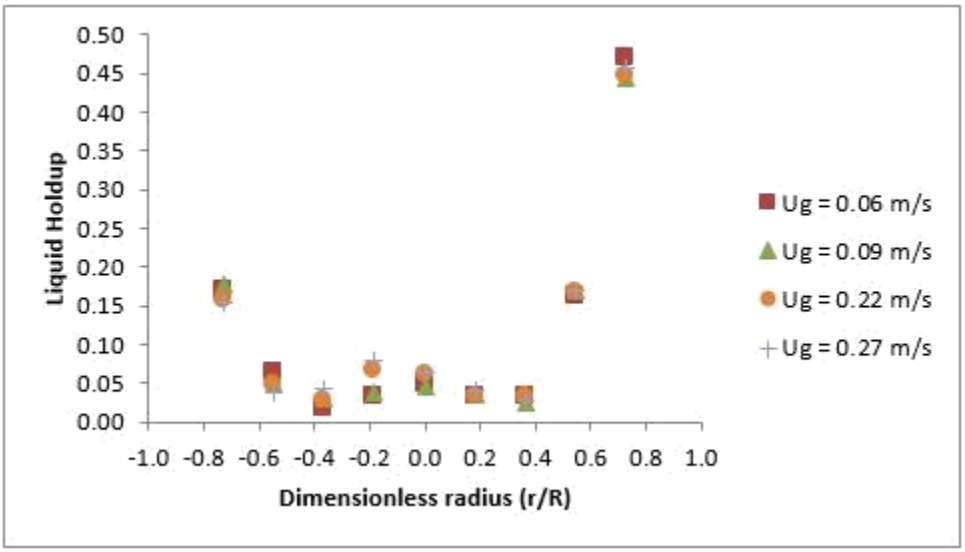

Figure 7. The Liquid Holdup for Different Gas Flow Rate With Constant Ul = 0.012 m/s Single Inlet Near the Wall at Axial Position Z/D = 5.

Although the variation is quite uniform, there is a slight increase of holdup for both phases towards the sides of the column. Variation of the liquid holdup near wall can be due to wall effect. The wall effect is significant for small diameter column and creates flow bypassing and results in a large holdup in those areas.

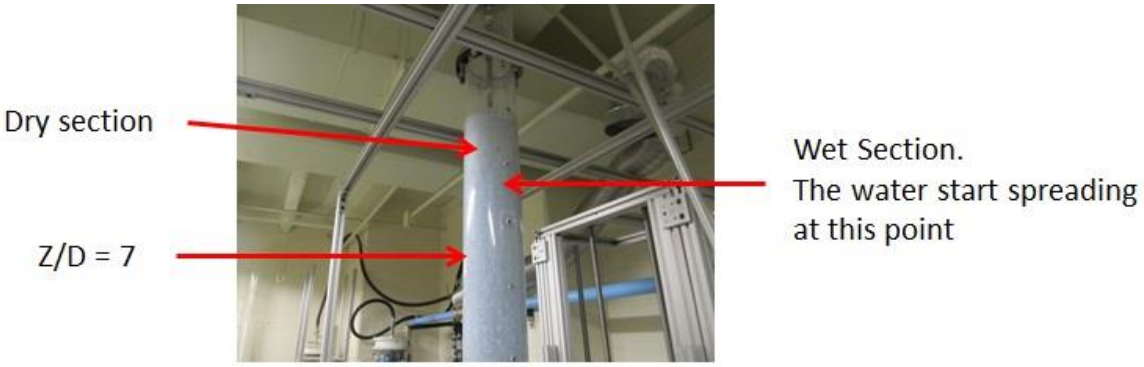

Figure 8. Liquid Distribution for Single Inlet Near The Center

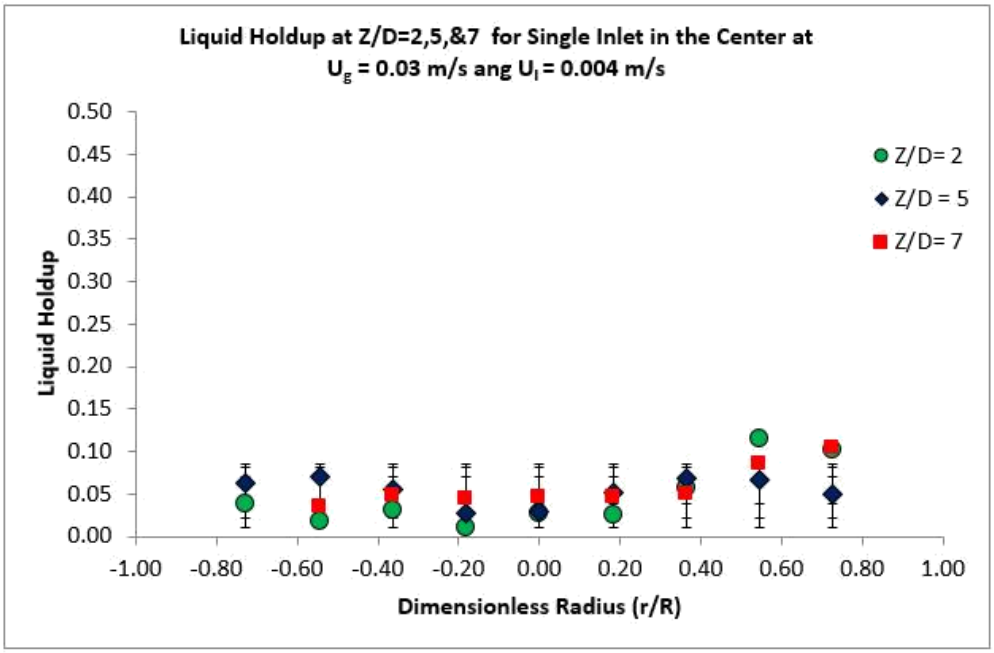

Figure 9. Liquid Holdup for Single Inlet in the Center in TBR 0.14m (ID)

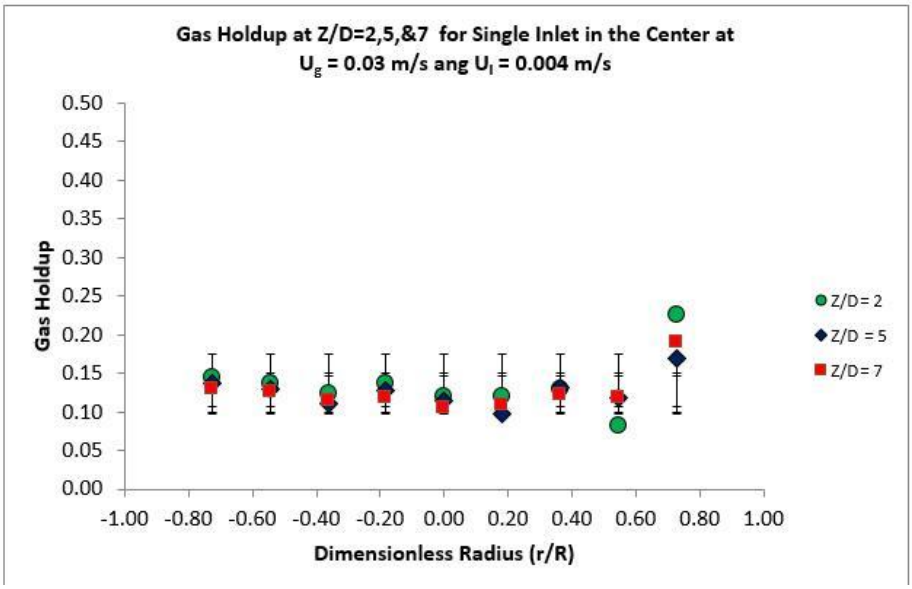

Figure 10. Gas Holdup for Single Inlet at the Center in TBR of 0.14m Internal Diameter (ID)

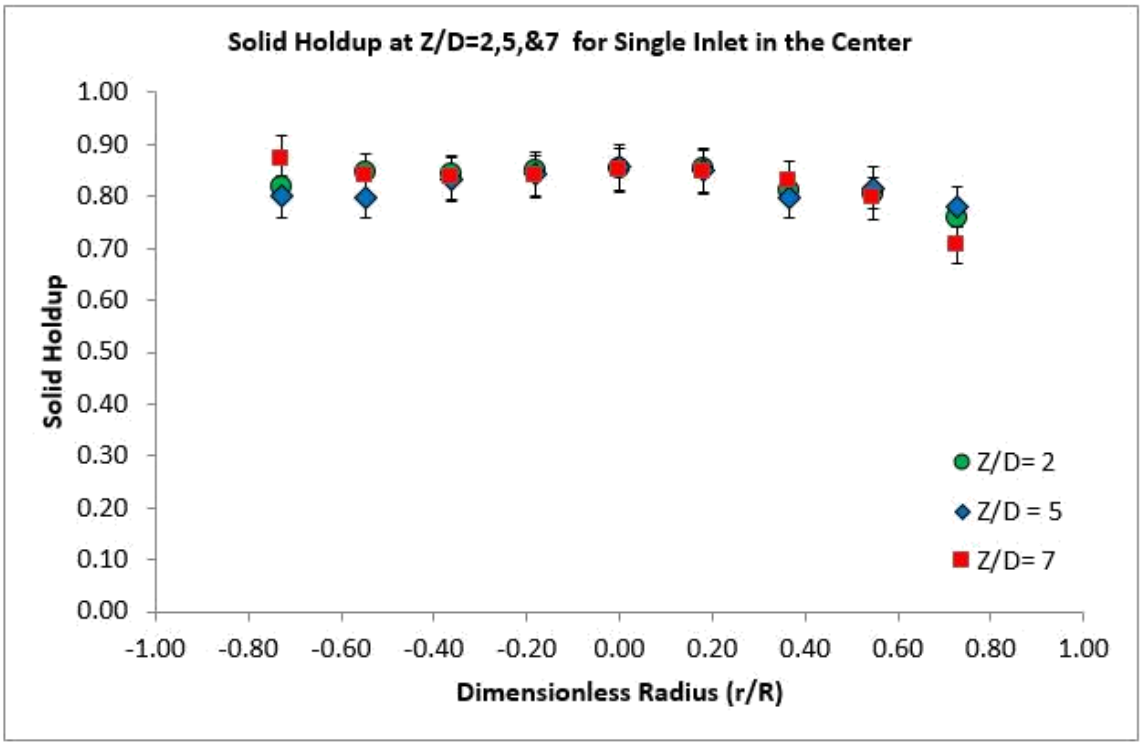

Figure 11. Solid Holdup for Single Inlet in the Center in TBR of 0.14m Internal Diameter (ID)

The solid holdup is also measured and plotted (Figure 11). There is slight maldistribution seen at Z/D=7. It is because of loose packing at the top. The gas and liquid flow can slightly disturb the packing arrangement. Toward the bottom, the packing is quite uniform, and it is due to the catalyst weight on top.

Figure 12 showed the effect of different gas velocity on liquid holdup at Z/D=5. There is maldistribution in all the cases. In this case also increasing superficial gas velocity is not improving the liquid distribution at this location for this kind of distributor.

4.3 PHASE HOLDUP WITH PROPER SHOWER INLET

This inlet distributor was aimed to give a homogenous distribution of gas and liquid. The Figure (13, 14, 15) show the phase holdup calculation at U_g = 0.03m/s and U_l = 0.004 m/s. The solid holdup shows almost uniform distribution along the radial direction at all axial position. A slight maldistribution is observed radially for both gas and liquid phase, but the trend is similar at all axial locations. This can be due to the fact that liquid is evenly spreading at the top of the bed, and the driving force is uniformly distributed cross sectional along the bed height.

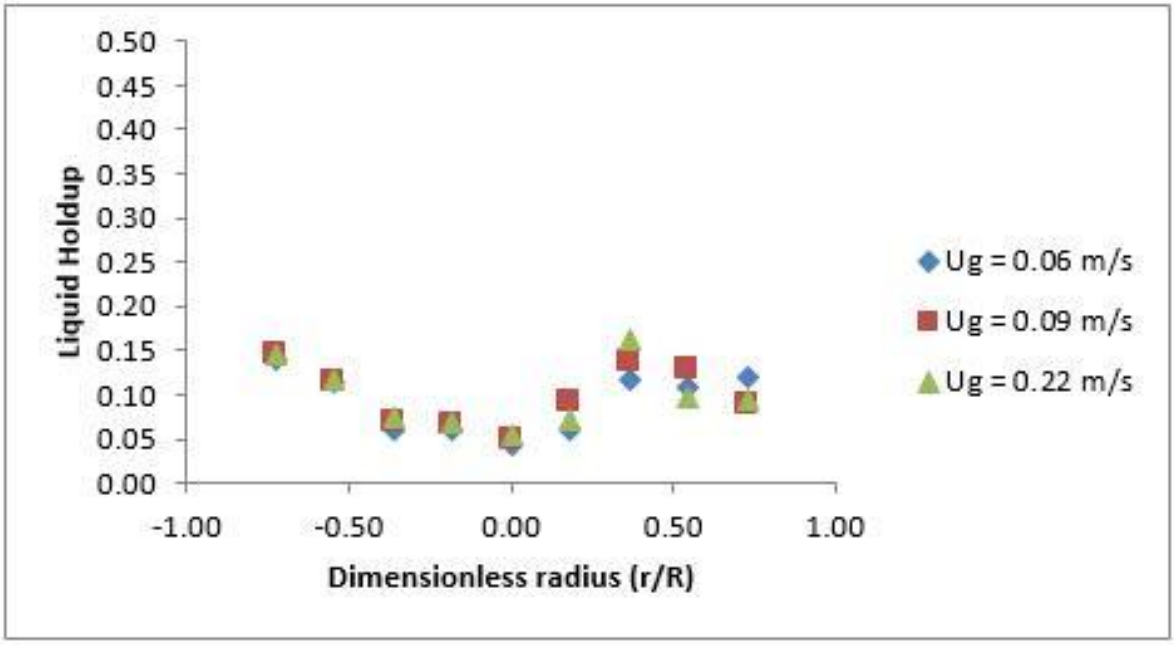

Figure 12. The Liquid Holdup for Different Gas Flow Rate with Constant Ul = 0.012 m/s Single Inlet In The Center At Axial Position Z/D = 5.

The methodology to determine holdup are similar to Gamma-Ray Computed Tomography technique (CT). Hence, results obtained from CT can be used to validate these results of GRD. Kuzeljevic (2010) et al. conducted study on TBR using CT and

they used a column of 0.163m diameter, catalyst bed height of 0.68 m, glass beads of diameter 0.003 m as a catalyst, bed porosity of 0.41, water and air as a gas and liquid medium and results are shown in Figure 16. These conditions are almost similar to the experimental condition of this study. Figure 17 shows that variation of liquid holdup Z/D=5 for various U_g with fixed U_l = 0.004 m/s. The comparison of Figure 16 and from Kuzeljevic study indicates that the TBR results obtained from GRD are in good agreement with the trend showed by CT results.

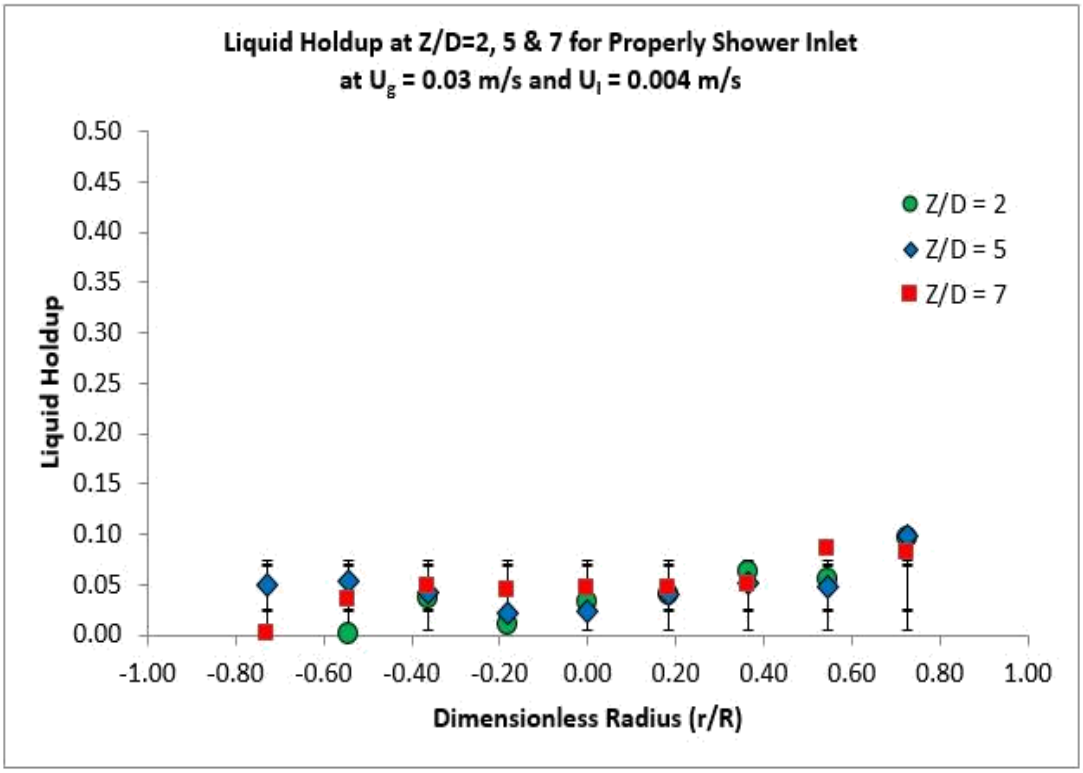

Figure 13. Liquid Holdup from GRD for TBR 0.14 m Internal Diameter (ID) at the Different Axial Position of Z/D 2, 5 and 7.

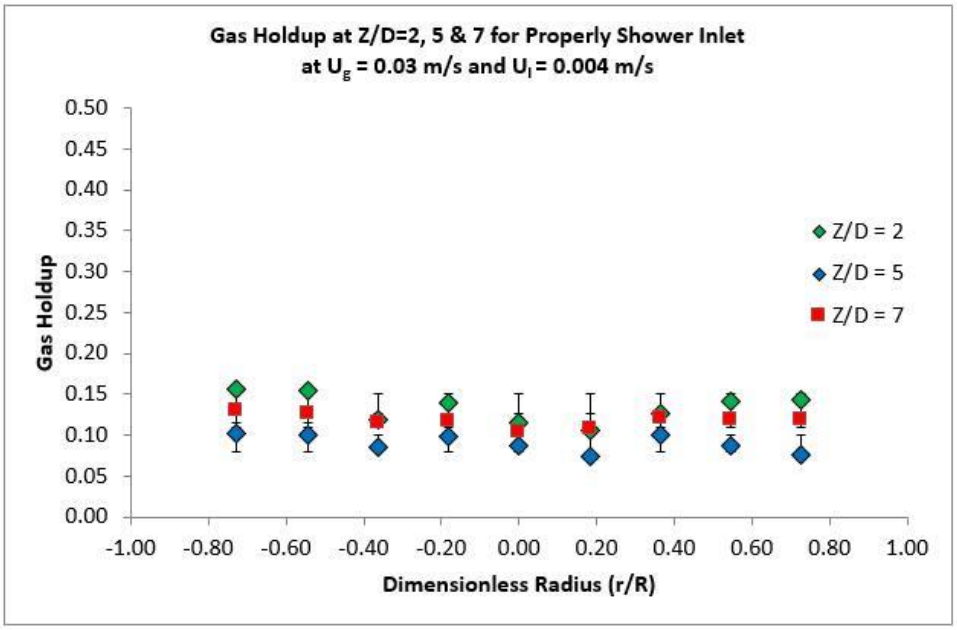

Figure 14. Gas Holdup from GRD For TBR 0.14m Internal Diameter (ID) at Different Axial Position of Z/D 2, 5 And 7.

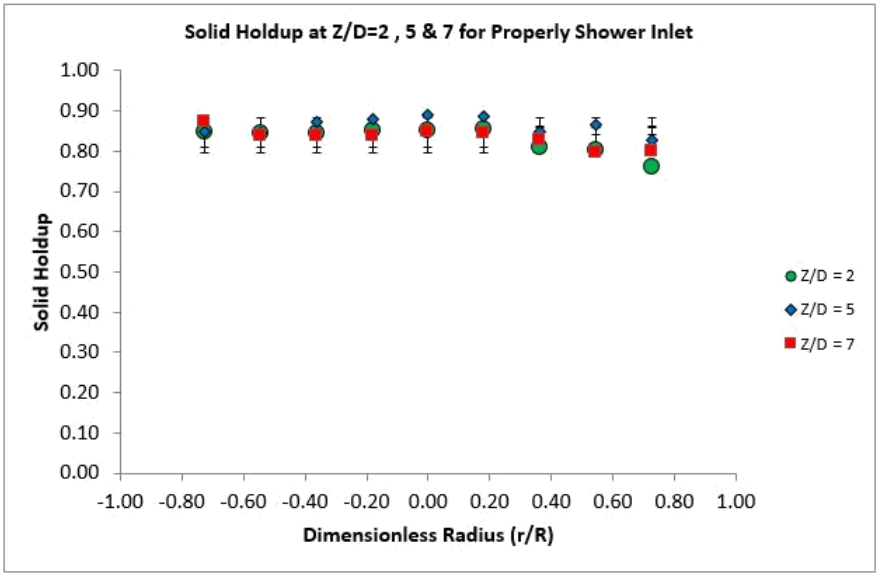

Figure 15. Solid Holdup from GRD For TBR 0.14m Internal Diameter (ID) at Different Axial Position Of Z/D 2, 5 And 7.

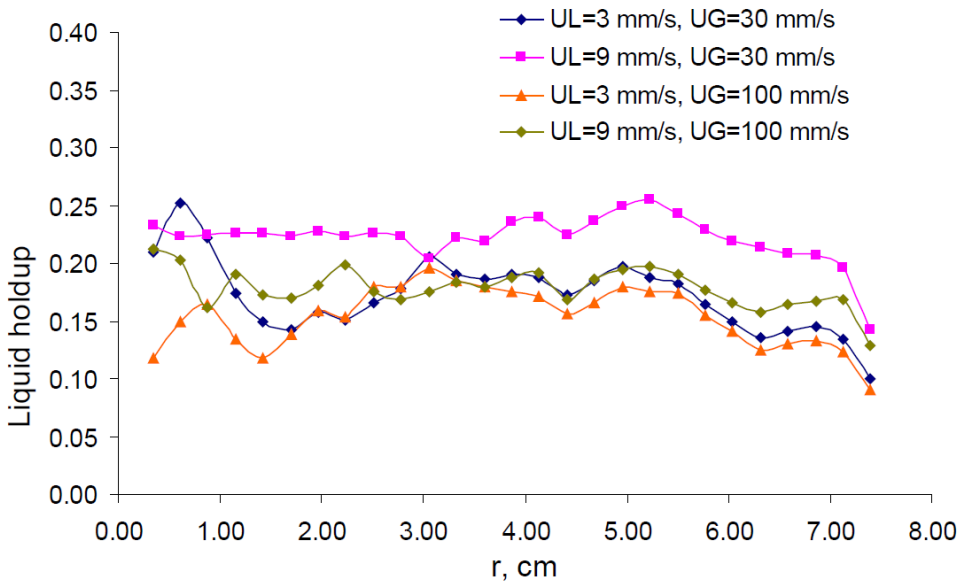

Figure 16. Liquid Holdup for TBR from Gamma Ray Computed Tomography (Taken from Kuzeljevic, 2010)

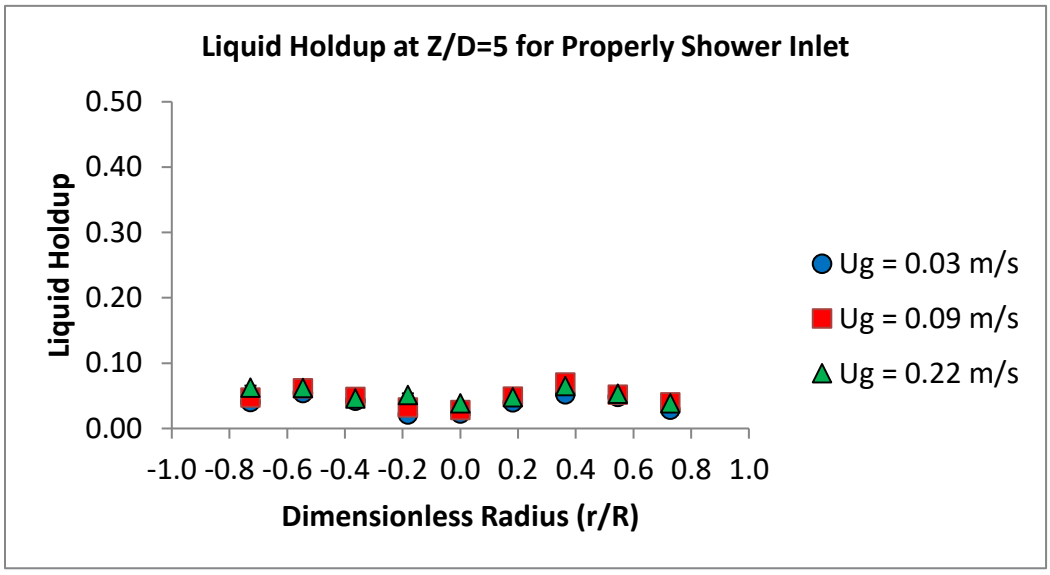

Figure 17. The Liquid Holdup for 0.14m TBR From GRD With Different Ug

5. REMARKS

GRD has been able to identify maldistribution of phases in the catalyst bed of TBR. Also, GRD has been able to measure line average diameter profile of liquid, gas, and solid holdups. This technique is flexible and easily applied to various sizes of the reactor. Also, this technique can even be implemented at extreme conditions of high pressure and temperature as seen in the industries. It is found that inlet distributor plays a vital role in flow distribution of phases along the catalyst bed of the reactor. The distributor with good distribution at inlet results in early spreading of liquid uniformly than compared with the case, when the flow is not uniform at the inlet. The effect of superficial gas velocity on liquid distribution is not significant, and the optimum distribution was seen to be in the middle of the reactor. Some of the other factors which affect flow distribution are packing material, operating conditions, etc. CT results of TBR obtained from literature are used to validate GRD results of TBR, and it is seen to be in good agreement. These kind of study are very critical to provide benchmark data for CFD validation. It helps to produce better hydrodynamic models capable of predicting maldistribution in TBR. This study is still in its nascent stage, and further studies are needed using different types of packing material, various sizes of the reactor. This research can advance knowledge in maldistribution of phases in TBR.

ACKNOWLEDGEMENT

The authors wish to acknowledge the Ministry of Science, Technology and Innovation Malaysia (MOSTI) for sponsoring the primary author’s study within the Chemical and Biochemical Engineering Department at Missouri University of Science

and Technology. Also, the primary author would like to acknowledge the use of the gamma ray, experimental facilities set-up and materials that were used in this work and funded by professor Al-Dahhan's research fund.

REFERENCES

Al-Dahhan, M., Kemoun, A., & Cartolano, A. (2006). Phase distribution in an up flow monolith reactor using computed tomography. AIChE Journal, 52, 745.

Alvarez, A., Ramrez, S., Ancheyta, J., & Rodrguez, L. (2007). Key role of reactor internals in hydroprocessing of oil fractions. Energy and Fuels, 21, 1731.

Atta, A., Hamidipour, M., Roy, S., Nigam, K. D. P., & Larachi, F. (2010). Propagation of slow/fast-mode solitary liquid waves in trickle beds via electrical capacitance tomography and computational fluid dynamics. *Chemical Engineering Science, 65*(3), 1144-1150.

Bazer-Bachi, F., Haroun, Y., Augier, F., & Boyer, C. (2013). Experimental evaluation of distributor technologies for trickle-bed re-actors. Industrial and Engineering Chemistry Research, 52 , 11189

Bazmi, M., Hashemabadi, S., & Bayat, M. (2013). Flow maldistribution in dense- and sock-loaded trilobe catalyst trickle-bed reactors: Experimental data and modeling using neural network. Transport in Porous Media, 97, 119.

Bonilla, J. A. (1993). Don't neglect liquid distributors. Chemical Engineering Progress, 89, 47.

Boyer, C., Koudil, A., Chen, P., & Dudukovic, M. (2005). Study of liquid spreading from a point source in a trickle bed via gamma-ray tomography and cfd simulation. Chemical Engineering Science, 60, 6279.

Chen, J., Rados, N., Al-Dahhan, M. H., Duduković, M. P., Nguyen, D., & Parimi, K. (2001). Particle motion in packed/ebullated beds by CT and CARPT. *AIChE Journal, 47*(5), 994-1004.

Kuzeljevic, Z. (2010). Hydrodynamics of Trickle Bed Reactor: Measurement and Modeling.. Ph.D. thesis Washington University, St Louis, MO, USA.

Llamas, J. -., Pérat, C., Lesage, F., Weber, M., D'Ortona, U., & Wild, G. (2008). Wire mesh tomography applied to trickle beds: A new way to study liquid maldistribution. *Chemical Engineering and Processing: Process Intensification, 47*(9-10), 1765-1770.

Llamas, J. D., Lesage, F., & Wild, G. (2009). Influence of gas flow rate on liquid distribution in trickle-beds using perforated plates as liquid distributors. *Industrial and Engineering Chemistry Research, 48*(1), 7-11.

Maiti, R., & Nigam, K. (2007). Gas-liquid distributors for trickle-bed reactors: A review. Industrial and Engineering Chemistry Research, 46, 6164.

Marcandelli, C., Lamine, A., Bernard, J., & Wild, G. (2000). Liquid distribution in trickle- bed reactor. Oil and Gas Science and Technology, 55, 407.

Mederos, F., Ancheyta, J., & Chen, J. (2009). Review on criteria to ensure ideal behaviors in trickle-bed reactors. Applied Catalysis A: General, 355, 1.

Ravindra, P., Rao, D., & Rao, M. (1997). Liquid flow texture in trickle-bed reactors: An experimental study. Industrial and Engineering Chemistry Research, 36, 5133.

Roy, S. (2006). Phase Distribution and Performance Studies of Gas-Liquid Monolith Reactor. Ph.D. thesis Washingthon University, St Louis, MO.

Tsochatzidis, N. A., Karabelas, A. J., Giakoumakis, D., & Huff, G. A. (2002). An investigation of liquid maldistribution in trickle beds. *Chemical Engineering Science, 57*(17), 3543-3555.

Schubert, M., Hessel, G., Zippe, C., Lange, R., & Hampel, U. (2008). Liquid flow texture analysis in trickle bed reactors using high-resolution gamma ray tomography. Chemical Engineering Journal, 140,

SECTION

2. OVERALL CONCLUSION AND RECOMMENDATION

In this section overall conclusion and the summary of the key findings of this work alongside with recommendations for future work in TBR are presented.

2.1. OVERALL CONCLUSION

The overall objective of this work is to develop the non-invasive gamma-ray densitometry technique to identify flow regime, gross maldistribution and liquid distribution. The investigation can be applied while the trickle bed reactor was in operation or online. The local liquid and gas velocities, phase saturation and their time series have been studied and investigated for the first time by developing, implementing and validating by the two-tip optical fiber probe technique. For the overall conclusion, the findings were consistent with what reported in the literature. The measurements and studies can be applied in various sizes of trickle bed reactor operated in the industrial conditions.

2.2. FLOW REGIME IDENTIFICATION USING ON-LINE GAMMA RAY DENSITOMETER FOR TRICKLE BED REACTORS

The key findings of the flow regime identification studies are briefly summarized as follows:

1. The slope change in mean and standard deviation plot with varying liquid flow rates and at different constant gas flow rate is used to identify the regimes. The

transition region is recognized, and it is found to same for all the axial measurement at the center of the reactor.

2. The flow distribution is quite uniform along the axial length at the center of the reactor. Pressure drop measurement also showed similar transition trend which indicates the overall and line average phenomena at the center of the reactor are behaving in a comparable manner.
3. To precisely locate the flow regime transition point, the GRD signal obtained at the middle of the reactor (Z/D=5, r/R=0) is verified on another time domain (Autocorrelation), frequency domain (Spectral Analysis) and state space (Kolmogorov Entropy). The identified flow regimes are a trickle and pulse flow.
4. Autocorrelation presented that in trickle flow the signals could be correlated, and there is no distinguishable correlation exists in pulse flow.
5. The spectral analysis identified the flow regime based on power law fall. Kolmogorov entropy which is state space analysis notable flow regime based on the trend of change in disorder or unpredictability in the system.

2.3. NOVEL MEASUREMENT TECHNIQUE BASED ON OPTICAL PROBE TO MEASURE LOCAL FLOW DYNAMICS IN PACKED BED REACTORS

The key findings of optical fiber probe are briefly summarized as follows:

1. New developed optical fiber probe successful measured the local liquid and gas velocities and saturations.
1. The local liquid and gas velocities shows non-homogenous gas/liquid distributions, with the most dominating positive velocity range of 0-5 m/sec.

2. The back-mixing is seen to be more at the bottom because as the force field dictating the movement of both the phases are same.
3. The values of liquid saturations are increasing on increasing the liquid flow rate. The center location (r/R =0) seems to have good distribution of liquid and gas along the axial direction as local liquid saturation's are not much varying along the axial length at these flow conditions.
2. This technique is validated with Industrial X-Ray Digital Radiography Technique (DIR) (Mohd Salleh et al. (2014)). The local liquid flow dynamics measured using the two-tip optical probe in a trickle bed reactor are in good agreement with experiments by Schubert et al. (2010b) and Sankey et al. (2009).

2.4. OVERALL DISTRIBUTION IDENTIFICATION AND EFFECT OF INLET DISTRIBUTOR ON THE PHASE HOLDUP IN A TRICKLE BED REACTOR USING GAMMA-RAY DENSITOMETRY (GRD)

The key findings of this work are briefly summarized as follows:

1. For the single inlet distributor in the center, the liquid holdup and gas holdup measured from the GRD showed almost uniform distribution at all measured axial position, of which the best distribution is seen in the middle of the reactor (Z/D = 5).
2. The distribution is quite uniform but there is slight increase of holdup for both phases towards the sides of the column. This variation of the liquid holdup near the wall can be due to wall effect.
3. There is slight maldistribution seen at the bottom of the column for the single inlet distributor near the wall.

4. Inlet distributor plays a vital role in flow distribution of phases along the catalyst bed of reactor.

2.5. RECOMMENDATIONS FOR FUTURE WORK

- The current work is used only glass beads with the similar size. It is recommended to used different types and size of any solid materials that can mimics solid phases in the industrial. Real types of catalysts with different sizes also can be used to get better results.
- Various size of trickle bed reactor can be recommended. The results obtained can be compared and analyzed as the effect of reactor size to the findings.
- This work presents a phase holdup from GRD technique. It is recommended that, a validation process should be performed by Computed Tomography with gamma-ray or X-ray as a source of radiation.
- In future studies, a computational fluid dynamics (CFD) should be implemented to be validated against the experimental data obtained from TTOFP with the used inlet distributor. Information obtained from the hybrid measurement technique provides detailed understanding of the relation between the local velocities and inlet distributor effect.
- A single probe that combines the measurements of the local velocities, phase saturation and flow regime and maldistribution identifications, needs to be considered and implemented based on the developed optical fiber probe.

APPENDIX A.

PROCEDURE MAKING TWO-TIP OPTICAL FIBER PROBE

Step by Step Procedure for Making the 2-Point Probe

1. Using scissors, cut two lengths of fiber – each approximately 2 meters in length.
2. Repeat the following sequence for each of the two fibers:
    a. Strip about 1" of the jacket off one end the fiber.
    b. Hang the fiber from the stand and attach the weight to the stripped end, leaving about ½" of the stripped fiber exposed.
    c. Use the hydrogen/oxygen torch to create a small, intense flame and cut the fiber just above the weight. As the glass melts, the weight pulls on the fiber which eventually snaps creating the tapered end. The size of the flame is shown below in Figure 1.

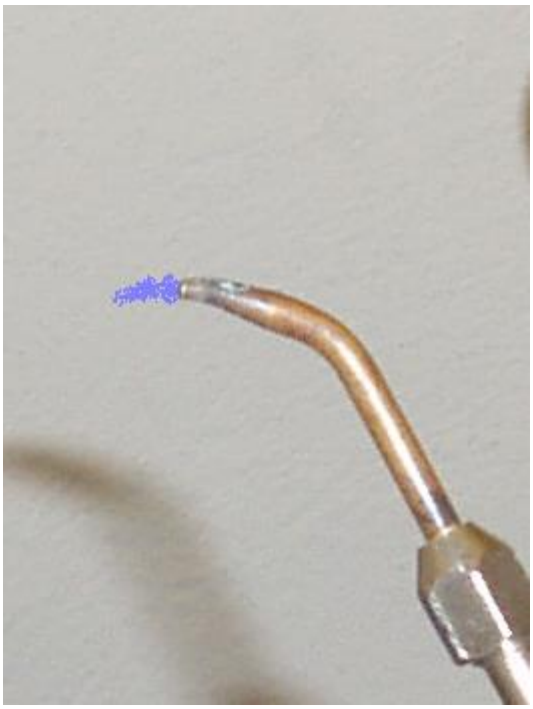

Figure 1. Size and Shape of Intense H_2/O_2 Flame.

    d. Under the microscope, use the diamond-tipped scribe to trim the tapered end of the desired geometry. (see Figure 2 below)

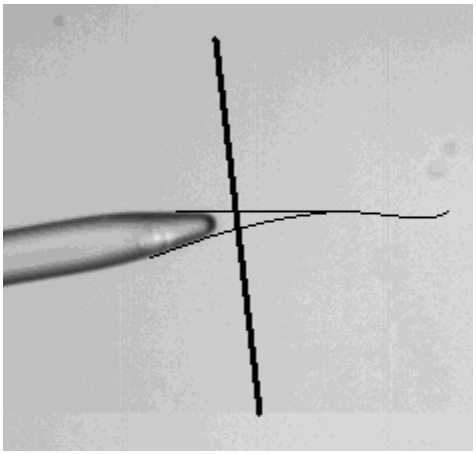

Figure 2. Typical Tip After the Flame Cut; Typical Trim Point and Resulting Tip After Flame Polishing.

e. Using the torch – only a gentle hydrogen flame – polish the very tip of the fiber. This melts the flat end left by the scribe into a more rounded point. If a very intense flame is used, it will melt the glass too quickly and actually blow the tip over.

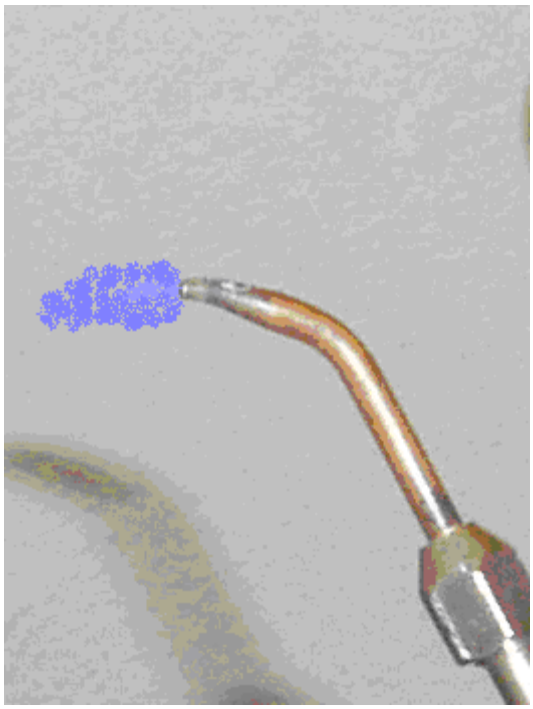

Figure 3. Flame Size and Shape for Flame Polishing.

f. Ensure that about 10 mm of the glasses (including the tip) is exposed beyond the jacket. If not, use the stripper to strip off any excess of the jacket.
g. Test the fiber.
    i. On the back end of the probe, strip off about 7 mm of the jacket and use the fiber cleaver to make a flush cut of the fiber (almost at the point where the jacket is just removed).
    ii. Apply a small amount of index matching gel to the back end of the fiber and mate it with a coupler using the grey PVC connector. It will help to tape the coupler (and fibers) in place to make sure they don't move during testing. A reliable connection is made when the tip is the brightest.
    iii. With one channel of the probe now connected to the Fiber box, check to make sure that the voltage drops are acceptable by dipping the probe tip repeatedly in a glass of water.
    iv. If the voltage drops are not acceptable, first try repeating step e. (The most common problem is under-polishing the tip.) If that does not work, remake the tip again.

3. With all two of the fiber tips now made and functioning well. Insert the two fibers, back-ends first, into the section of stainless steel tubing (bend the tubing if required). Leave about 1 ½" of the fiber exposed from the tip of the tubing. This will help to keep the fibers together so that they can be more easily aligned in the jig.
4. Place the jig in the lockable tweezers so that the triangle is pointing downward toward the table and align the tubing/fibers with the face of the jig. (see Figure 4 below)

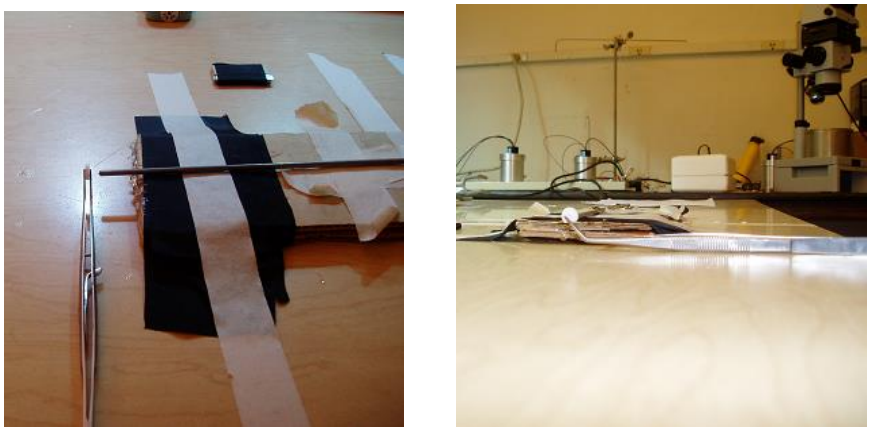

Figure 4. Positioning of the Jig.

5. Take one fiber and thread it into the bottom-most hole in the jig.
6. Thread the next fiber into the center hole and then thread the remaining two fibers into the two uppermost holes.
7. Identify which fiber is threaded into each hole of the jig by gently tugging on the end of each fiber to see which moves. Mark the ends with the Sharpie so that they can be easily identified.
8. The next four steps will have to be done quickly (within the 5 minute cure time of the epoxy).
    a. Mix the epoxy thoroughly with a toothpick and apply the epoxy only along the jacket of the fibers (do not place epoxy on the glass of the fiber). Start about 3 inches from the exposed glass and apply the epoxy to the upper and undersides of the fiber bundle being careful not to pull the fiber ends out of the jig. Continue to cover the fiber bundle with epoxy until you are about 1 inch away from the exposed glass.
    b. Holding the fibers in place, pull the stainless steel tubing up to the tips. As the tubing moves it will pull the epoxy along with it, so be sure to clean off any excess with a toothpick. Pull the tubing to about ¼" away from the exposed glass.
    c. Having identified which fiber is threaded into each hole, adjust the lengths of the fibers in the jig by pulling on the end of the appropriate fiber. The 3

outer fibers should all be set at the same length with the central fiber approximately 2 mm longer.

d. With the fiber lengths now set in the jig, hold the back end firmly and gently push the tubing so that the glue/tubing is almost near the exposed glass. Be sure to remove any excess glue from the SS tubing.

9. Allow the glue to dry. Wait at least 30 minutes to allow the glue to cure more.
10. Once the glue has dried, carefully pull the probe from the jig and place the probe securely so that the probe tips are safe from hard impacts.
11. Secure any appropriate fittings on the probe (for insertion into a reactor) by running them up the back of the probe.
12. Plug in the fibers to the fiber box.
13. The 2-point probe is now ready for use.

APPENDIX B.

MATLAB PROGRAM FOR TWO-TIP OPTICAL PROBE

A: Plotting and Smoothing Progran

```
clear all;
format short g;
format compact;

a=load('Fittest1.txt');
data_points = length(a);
N = 1000;
lolim1 = -0.02;  %min
lolim2 = -0.3;   %max
uplim1 = 1.5;    %max
uplim2 = 1.4;    %min threshold *dominan
x=1:N+1;

time = 52;  %total measurement time
dt = time/data_points;
t = linspace(0,dt*(N+1),N+1);

for i=1:data_points/(N+1);
    upper=a(N*i:N*(i+1),4)-uplim2;
    lower=a(N*i:N*(i+1),2)-lolim2;
    for k=1:N+1
       if upper(k) > (uplim1+uplim2)/2-uplim2
           upper_n(k) = 1;
       else
           upper_n(k) = 0;
       end
       if lower(k) > abs((lolim1+lolim2)/2-lolim2)
           lower_n(k) = 1;
       else
           lower_n(k) = 0;
       end
    end
    s=1;
    figure(s); set(s,'Position',[690 607 987 373]);
    subplot(211), plot(x,upper,'b',x,upper_n,'r'); grid;
    ylim([-1 2]);
    xlim([0 N]);
    set(gca,'FontSize',10);
    xlabel('x','FontSize',10);
    ylabel('Volts','FontSize',10);
    plot_title = ['Optical Probe data for x = ',num2str(N*i),' and y =
',num2str(N*(i+1))];
    title(plot_title,'FontSize',10)

    subplot(212), plot(x,lower,'r',x,lower_n,'m'); grid;
    ylim([-1 3]);
    xlim([0 N]);
    fprintf('i =%d, x =%6d, y =%6d\n',i,N*i,N*(i+1));
    set(gca,'FontSize',10);
    xlabel('x','FontSize',10);
    ylabel('Volts','FontSize',10);
    plot_title = ['Optical Probe data for x = ',num2str(N*i),' and y =
',num2str(N*(i+1))];
    title(plot_title,'FontSize',10)
```

```
    [tua,tud,du]=findtimes(upper_n,0);
    [tla,tld,dl]=findtimes(lower_n,0);

    s=2;
    figure(s); set(s,'Position',[690 160 987 372]);
    subplot(211), plot(du,'b'); grid;
    ylim([-1 2]);
    set(gca,'FontSize',10);
    xlabel('x','FontSize',10);
    ylabel('Differential','FontSize',10);
    plot_title = ['Differential Plot for x = ',num2str(N*i),' and y =
',num2str(N*(i+1))];
    title(plot_title,'FontSize',10)
    subplot(212), plot(dl,'r'); grid;
    ylim([-1 3]);
    set(gca,'FontSize',10);
    xlabel('x','FontSize',10);
    ylabel('Differential','FontSize',10);
    plot_title = ['Differential Plot for x = ',num2str(N*i),' and y =
',num2str(N*(i+1))];
    title(plot_title,'FontSize',10)
    pause;
end
```

B: Liquid and Gss Velocity Calculation

```
function [ outp ] = VelocityFinder1
clear all

f1=['……..txt'];

format short g;
format compact;
for ki=1:1
            a=load(f1);
            data_points = length(a);
            N = 100000;
            perc_meas =0.50;  % 50% measurment
            num_frame=500;    % number of frame
            upthresh=( max(a(:,2))+min(a(:,2)))/2
            lothresh=( max(a(:,3))+min(a(:,3)))/2

           x=1:N+1;
            time =(8192 * (num_frame*perc_meas))/40000
            dt = time/data_points;
            t = linspace(0,dt*(N+1),N+1);
            z=1;
            for i=2:data_points/(N+1);
                upper=a(N*i:N*(i+1),2);
                lower=a(N*i:N*(i+1),3);
                for k=1:N+1
                    if upper(k) > upthresh
                        upper_n(k) = 1;
                    else
                        upper_n(k) = 0;
```

```
                    end

                    if lower(k) > lothresh
                        lower_n(k) = 1;
                    else
                        lower_n(k) = 0;
                    end
                end
                 s=1;

   %Findind the time

                [tua,tud,du]=findtimes(upper_n,0);
                [tla,tld,dl]=findtimes(lower_n,0);

                [z1,z2]=size(tla);
                [z1,z3]=size(tua);

   % sorrting the data and found the matching signal
                 for ii=1:z2
                       for jj=1:z3
                             if abs(tla(ii)-tua(jj)) <=1500
                                   if abs(tla(ii)-tua(jj)) ~=0
                                       if (tla(ii)-tua(jj)) >0

                                          vv = 0.1/(t(tla(ii))-
t(tua(jj)));
                                           if vv < 50
                                             vl(z,1)=vv;
                                             vl(z,2)=tla(ii);
                                             vl(z,3)=tua(jj);
                                             vl(z,4)=i
                                             z=z+1
                                           end
                                       end
                                   end
                             end
                       end
                    if z > 75
                    xlswrite(f1(1:9),vl);
                    break;
                    end;
                 end

            end

end

function [tx_arrive,tx_depart,dx]=findtimes(x,thresh)

dx = diff(x);
tx_depart=find(dx < -thresh);
tx_arrive=find(dx >  thresh);
end
```

C: Calculation Progarm for Gas Holup

```
%Develop by Vineet Alexander

clear all
f=load('…….txt');  %% loading text file
y=f(:,2);  %% extracting 2nd coloumn
l=f(:,3);   %% extracting 4th coloumn
upperthreshold= (max(y)+min(y))/2;  % for finding the upperthreshold
value
lowerthreshold=(max(l)+min(l))/2; % for finding the lowerthreshold
value
ju=0; jl=0; jud=0;jld=0;          %ju=no of transtion from 0 to 1(upper)
mu=0; ml=0;                       %ml=no of transiton from 1 to 0(lower)
                                  %jud=no of data points having 1 value
                                  %value(upper)
for i=1:length(y)
      if y(i)>upperthreshold
        k(i)=1;
        jud=jud+1;                  %% no of data points having 1 value
    elseif  y(i)<upperthreshold;
        k(i)=0;                     %%% loop for normalizing
    end
    if l(i)>lowerthreshold
        n(i)=1;
        jld=jld+1;                  %% no of data points having 1 value
    elseif l(i)<lowerthreshold
        n(i)=0;
    end

end
for i=1:length(y)-1
 if k(i+1)>k(i)
        ju=ju+1;                       %% for finding no of peaks
 elseif k(i+1)<k(i)
        mu=mu+1;
 end
    if n(i+1)>n(i)
        jl=jl+1;
    elseif n(i+1)<n(i)
        ml=ml+1;
    end
end

if ju>mu
    upperholdup=((jud-ju)/(length(y)-1))
elseif mu>ju                                    %% to find the holdup
    upperholdup=((jud-mu)/(length(y)-1))
elseif mu==ju
    upperholdup=((jud-mu)/(length(y)-1))
end

if jl>ml
```

```
    lowerholdup=((jld-jl)/(length(y)-1))
elseif ml>jl                                    %% to find the holdup
    lowerholdup=((jld-ml)/(length(y)-1))
elseif ml==jl
    lowerholdup=((jld-ml)/(length(y)-1))
end
```

APPENDIX C

PROGRAM OF KOLMOGOROV ENTROPY CALCULATION

```
%*****************************************************************
%Topic      : Kolmogorov Entropy Calculation
%Input      : Data in excel
%Output     : Kolmogorov Entropy (KE)
%*****************************************************************

%-----------------------------------------------------------------
%1. Load the data
y=xlsread('datafile.xlsx');
%-----------------------------------------------------------------

%-----------------------------------------------------------------
%2. Calculate the mean, cut off length L.
%   L should be three times the average absolute deviation (AAD)
%-----------------------------------------------------------------
 MeanData = mean(y);
 Deviat = abs(y-MeanData);
 SumDeviat = sum(Deviat);
 LengthData =length(y);
 AAD = SumDeviat/LengthData;
 L=3*AAD;
%-----------------------------------------------------------------
%3. Initial the parameter
%
%-----------------------------------------------------------------
n=50;          %vector elements
m=1000;        %number of pair vector
fulltotb=0;
storeb=0;
s=80;          %can be changed between 80-100.

%-----------------------------------------------------------------
%4. Main loop for
%   a. Setting randomly initial vector pair
%   b. Calculate the difference between the pair X1 & X2
%   c. Find the maximum value of the difference (diff1)
%   d. Compare with the L and store the value of b when difference < L
%-----------------------------------------------------------------

fprintf('k\t   vec1\t   vec2\n');
for k=1:m                  %Create initial # vector pair
    vec1 = randi([1 200],1,1);
    vec2 = randi([1 200],1,1)+n;

    if (abs(vec1-vec2) > n)
         tempb=0;
         fprintf('%d\t   %d\t   %d\n',k,vec1,vec2);
         for i=1:s           %for next value of vector i.
            X1 = y(vec1+i:vec1+n+i-1);
            X2 = y(vec2+i:vec2+n+i-1);
            X12=[X1 X2]';
            diff1=abs(X1-X2);
            maxdiff(k) = max(diff1);   %Find the maximum value
            if (maxdiff(k) <= L)
                tempb=tempb+1;         %Count the b value
```

```
            else
                break;
            end
          storeb(k)=tempb;           %Store the b value
          fprintf('i=%d Value of b = %3d\n',i,storeb(k));
          end      %for i
      end          %end for if vec1~= vec2
end                %for k

%-------------------------------------------------------------------
%5. Calculate the
%   a. Average of b value.
%   b. Calculate the Kolmogorov Entropy.
%-------------------------------------------------------------------

storeb(storeb==0)=[];      %Eliminate the 0 value
fulltotb=sum(storeb);      %Sum the b value

Average_b=fulltotb/length(storeb);
fprintf('Number of b = %4d, Sum of b = %6d Average of b = %6.2f
\n',length(storeb),fulltotb,Average_b);

fs = 66.67;
KE = -fs*log(1-(1/Average_b));  %Calculate the Kolmogorov Entropy
fprintf('KE = %6.5f\n',KE);
```

VITA

Mohd Fitri Abdul Rahman was born in Perak, Malaysia. He grew up in Kuala Kangsar, Perak and went to Clifford Primary and Secondary School. He was enrolled in science matriculation program in Universiti Pertanian Malaysia (UPM). He received his B.S. in Industrial Chemistry and M.S. in Quantum Chemistry in May 1994 and February 2000, respectively, from Putra Malaysia University (formally known as Universiti Pertanian Malaysia), Serdang, Selangor, Malaysia. He worked in the research field at Malaysian Nuclear Agency for almost nine years before joining the Missouri University of Science and Technology, Rolla, Missouri, USA, where he earned his Ph.D. in Chemical Engineering in May 2017.

Mohd Fitri Abdul Rahman has been a member of the American Institute of Chemical Engineers since 2010. He has attended several conferences related to his research interests and published two conference papers; additionally, three journal papers have been submitted and currently are in process. His research interests involve hydrodynamics in multiphase systems.